The influence of a tidal inlet system on a nearby mega-feeder nourishment

D.C.A. Dane

Msc Thesis

January 2020

TU Delft

The influence of a tidal inlet system on a nearby mega-feeder nourishment

by

D.C.A. Dane

In partial fulfilment of the requirements for the degree of

Master of Science
in Civil Engineering

at the Delft University of Technology,
to be defended publicly on Tuesday January 7, 2020 at 14:00 PM.

Student number:	4592239	
Chairman:	Prof. dr. ir. S.G.J. Aarninkhof	TU Delft
Thesis committee:	Ir. Dr. J. Hopkins,	TU Delft, Supervisor
	Ir. Dr. M. A. de Schipper,	TU Delft
	Ir. R. McCall,	Deltares
	Ir. Dr. J. E. A. Storms,	TU Delft

TU Delft

Abstract

All over the world coastal communities are at risk due to sea-level rise and intensifying weather conditions. Many sandy beaches are eroding as a result of human-induced factors. Currently, the preferred coastal protection measure in the United States are beach nourishments. In Europe, there also is a general shift from hard to soft coastal protection measures. However, beach nourishments are not a long-term solution. Recently, in the Netherlands, a new concept called a large-scale (mega-feeder) nourishment has been introduced (the Sand Engine). Numerous studies on this new concept have been conducted. However, not for a mega-feeder nourishment nearby a tidal inlet system. About 10% of the world's beaches consist of barrier islands. Emphasizing the importance of investigating the development of a mega-feeder nourishment nearby a tidal inlet system, under various hydrodynamic conditions. Therefore the research question is as follows:

How does a nearby tidal inlet system influence the development of a mega-feeder nourishment?

The research question is answered by investigating the effects various hydrodynamic conditions have on the development of a mega-feeder nourishment nearby a tidal inlet system. This is done for fixed morphodynamic features, such as the dimensions of the tidal basin and the dimensions and orientation of the tidal inlet. The only variable morphodynamic feature is the alongshore position of the mega-feeder nourishment. Four distinct hydrodynamic scenarios are modelled to investigate their effects on a mega-feeder nourishment. The tidal range (η), significant wave height (H_s), peak wave period (T_p) and peak wave direction (D_p) are varied. This resulted in the following hydrodynamic scenarios:

- Mild wave conditions (η = 1.5m; H_s=1.0m and D_p=0°);
- Oblique wave conditions (η = 1.5m; H_s=1.0m and D_p=-45°);
- Storm wave conditions (η = 1.5m; H_s=variable and D_p=0°);
- High tidal range (η = 3.0m; H_s=1.0m and D_p=0°).

These hydrodynamic conditions and their effect on a mega-feeder nourishment are modelled by utilizing a process-based numerical model called Delft3D. In Delft3D, two locations of the mega-feeder nourishment per hydrodynamic scenario are evaluated. A mega-feeder nourishment is placed at an alongshore distance of 2 kilometers and 5 kilometers from the tidal inlet. This to get insight in the tidal flow nearby a tidal inlet and up to what alongshore distance this tidal flow affects the development of a mega-feeder nourishment. The hydrodynamic conditions were simplified, meaning steady wave characteristics and a single M2 tidal constituent. Using real time-varying hydrodynamic conditions yields similar results compared to the simplified hydrodynamic conditions. Therefore, simplifying the hydrodynamic conditions is justified.

The results show that there will be additional erosion near a tidal inlet if the mega-feeder nourishment is located inside the influence of the tidal inlet. The influence is the alongshore distance where the currents owing to the tidal inlet (residual currents) still affects the total alongshore sediment transport (larger than 50 $m^3/6y/m$). The alongshore distance of the influence increases with an increasing tidal range (tidal prism).

However, there is no shoreline retreat owing to the tidal inlet at the location (2km from the tidal inlet) of the mega-feeder nourishment over a time period of 6 years. Only the adjacent coast on the inlet-side of the mega-feeder nourishment erodes significantly more than without a tidal inlet, with an increasing magnitude in the shoreline retreat towards the tidal inlet. Hence, it is expected that if the mega-feeder nourishment is placed close to the tidal inlet (i.e. several hundreds of meters), then the influence of the currents owing to the tidal inlet will enhance the shoreline retreat at the location of a mega-feeder nourishment.

To conclude, the tidal inlet does influence the development of a mega-feeder nourishment nearby a tidal inlet (order several hundreds of meters). However, this is not necessarily seen in the retreat of the shoreline but instead in deeper depth contours. The governing process in the sediment transport at a mega-feeder nourishment is the incident wave angle for small tidal ranges ($\eta < 1.5m$) and mild wave conditions (H_s > 1m). However, for a large tidal range ($\eta > 3.0m$) the residual currents owing to the tidal inlet will become the governing process.

Preface

Before you lies the masters thesis which concludes the Master of Science in Hydraulic Engineering at the faculty of Civil Engineering and Geoscience, Delft University of Technology (TU Delft). Coming from the HBO, this thesis does not only complete my study career at the TU Delft, but also my study career in general.

First I would like thank my graduation committee Julia Hopkins, Matthieu de Schipper, Robert McCall, Joep Storms and Stefan Aarninkhof for their valuable feedback and steering me in the right direction during the kick-off and progress meetings. I would like to thank Julia in particular as my day-to-day supervisor. Julia was always available to give answers to my questions and give me valuable feedback. You were truly a **day-to-day** supervisor. I also very much enjoyed that there was time for some small chit-chats during our weekly meetings. Thank you Matthieu for your enthusiasm towards my thesis and helping me think about interesting approaches to problems I've encountered.

Secondly, I would like to thank my friends at the TU Delft for the fun and serious times when needed. I would not have been able to pass my premaster in one year without you guys. Furthermore, I would like to thank my friends at home for their interest in my thesis and allowing to get my mind off of my thesis, which was often necessary. We know each other for a long time now and I am confident that we will continue to do so now that we are all going to work full-time jobs.

Last and most importantly, thank you mom and dad! Without your support I would not have been able to study whatever I wanted. I am so grateful for the opportunity you have given me during my entire life! You were always ready to cheer me up and to help me during my study career.

D.C.A. Dane
Delft, January 2020

List of Figures

List of Tables

Nomenclature

Abbreviations

Table 1: Abbreviations used in the report

Abbreviation	Description
2DH	Two dimensional horizontal
Active depth	Depth in which the majority of total alongshore sediment transport takes place
D_p	Peak wave direction
e1	Course outer grid of the ebb-tidal simulation (model 1)
e3	Fine inner grid of the ebb-tidal simulation (model 1)
H_s	Significant wave height
Incident wave angle	Wave angle relative to the shoreline orientation
Influence (reach)	The distance where the RTF TAST is more than 50 m³/6y/m from the tip of the barrier island (start of the tidal inlet).
Inlet-side	The side of the mega-nourishment closest to the tidal inlet
M2 tidal constituent	Tidal constituent owing to the moon (principal lunar semi-diurnal)
Mega-feeder nourishment	A mega-nourishment with a feeder function to the adjacent coast
Mega-nourishment	A large-scale nourishment
MHW	Mean High Water Level
Model 1	Simulations of the ebb-tidal delta model (ebb-tidal delta simulations)
Model 2	Simulations of the mega-nourishment model (simplified simulations)
Morfac	Morphological Acceleration factor
MSL	Mean Sea Level
η	Tidal range
NGDC	National Geophysical Data Center
NOAA	National Oceanic and Atmospheric Administration
Non-inlet-side	The side from the centroid of the mega-nourishment that is not the closest to the tidal inlet
t1	Course outer grid of the simplified simulations (model 2)
t2	Intermediate grid of the simplified simulations (model 2)
t3	Fine inner grid of the simplified simulations (model 2)
Rel.	Relative to
RTF current	Absolute difference in the flow field for the tidal inlet being open and closed. This is the flow field owing to the tidal inlet.
RTF TAST	Absolute difference between the total alongshore sediment transport for the tidal inlet being open and closed. This is the TAST owing to the tidal inlet.
TAST	Total alongshore sediment transport
Total transported RTF TAST	Total transported total alongshore sediment transport owing to the tidal flow in the tidal inlet. This is a integral of the RTF TAST over the x-direction
T_p	Peak wave period
UTM	Universal Transverse Mercator
WGS84	World Geodetic System 1984

Units

Table 2: Units used in the report

Abbreviation	Description
kg	Kilograms
km	Kilometers
m	Meters
min	Minutes
s	Seconds
y	Years

Simulations

Table 3: Names and simulation ID's used to refer to certain models and their hydrodynamic conditions. The first column shows the ID the simulation has. The second column shows how this ID is abbreviated. The third column shows the name of the hydrodynamic conditions used for the model. The fourth column shows whether the tidal inlet is open or closed. The last column shows the alongshore distance of the mega-feeder nourishment to the tip of the barrier island.

Run ID	Run ID abbr.	Hydrodynamic conditions	Tidal inlet	Dist. [km]
Nour_Run_1.1	_11	Mild wave conditions	open	2.0
Nour_Run_1.2	_12	Mild wave conditions	open	5.0
Nour_Run_1.3	_13	Mild wave conditions	closed	2.0
Nour_Run_1.4	_14	Mild wave conditions	closed	5.0
Nour_Run_2.1	_21	Oblique wave conditions	open	2.0
Nour_Run_2.2	_22	Oblique wave conditions	open	5.0
Nour_Run_2.3	_23	Oblique wave conditions	closed	2.0
Nour_Run_2.4	_24	Oblique wave conditions	closed	5.0
Nour_Run_3.1	_31	Storm wave conditions	open	2.0
Nour_Run_3.2	_32	Storm wave conditions	open	5.0
Nour_Run_3.3	_33	Storm wave conditions	closed	2.0
Nour_Run_3.4	_34	Storm wave conditions	closed	5.0
Nour_Run_4.1	_41	High tidal range	open	2.0
Nour_Run_4.2	_42	High tidal range	open	5.0
Nour_Run_4.3	_43	High tidal range	closed	2.0
Nour_Run_4.4	_44	High tidal range	closed	5.0
Real_Run_5.1	_51	Real tide	open	2.0
Real_Run_5.2	_52	Real tide	open	5.0
Real_Run_5.3	_53	Real tide	closed	2.0
Real_Run_5.4	_54	Real tide	closed	5.0
Real_Run_6.1	_61	Real waves	open	2.0
Real_Run_6.2	_62	Real waves	open	5.0
Real_Run_6.3	_63	Real waves	closed	2.0
Real_Run_6.4	_64	Real waves	closed	5.0
Ebb_Run_1.0	-	Mild wave conditions	open	-

Contents

1

Introduction

1.1. Background

All over the world coastal communities are at risk due to sea-level rise and intensifying weather conditions. Moreover, the coastal population could grow from 1.2 billion people in 1990 to 1.8 - 5.2 billion people in 2080 [Nicholls et al., 2007]. Luijendijk et al. [2018] found that 31% of the world's shorelines are sandy beaches. Of these sandy beaches, 24% have structural erosion with erosion rates exceeding 0.5 meters per year. Four of the seven top most erosive beaches are human-induced. Furthermore, it was found that 37% of the sandy marine protected beaches are subjected to erosion rates larger than 0.5 meters a year, emphasizing the increasing importance of coastal protection measures.

Currently, the preferred coastal protection measures in the United States of America (USA) are beach nourishments [Basco, 1999, Campbell and Benedet, 2004], these are often done out of emergency. Also in Europe, there has been a general shift from hard to soft protection measures [Hanson et al., 2002], such as beach nourishments. However, beach nourishments are not a long-term solution and relatively expensive. Recently, in the Netherlands, a large-scale (mega-feeder) nourishment called "de Zandmotor" (the Sand Engine) was constructed. The Sand Engine had 21 million cubic meters of sand to protect about 10 kilometers of relatively straight coast. The sediment is expected to feed the adjacent coast over a period of approximately 20 years. One of the main advantages of a mega-feeder nourishment is that it is needed about once every 20 years to maintain the coastline, opposed to frequent renourishments of once every 2-5 years for beach nourishments [Stive et al., 2013]. The sediment will slowly diffuse along the coast thus feeding the adjacent shore. This diminishes the need for frequent renourishments. Moreover, the Sand Engine has created additional space for recreational use.

Although the Sand Engine is still in the pilot phase, the Sand Engine has already been declared a success [Oost et al., 2016], looking at the coastal management and lifetime of the Sand Engine. During the first 18 months, the shoreline has retreated about 150 meters at the mega-nourishment. Meanwhile the adjacent shoreline has prograted up to 200 meters, preventing erosion at the adjacent coastal cells. The volumetric loses were 1.8 million cubic meters, which accounts for about 10% of the total volume of sediment nourished. Only a small amount of sediment was lost. About 70% of the lost sediment was found on the adjacent coasts and dunes [de Schipper et al., 2016]. After 4 years, 95% of the sand supplied in the Sand Engine is still within the measuring area. Thereof 80% of the sand is still within the contours of the in 2011 constructed Sand Engine. This concludes that the lifetime of the Sand Engine will be longer than 20 years [Taal et al., 2016].

1.2. Problem description

The Sand Engine has only been applied on a straight coastal stretch in the Netherlands. Although the pilot has been declared a success, there is still a lot unknown. There are numerous studies and master theses about the concept ”mega-nourishment” and the evaluation of the Sand Engine, since the introduction of the Sand Engine. However, quite often the shorelines are not straight sandy beaches similar to the coast where the Sand Engine has been constructed.

Furthermore, about 10% of the world’s beaches consists of barrier islands [Stutz and Pilkey, 2012]. Most of the worlds barrier islands are found in the United States (24%), Mexico (11%), Russia (8%) and Australia (7%). These barrier islands often form a chain of barrier islands and have tidal inlets at both or either side of the barrier island. Hence, it is important to investigate the effect a tidal inlet system has on the development of a mega-feeder nourishment.

There has been a master’s thesis about nourishment strategies for the Ameland barrier island [Bak, 2017]. This thesis did include a mega-feeder nourishment nearby a tidal inlet. However, this thesis primary scope was the effect of sediment grain size and whether the nourishment would be viable with hydrodynamic conditions specific to Ameland. It is still unclear how a mega-feeder nourishment will behave adjacent to a tidal inlet system under various hydrodynamic conditions. Also it is not known from what distance the tidal inlet will affect the development of a mega-feeder nourishment.

1.3. Research objectives

This thesis will investigate the effects different hydrodynamic conditions have on the development of a mega-feeder nourishment nearby a tidal inlet. Hence, key morphodynamic features, such as the dimensions of the tidal basin and the dimensions or orientation of the tidal inlet, are kept constant. Therefore, the results will give insight into what the effects are of a tidal inlet system on a nearby mega-feeder nourishment. This will lead to the following research question:

> *How does a nearby tidal inlet system influence the development of a mega-feeder nourishment?*

Many parameters can influence the impact of a tidal inlet system on the development of a mega-feeder nourishment. Therefore, the following sub-questions will assist in answering the research question:

- How does a mega-feeder nourishment nearby a tidal inlet develop over time under various hydrodynamic conditions?
- What processes are important in the development of a mega-feeder nourishment owing to the tidal inlet?
- What is the effect of the tidal prism on the development of a mega-feeder nourishment?
- What alongshore distance from the tidal inlet will influence the development of a mega-feeder nourishment?

1.4. Relevance

The findings of this thesis will help to understand the effect nearby tidal inlet systems have on the development of a mega-feeder nourishment for different hydrodynamic conditions. If this thesis is a success then we can determine whether a mega-feeder nourishment solution is viable nearby a tidal inlet system and what morphological response might be expected. The study will be set up in such a way that the morphological response for a range of hydrodynamic conditions is approximately known, which might help in future designs of a

mega-feeder nourishment. As 10% of the world's beaches consists of barrier island with tidal inlets on both or either side [Stutz and Pilkey, 2012], it is essential to have a feeling of what might happen to a mega-feeder nourishment.

1.5. Thesis outline

The contents of this thesis consists of 7 chapters. First, chapter 2 will describe the theory which is relevant to this thesis. The theory describes what is already known and is used to explain the results or build the model. Furthermore, the relevant hypotheses to the research and sub-questions are formulated based on the knowledge gained in the literature study. Chapter 3, will describe how the research question will be answered and what tools are used. Moreover, the methods used to analyze the results are elaborated on. Chapter 4 will elaborate on the results of the simplified model. The results are discussed in chapter 5, including a discussion on what a tidal inlet system nearby a mega-feeder nourishment could mean for the design of a mega-feeder nourishment. Finally, in chapter 6, the conclusions are presented and in chapter 7 the recommendations of the thesis are described.

2

Theoretical background

2.1. Tidal inlet systems

Tidal inlet systems are formed due to large discharges in a tidal inlet. These large discharges will cause a strong sediment exchange with the adjacent coast, the tidal basin and the ebb-tidal delta [Bosboom and Stive, 2015]. The tidal inlet is connected with multiple systems which develop and are classified in their own ways. This section will discuss the different parts which make up a tidal inlet system and how these are classified.

2.1.1. Tidal inlet system definition

The tidal inlet system is the definition encompassing all components in a tidal inlet system. A tidal inlet system is often a highly dynamic system in which rapid changes in the bathymetry are not uncommon. The tidal inlet system consists of five main components: ebb-tidal delta, tidal gorge, flood-tidal delta, tidal basin and the adjacent coast.

Tidal basin

The tidal basin is the area which is filled with water. It is often characterized by meandering, braided and/or branched channels [Bosboom and Stive, 2015]. The tide is the main driver behind the volumetric exchange of water with the tidal basin. In essence, the tide causes a water level difference, which results in water to be transported in or out of the tidal basin. The surface area of the tidal basin and the tidal range determines the amount of water to be transported in the tidal basin. This volume of water which is transported in and out of the tidal basin within one tidal cycle, is called the tidal prism. For short basins, the water level inside the tidal basin can directly follow the water level of the ocean. Therefore the tidal prism for a short basin is proportional to the tidal range times the mean surface area of the tidal basin. For long tidal basins, the water has to propagate inside the tidal basin. As a result, the water level in the tidal basin can no longer instantaneously follow the water level in the ocean. This reduces the tidal prism compared to a short basin.

Flood-tidal delta

The flood-tidal delta is the delta that is located in the tidal basin, which often spans the entire tidal basin if there is an abundant sediment supply. One of the locations where there is abundant sediment supply is in the Wadden Sea. The flood-tidal delta contains sediment which is accumulated during flood flows of the tide or during storm surges.

Tidal gorges

The tidal gorge connects the flood-tidal delta to the ebb-tidal delta. Many tidal gorges have barrier islands at both sides of the gorge and are often part of a larger system. The tidal gorge is where the currents are the largest. This means that most of the sediment is transported through the tidal gorge. The sediment is deposited on or transported to the flood-tidal delta or ebb-tidal delta. The currents in the tidal gorge are caused by a water level difference, waves or wind. If the tide is the governing factor of the currents inside the tidal gorge then it is called a tidal inlet [Escoffier, 1940].

Ebb-tidal delta

The ebb-tidal delta is the delta located on the ocean-side of the tidal inlet system. The ebb-tidal delta is formed due to the divergence of the flow from inside the tidal gorge. It is further shaped by the waves and the tides. The waves will enhance shore-wards sediment transport and will limit the overall size of the ebb-tidal delta [Hageman, 1969]. Meanwhile, the magnitude of the currents caused by the tide will enhance seaward sediment transport. Therefore, the size and shape of the ebb-tidal delta is a balance between the shore-wards sediment flux caused by the waves and seawards sediment flux caused by the tidal currents [Bosboom and Stive, 2015]. Hence, with varying forcing will come various ebb-tidal delta shapes.

2.1.2. Global geology of tidal systems

About 10% of the global shorelines consists of coasts interrupted with tidal inlets (barrier islands). The majority of barrier islands are located along trailing edge margins [Douglas Glaeser, 1978]. Out of all barrier islands on trailing margins and marginal seas, 73% is located on coastal plains. Furthermore, on leading edge margins this is 58% (if the barrier islands are located in deltas). Deltas provide the sediment and low gradient foreshore conditions to enable barrier islands to exists. On average barrier islands on coastal plains are about 10 kilometers long and the tidal inlets are generally about 1 kilometer wide [Stutz and Pilkey, 2012].

2.1.3. Tidal inlet systems classification

Tidal inlet systems come in many shapes and sizes. Their shapes are often dependant on the overall hydrodynamic conditions. These hydrodynamic conditions can be subdivided into three tidal current energy conditions, which can be directly related to the tidal range [Davies and Moses, 1964, Hayes, 1979].

- *Microtidal coasts* Tidal range between 0 and 2 meter;
- *Mesotidal coasts* Tidal range between 2 and 4 meter;
- *Macrotidal coasts* Tidal range larger than 4 meter.

Furthermore, the wave energy can be divided into low, medium and high wave energy. Based on the tidal range and wave energy, Hayes [1979] and Davis and Hayes [1984] classified barrier island shorelines into five distinct subjective morphological types (Figure 2.1):

- *Wave-dominated* Long continuous barriers islands, few inlets, washovers abundant;
- *Mixed-energy (wave dominant)* Increasing number of tidal inlets, large ebb-tidal deltas, drumstick barriers islands (like the Wadden barrier islands);
- *Mixed-energy (tide-dominant)* Abundant tidal inlets, large ebb-tidal deltas, drumstick barriers islands;

- *Tide-dominated (low)* Occasional wave-built bars, transitional forms;
- *Tide-dominated (high)* Predominant tidal-current ridges, extensive salt marshes and tidal flats.

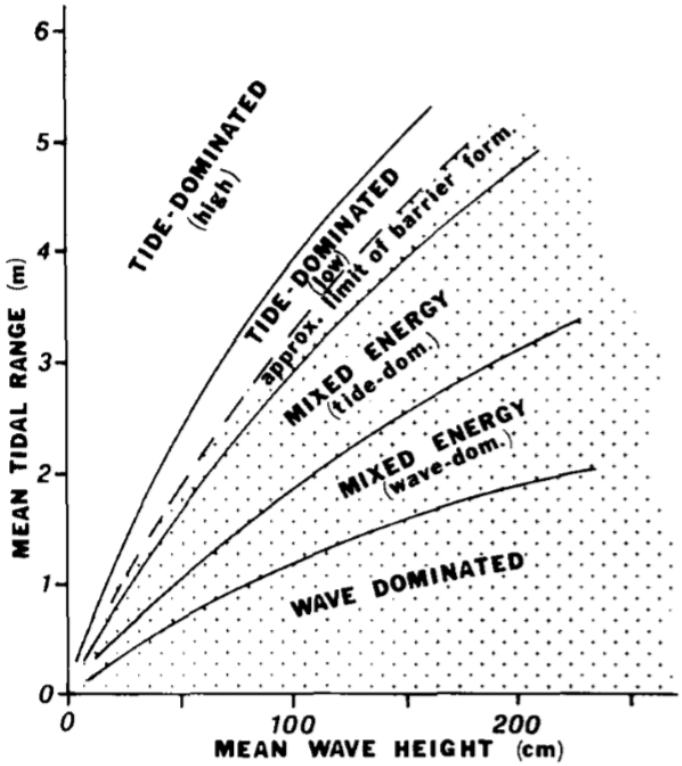

Figure 2.1: Hydrodynamic classification based on the general relationships between tidal range and wave height (Davis and Hayes [1984] modified after Hayes [1979]).

2.2. Important physical processes

Several physical processes are important in the diffusion of a mega-feeder nourishment and owing to the tidal inlet. The most general formula to describe the movement of sediment is:

$$\begin{aligned} \langle S_b \rangle &\propto \langle u|u|^2 \rangle \\ \langle S_s \rangle &\propto \langle u|u|^3 \rangle \end{aligned} \tag{2.1}$$

S_b Bed load sediment transport
S_s Suspended load sediment transport
u Flow velocity

Sediment transport is proportional to the flow velocity (see Equation 2.1). The bed load transport is proportional to the third power of the flow velocity and the suspended load transport is proportional to the fourth power of the flow velocity. This implies that the suspended load transport is more susceptible to the flow velocity compared to the bed load transport with flow velocities larger than 1 m/s. The flow velocity can be influenced by many processes found in the nearshore zone. The processes which influence the flow velocity are briefly discussed in this section. The transport is categorized into cross-shore sediment transport processes and alongshore sediment transport processes.

Cross shore processes

Roelvink and Stive [1989] describes sediment transport in the cross-shore direction as follows (assuming that $\overline{u} << u_{lo} << u_{hi}$):

$$\begin{aligned} u &= \overline{u} + u_{lo} + u_{hi} \\ \langle u|u|^2 \rangle &= \underbrace{3\langle \overline{u}|u_{hi}|^2 \rangle}_{1} + \underbrace{\langle u_{hi}|u_{hi}|^2 \rangle}_{2} + \underbrace{3\langle u_{lo}|u_{hi}|^2 \rangle}_{3} + \dots \end{aligned} \tag{2.2}$$

$\overline{u}$ Time-mean component (streaming outside surf zone, undertow in surf zone)
u_{lo} Low-frequency motion at wave-group scale
u_{hi} High-frequency motion at short wave scale

The cross-shore sediment transport mainly consists of three components. The first component is related to the transport by the mean current (underlined by a 1 in equation 2.2). The transport is onshore directed outside of the surf zone and is caused by the wave boundary layer. Inside the surf zone this is offshore directed due to a return current (the undertow). The second component is related to wave skewness (underlined by a 2 in equation 2.2). Wave skewness always results in an onshore directed flow as shoaling waves are positively skewed. The amplitude of the crest of the waves are higher than the trough of the waves. As a result, there is a net onshore directed sediment transport ($u^3 > 0$). The last component is related to the influence of long waves (underlined by a 3 in equation 2.2). The sediment transport owing to long waves is offshore directed outside of the surf zone. Due to the long waves still being bound to the wave group. The trough of the bound long waves coincide with the highest velocities of the group. Therefore the net transport of the bound long waves are offshore directed. In the surf zone the bound long waves are no longer in phase with the wave group. Hence, the highest velocities do not necessarily coincide with the trough of the long waves. As a result, the direction of the sediment transport might change inside the surf zone owing to the long waves.

Alongshore processes

The alongshore sediment transport consists of a couple of different processes (see Bosboom and Stive [2015], page 346). Assuming that stirring due to short waves is the dominant process then the alongshore sediment transport is approximately as shown in equation 2.3.

$$\langle S_y \rangle \propto \hat{u}^2 V \tag{2.3}$$

S_y Alongshore sediment transport (per unit width) [m²/m/s]
$\hat{u}$ Magnitude of the combined wave-current velocity vector
V Alongshore current velocity at some level above the bed

The most important factor in the alongshore sediment transport is the stirring up of sediment due to the short waves ($\hat{u}$). Subsequently, the sediment is transported by the alongshore currents. The stirring up of sediment can be caused by the orbital wave motion. The stirring up has two peak moments. One occurs when the velocities near the bottom are the largest. The other is owing to wave breaking, which stirs up sediment. This is a result of the increased turbulence which suspends sediment into the upper part of the flow when the waves are breaking. The largest alongshore sediment transport is located where the waves are breaking, most often this is just seaward of the breaker bar.

Waves and tides

The previous sections discussed the important processes found for the cross-shore sediment transport and alongshore sediment transport. The orbital motion of the short waves was important in both. Therefore the magnitude of these velocities will be discussed briefly. The near-bed peak velocity in shallow water according to linear wave theory is shown in equation 2.4.

$$\hat{u} = \sqrt{gh}\frac{H}{2h} \tag{2.4}$$

y Flow velocity [m/s]
$\hat{h}$ Water depth [m]
H Wave height [m]

The alongshore sediment transport is proportional to the wave height where the waves break ($H_b^{2.5}$) [Bosboom and Stive, 2015]. Moreover, the alongshore sediment transport is proportional to the significant wave height where the waves break times the sinusoidal of two times the angle of wave incident ($S \propto H_{s,b} * sin(2 * \phi_b)$), according to one of the most basic bulk alongshore sediment transport formulations, namely the CERC formulation (the $sin(2 * \phi_b)$ is also called the $s, \phi - curve$).

The tide propagates as a wave along the coast around the amphidromic point (point where tide vertical tide is always 0 meter). This introduces a tidal current along the coast. The tidal current is not uniform in the cross-shore direction but decreases towards the coast. The tidal velocity is proportional to the gradient of the tidal wave, assuming that the tidal wave is in very shallow water (see equation 2.5).

$$v \propto \sqrt{h\frac{\partial \eta}{\partial y}} \tag{2.5}$$

V Tidal current [m/s]
η Tidal amplitude [m]
y Tidal wavelength [m]
h Water depth [m]

Typically the tidal amplitude is O(1)m and the tidal wavelength O(10^6)m (1000km), the water depth is in the order of magnitude of O(10)m. This will result in tidal current of approximately O(10^{-2}) to O(10^{-1}) m/s.

The tide can also be asymmetric and skewed. This means that the tide is not a perfect sinusoidal wave. Due to the power of the sediment transport (see equation 2.1), the asymmetric nature of the tidal wave may lead to a net sediment transport.

Tidal inlets

A simple estimation of the mean tidal current in the tidal inlet for a short basin, based on gradients between the basin and the ocean is (Page 240 of Bosboom and Stive [2015]):

$$u_s(x,t) = \frac{\partial \eta_0}{\partial t}\frac{A_b}{A_s} \tag{2.6}$$

$u_s(x,t)$ Mean current in the tidal inlet at location x
A_b Basin surface area upstream of x
A_s Channel cross-sectional area at x

The currents in the tidal inlet might be strong enough to form a tidal jet. This is when the tidal flow has enough momentum such that the flow cannot spread out fast enough when flowing into the ocean. In this situation the highest velocities are in the tidal inlet. Furthermore, a tidal jet may cause a residual flow near the tip of a barrier island to always be directed towards the tidal inlet [Bosboom and Stive, 2015]. Thus creating a flow pattern which has the same direction in both the ebb and flood situation (see Figure 2.2).

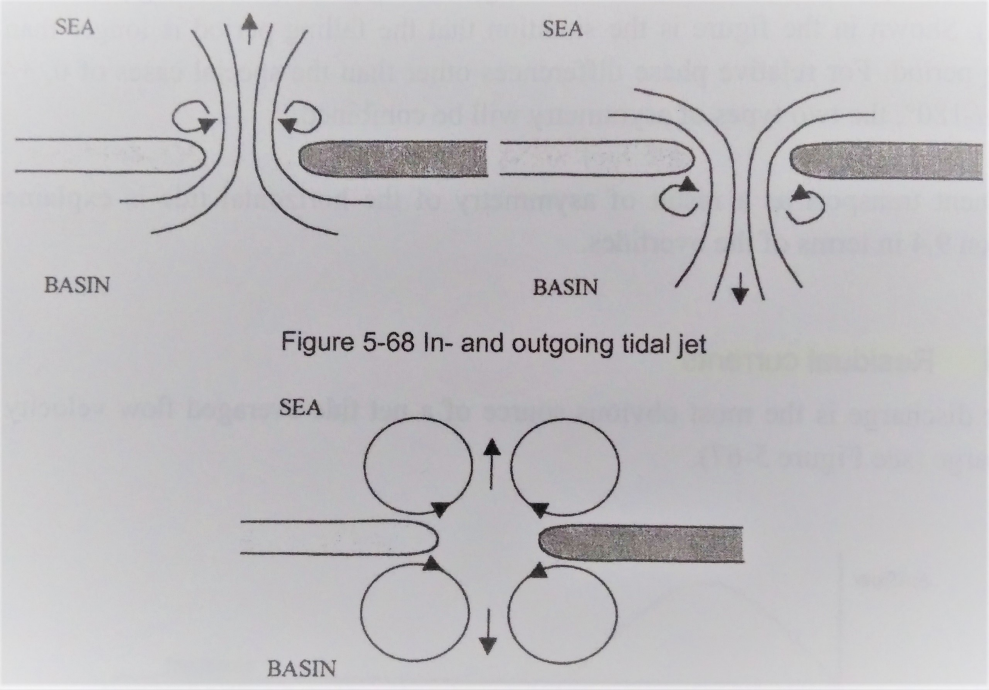

Figure 2.2: Schematized tidal residual currents at a tidal inlet (Bosboom and Stive [2015], p.250).

2.3. Analysis of the Sand Engine

The Sand Engine is the only existing mega-feeder nourishment to date. The Sand Engine is currently being observed and the morphological response is being investigated. Initially along the dutch coast, beach and foreshore nourishments were the preferred choice. Every approximately 5 years a nourishment was conducted to maintain the beach at a fixed line. The Sand Engine will decrease the nourishing frequency from once every 5 years to once every 20 years [Zuid-Holland, 2010], nourishing a huge amount of sediment locally instead of small nourishments along the entire coast. This will reduce the cost of maintaining the beach at a fixed position over time.

2.3.1. Characteristics of the Sand Engine and surroundings

There are many characteristics important in the design of a Sand Engine. The most important characteristics are:

- Bathymetry
- Wave climate
- Tide climate
- Grain size

Bathymetry

Without accurate bathymetry data, the model results are useless. The bathymetry used in the models for the Sand Engine was obtained from the Jarkus data (period from 1990 to 2005).

Wave climate

The wave climates were obtained by stations located in the North Sea. Two stations were used, EUR station (RD coordinate: xRD = 9963 m, yRD = 447601 m) and the MPN station (MPN xRD = 80443 m, yRD = 476683 m) (Figure 2.3).

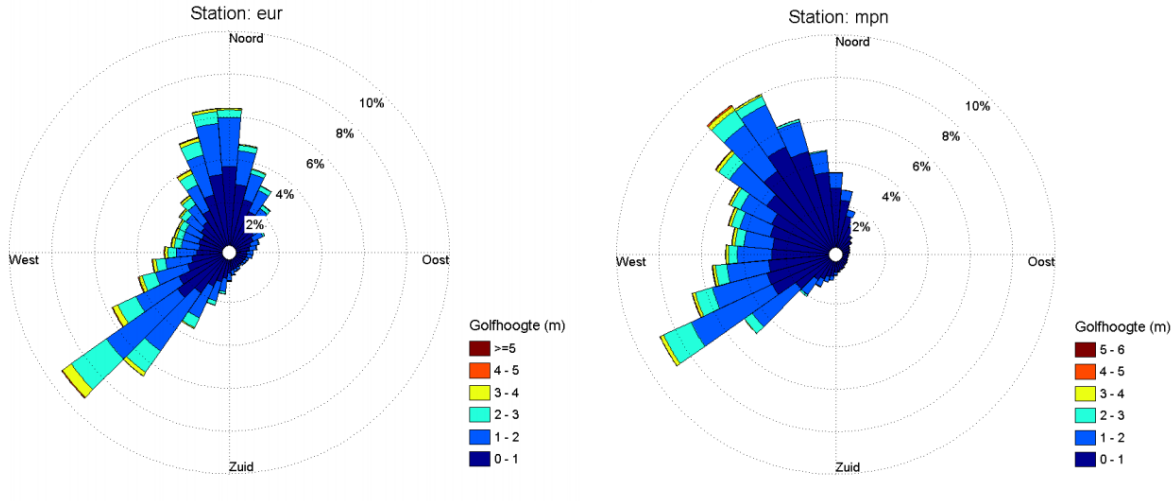

Figure 2.3: Wind rose containing information about the significant wave height and wave direction for measuring stations EUR and MPN [Deltaris [2009], p.7].

The highest and most frequent waves come from north-northwest and west-southwest (Figure 2.3). The annual mean significant wave height is 1.3 meter with a period of 5 - 6 seconds [Wijnberg [2002] cited in de Schipper et al. [2016]].

Tidal climate

The tidal wave propagates to the North along the Dutch coast. While propagating to the North, the tidal amplitude decreases. The tide at Scheveningen is asymmetric with a tidal amplitude of 1.98 m during spring tide and 1.48 m during neap tide. On average, the rising tide takes 4 hours and 21 minutes while the falling tide takes about 8 hours. The flood currents are 0.7 m/s northeast directed and 0.5 m/s southwest directed [Luijendijk et al., 2017]. Furthermore, there is a surge of 2.35 meters with a return period of 1 year at Hoek van Holland [Luijendijk et al., 2017].

Soil characteristics

The median grain size (D_{50}) is 242 μm with a standard deviation of approximately 50 μm [Luijendijk et al., 2017]. For the morphological calculations a median grain size of 215 μm was used [Zuid-Holland, 2010].

2.3.2. Morphological response

The purpose of the Sand Engine is to diffuse and supply the adjacent coastal cells with sediment, reducing the need for frequent re-nourishments at the adjacent coast.

Modelled morphological response to the Sand Engine

The morphological response was modelled using Delft3D [Lesser et al., 2004]. The expectation was that the Sand Engine could supply the adjacent beaches for approximately 20 years. The Sand Engine has been modelled for a time span of 20 years (Figure 2.4 shows the modelled morphological response over a time span of 10 years). Currently, the Sand Engine has existed for 7 years, therefore the Sand Engine should be somewhere between Figure 2.4c and 2.4d.

Observed morphological response

During the first 18 months, the shoreline retreated about 150 meters. Meanwhile, the shoreline of the adjacent coastal sections prograted up to 200 meters. The volumetric loses were 1.8 million cubic meters. This accounts for about 10% of the total amount of sediment nourished, only a small amount of sediment was lost. About 70% of the sediment was found on the adjacent coasts and dunes. During months of high wave energy conditions the alongshore sediment transport was dominant and during months of low wave energy conditions the cross-shore sediment transport was dominant [de Schipper et al., 2016]. After 4 years, 95% of the sand supplied in the Sand Engine is still within the measuring area. Thereof 80% of the sand is still within the contours of the in 2011 constructed Sand Engine. This concludes that the lifetime of the Sand Engine will be longer than 20 years. The volume of sediment diffused along the adjacent coast is almost enough to cope with a relative sea-level rise of 3 mm a year, for the upcomming 50 years [Taal et al., 2016].

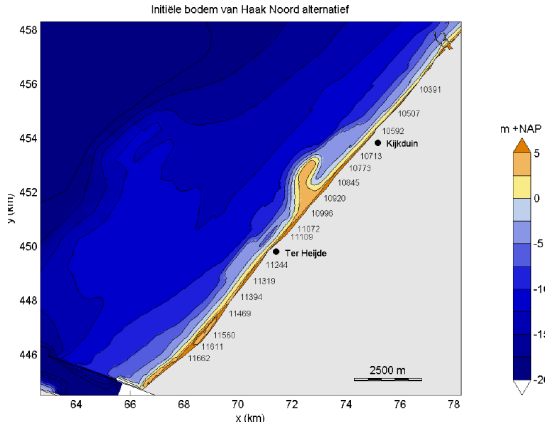

(a) Initial bathymetry of the Sand Engine (t=0 year)

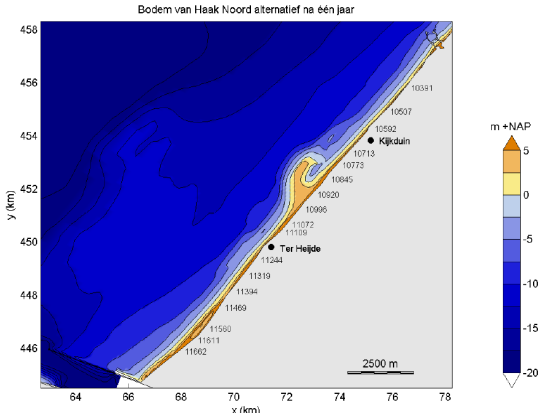

(b) Bathymetry of the Sand Engine after one year (t=1 year). The northern tip of the Sand Engine has propagated northward and slightly towards the coast.

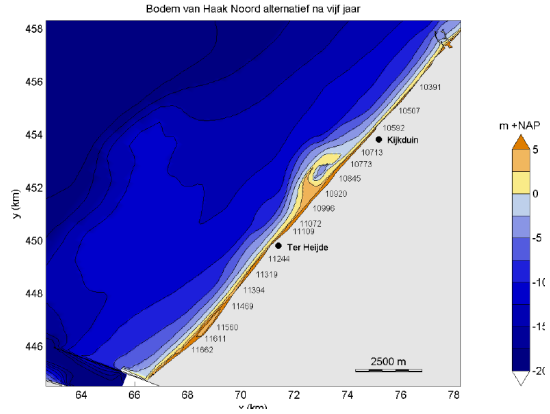

(c) Bathymetry of the Sand Engine after five years (t=5 years). The width of the Sand Engine has decreased and the length increased, thus the Sand Engine has diffused. Most of the sediment propagated towards the northeast.

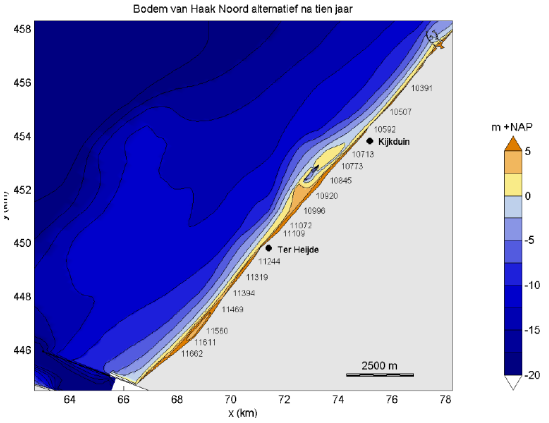

(d) Bathymetry of the Sand Engine after ten years (t=10 years). The Sand Engine has diffused even more. The sand now also has reached Kijkduin. Therefore no additional nourishments are needed.

Figure 2.4: The predicted morphological response of the Sand Engine at zero, one, five and ten years after the initial bathymetry, using a numerical model called Delft3D [Zuid-Holland, 2010]. A more state of the art model of the Sand Engine is shown in Luijendijk et al. [2017].

2.3.3. Important parameters in the morphological response of the Sand Engine

The wave-driven currents had the largest contribution to the total erosion [Luijendijk et al., 2017]. In the Luijendijk et al. [2017] paper, the observed morphological response was replicated in a model. One of the topics in this report is the sensitivity of the model by in/excluding certain processes. These are categorized into different runs. These runs are:

- Run A (reference run): Wave effects, vertical tide, wind-driven currents, surge levels and horizontal tide;
- Run B: Wave effects, vertical tide, wind-driven currents an surge levels;
- Run C: Wave effects, vertical tide and wind-driven currents;
- Run D: Wave effects and vertical tide;
- Run E: Wave effects only;
- Run F: Run E, but without wave effects.

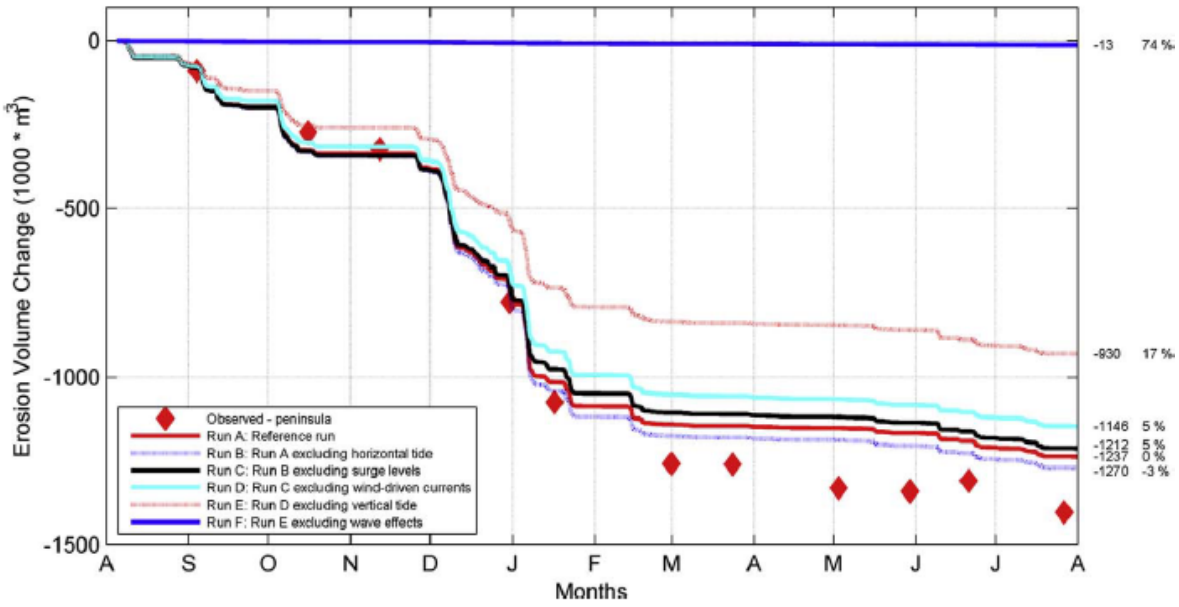

Figure 2.5: Volume changes of the Sand Engine over the study period (August 2011 - August 2012). This figure shows the relative contribution of the different environmental forcings. The y-axis on the left gives the final computed volume change per simulation. The y-axis on the right gives the difference with respect to the reference run in terms of percentage [Luijendijk et al., 2017].

Waves had the largest contribution to the morphological response of the Sand Engine (Figure 2.5). The erosion due to wave-driven currents give rise to approximately 75% of the total erosion. Furthermore, the vertical tide has the second biggest contribution to the erosion. On the contrary, the horizontal tide has almost a negligible impact on the erosion.

2.4. Hypothesis

It is expected that the presence of a nearby tidal inlet will enhance the erosion of a mega-nourishment. The tidal flow in the tidal inlet might have a high momentum preventing the flow from spreading out fast enough, this will result in a tidal jet. The magnitude of the currents inside the tidal inlet depend on the dimensions of the tidal basin and tidal inlet, and the tidal range. These parameters make up the tidal prism. This tidal jet will cause gyres at the adjacent coast of the barrier islands. These gyres will result in flow patterns always directed towards the tidal inlet near the barrier island tips (Figure 2.6). This will cause a net residual current, over a tidal cycle, towards the tidal inlet at the tips of the barrier islands [Bosboom and Stive, 2015].

Therefore it is expected that the tidal inlet will, in general, enhance the erosion of a mega-nourishment, given that the mega-nourishment is located within the range of influence of the residual currents. Eventually, with a large enough distance from the tidal inlet, the tidal inlet will not have an effect on the mega-nourishment anymore. This distance is not yet known but estimated to be in the order of hundreds of meters to several kilometers from the tidal inlet [Bosboom and Stive, 2015].

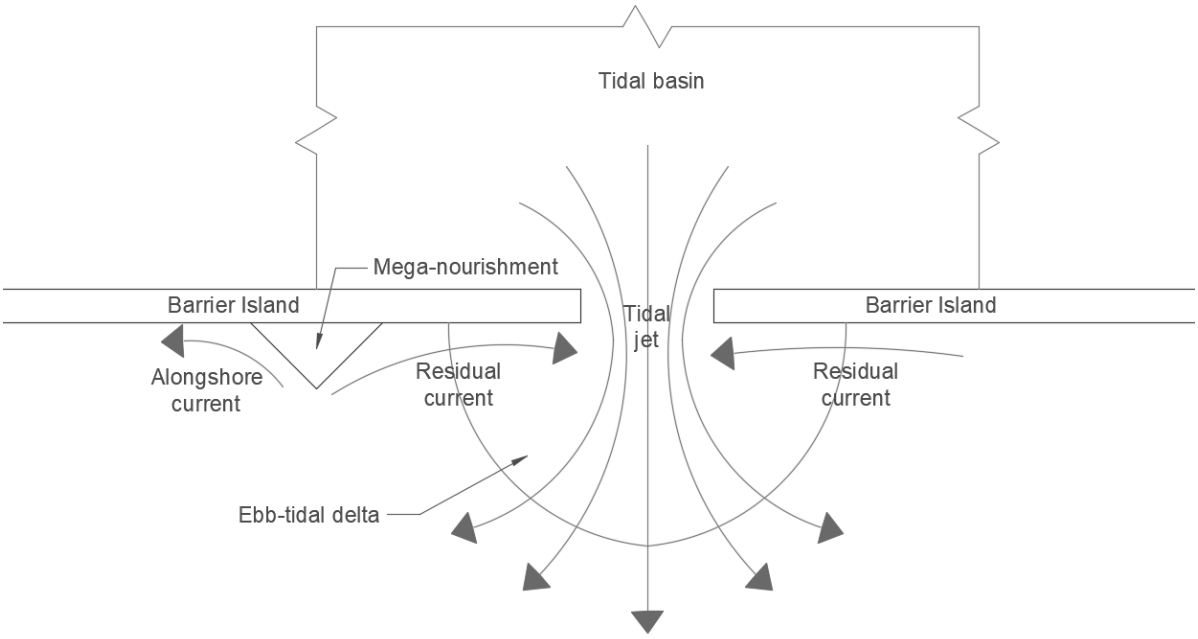

Figure 2.6: Schematic overview of the hypothesized processes and locations.

Question: How does a mega-feeder nourishment nearby a tidal inlet develop over time under various hydrodynamic conditions?

It is hypothesized that storm conditions will enhance the sediment transport at the mega-feeder nourishment owing to an increased magnitude in processes such as an undertow, long waves, up stirring and alongshore sediment transport. Furthermore, it is hypothesized that oblique waves towards the tidal inlet will transport sediment originating from the mega-feeder nourishment towards the tidal inlet owing to alongshore sediment transport, refraction and wave breaking. The alongshore sediment transport may be picked up by the flow towards the tidal inlet, transporting sediment towards the tidal inlet and enhancing erosion of the mega-feeder nourishment.

Question: What processes are important in the development of a mega-feeder nourishment owing to the tidal inlet?

It is hypothesized that the net residual currents as a result of the gyres will have a

significant impact on the erosion of the mega-feeder nourishment. Furthermore, it is hypothesized that high waves will enhance sediment transport.

Question: What is the effect of the tidal prism on the development of a mega-feeder nourishment?

The tidal range is proportional to the tidal prism and the tidal prism is proportional to the magnitude of the tidal currents inside the tidal inlet. Hence, if the tidal range increases then so will the tidal prism and tidal currents. The tidal current will generate gyres owing to tidal jetting. These gyres might result in flow patterns always directed towards the tidal inlet, adjacent (order several hundreds of meters to kilometers) to the tidal inlet. Therefore, an increasing tidal range and thus tidal prism, will increase the erosion of the mega-feeder nourishment owing to residual currents.

Question: What alongshore distance from the tidal inlet will influence the development of a mega-feeder nourishment?

It is hypothesized that tidal inlets will enhance erosion of the nearby (order hundreds of meters to several kilometers) mega-nourishment owing to the net residual currents as a result of the gyres at the tips of the barrier islands.

3

Methodology

The development of a mega-feeder nourishment adjacent to a tidal inlet is investigated by means of numerical process-based modelling. This is done by utilizing Delft3D version 4 release 7545 [Lesser et al., 2004], specifically the Flow, Wave and Sediment modules. The Delft3D-FLOW module solves the Navier Stokes equations for an incompressible fluid, under the shallow water and Boussinesq assumptions [Deltares, 2014b].

Furthermore, the Delft3D-WAVE (SWAN) module is utilized to solve the discrete spectral action balance equation [Deltares, 2014a]. The WAVE and FLOW modules are online coupled, meaning that the WAVE model has a dynamic interaction with the FLOW module. The effects of waves on currents and the effect of flow on waves are accounted for [Deltares, 2014a].

The sediment module calculates the sediment transport for bedload and suspended load transport of non-cohesive sediments and cohesive suspended load sediments (mud). The transport is calculated by solving the advection-diffusion equation [Deltares, 2014b]. The entire morphological feedback loop is shown in Figure 3.1 and elaborated on in Lesser et al. [2004].

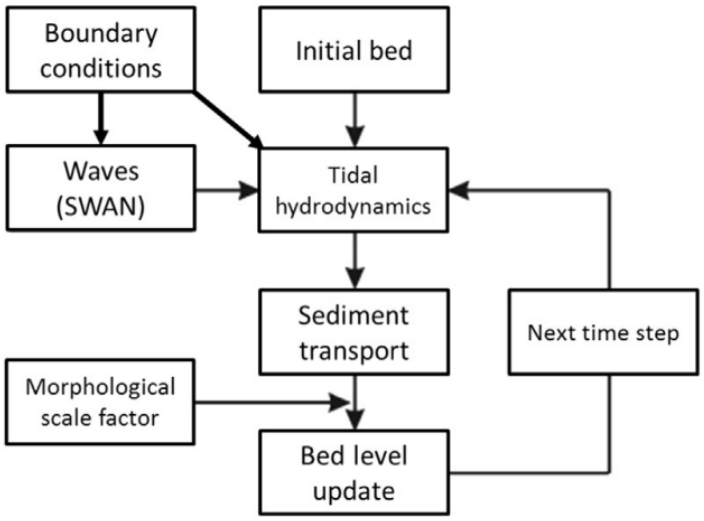

Figure 3.1: Overview of the morphodynamic feedback loop applied in Delft3D [Luijendijk et al., 2017]

3.1. Simplified model setup

Two models are constructed to obtain insight into the development of a mega-feeder nourishment nearby a tidal inlet. The first model (referred to as model 1) solely purpose is to build an ebb-tidal delta. This model will develop the bathymetry and hence the flow patterns required nearby a tidal inlet. The most significant change in the bathymetry occurs in the order of decades [van der Wegen, 2010]. Therefore, these models are run for 30 years worth of morphological change. The second model (referred to as model 2) uses the bathymetry results of the first model and includes the mega-feeder nourishment. In model 2 a more detailed grid is desired to capture the physical processes in the surf zone at the location of the mega-nourishment. This ensures a more accurate behavior of the mega-nourishment. The hydrodynamical and morphodynamical parameters are the same for model 1 and model 2. Furthermore, all models are run in 2DH mode, which means that the currents are depth-averaged. At last, the grids are constructed by utilizing domain decomposition allowing for grid refinement where desired [Deltares, 2014a].

3.1.1. Grid and bathymetry of the ebb-tidal delta simulations

The first model has a total of three rectilinear grids (see Figure 3.2). The first grid is the coarse outer grid (referred to as e1). This grid has a resolution of 300 by 300 meters, an alongshore length of 26.7 kilometers and a cross-shore length of 32.7 kilometers (in part owing to the large tidal basin). The second grid is the fine inner grid (referred to as e3). This grid is nested inside the e1 grid and has a resolution of 60 by 60 meters, an alongshore length of 7.8 kilometers and a cross-shore length of 6.4 kilometers. The e3 grid is located to the sea-ward side of the tidal inlet. Inside the e3 grid an ebb-tidal delta will develop. Therefore, this finer grid is desired to capture the highly variable flow patterns reasonably well. The third and final grid is the coarse wave grid (referred to as e1-wave). This grid is, in essence, the same as the e1 grid. However, the fine grid (e3) is not cut out of the coarse wave grid (e1-wave).

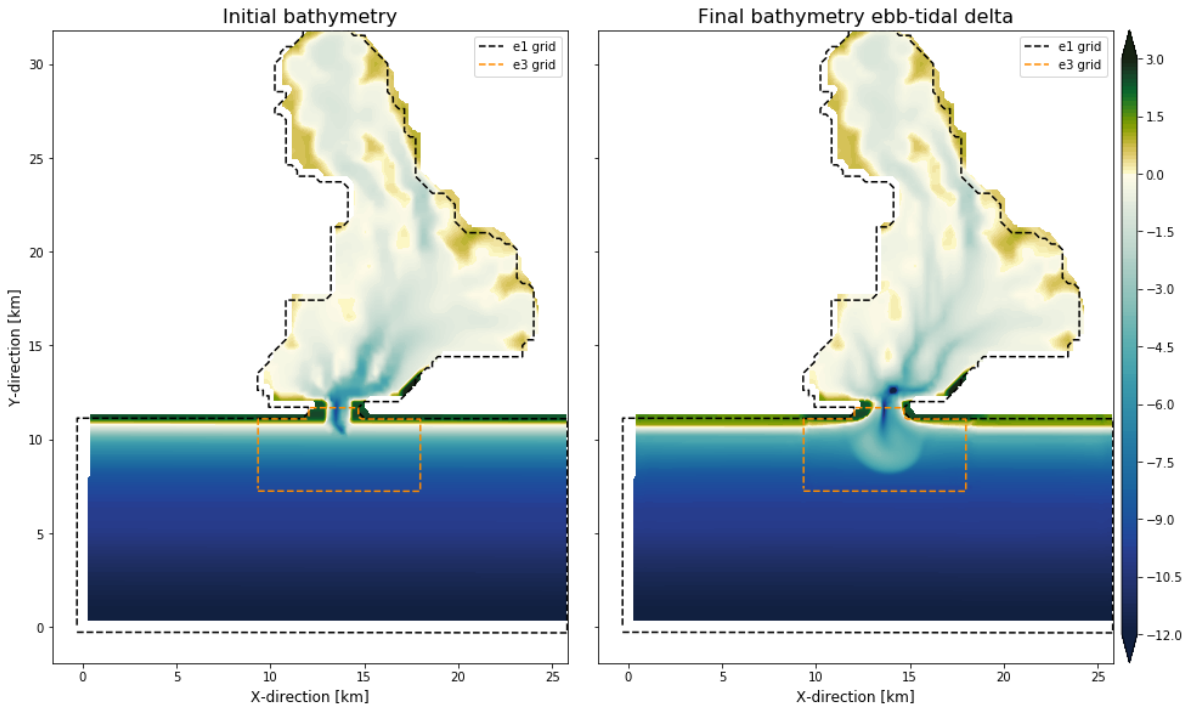

Figure 3.2: The left figure shows the initial bathymetry of the simplified model to build the ebb-tidal delta. The right figure shows the final bathymetry of the ebb-tidal delta model run. The black dashed line represents the boundary line of the coarse outer grid and the orange dashed line represents the boundary line of the fine inner grid.

The bathymetry of the coast is uniform in the alongshore direction (see figure 3.2), except for where the tidal inlet is located. The bathymetry is constructed from a sandy beach profile (1:150). A tidal inlet is placed at the center of the grid. The tidal inlet has a width of 1.3 kilometers and its deepest point is -9.8 meter below Mean Sea level (MSL). The tidal basin represents a large basin of which the tidal prism is in the order of 100 million cubic meters.

3.1.2. Grid and bathymetry of mega-nourishment simulations

The second model has a total of five rectilinear grids (see Figure 3.3). The first grid is the coarse outer grid (referred to as t1). This grid has a resolution of 300 by 300 meters and is used in the FLOW module. The grid extends 25.8 kilometers into the alongshore direction and 32.1 kilometers in the cross-shore direction. The second grid is the intermediate inner grid (referred to as t2). This grid is nested inside the t1 grid and has a resolution of 100 by 100 meters and is used in the FLOW module. The t2 grid extends 13.3 kilometers in the alongshore direction and 4.6 kilometers in the cross-shore direction. The main purpose of the t2 grid is to allow for a gradual transition to the fine grid, preventing hydrodynamic extremes as a result of the grid transition. Moreover, this grid is used to better capture the physics in the tidal inlet and ebb-tidal delta. The third and finest grid of the FLOW module is the fine inner grid (referred to as t3). The t3 grid has a resolution of 33.3 by 33.3 meters and is used in both the FLOW and WAVE modules. This grid extends 4.2 kilometers in the alongshore direction and 2.1 kilometers in the cross-shore direction. The location of this grid is varied based on the location of the mega-feeder nourishment, which will be elaborated on in chapter 3.2.

There are two more grids specifically used in the WAVE module. The fourth grid is the equivalent of the t1 grid but without the nested grids cut out (referred to as t1-wave). The same applies to the intermediate grid (t2-wave), which is the equivalent of the t2 grid in the FLOW module.

The results of the first model run acts as the input of the second model run. Therefore, the initial bathymetry of model 2 is the bathymetry of the final ebb-tidal delta simulation (see the right figure in Figure 3.2) including a mega-feeder nourishment. The mega-feeder nourishment is about 1 kilometers long and extends 0.5 kilometers into the ocean (see Figure 3.3). The position of the mega-feeder nourishment depends on the simulation, which will be described in chapter 3.2. This results in a nourished sediment volume of about 2.1 million m^3.

Furthermore, the dimensions of the tidal basin and tidal inlet are fixed in this thesis as the scope of the thesis is to investigate the effects of the hydrodynamics on the mega-nourishment. As a result, the resulting bathymetry after 30 years, which includes the ebb-tidal delta, is also fixed. Hence, the morphodynamics are fixed and only the hydrodynamics are varied. Therefore, the results of this thesis will only be applicable to this particular system.

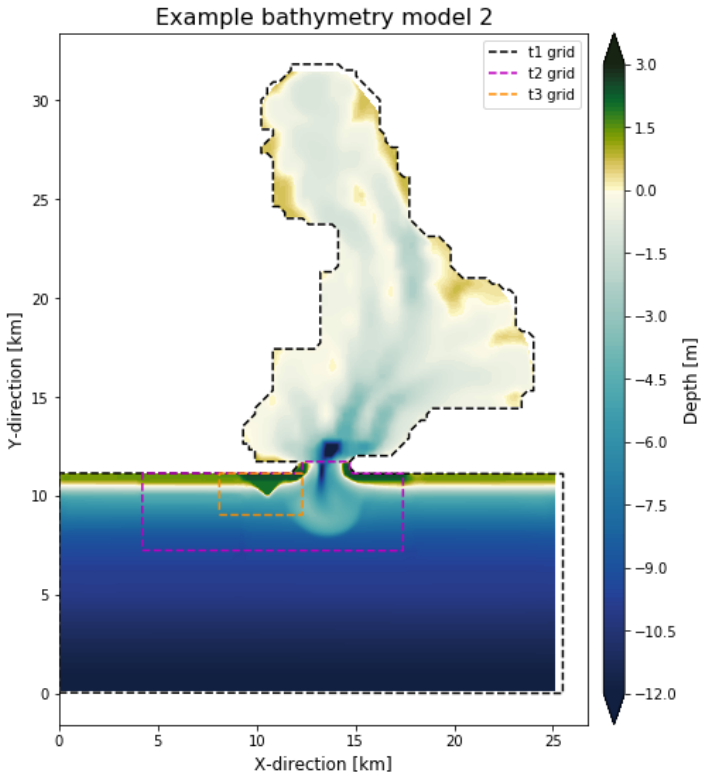

Figure 3.3: The grid and bathymetry of model 2 (the development of a mega-feeder nourishment). The mega-feeder nourishment is located at an alongshore distance of 2 kilometers from the tidal inlet with the tidal inlet being open. This is one of the scenarios further elaborated on in chapter 3.2. The black, purple and orange dashed lines represent the boundary of the t1, t2 and t3 grids respectively. The colors indicate the bathymetry used inside the model and are relative to MSL.

3.1.3. Boundary conditions used in the models

The water levels in the models are forced with a tide. This tide consists of only an M2 constituent. The amplitude of the M2 tidal constituent will vary based on the simulation (Table 3.2). The tidal range will vary between 1.5 and 3.0 meters.

The waves are forced with a spatially uniform, stationary mild wave conditions (H_s = 1.0 m; T_p = 5s) or with a spatially uniform, time-varying stormy wave conditions. The stormy wave conditions will have mild wave conditions for a majority of the time. However, twice a year storm conditions (H_s = 2.5 m; T_p = 8s) are imposed. These storm conditions are imposed for a month at a time every year in March and September (Figure 3.4). Moreover, the waves are imposed with a JONSWAP frequency-direction spectrum. The spectral space of model 1 is divided into 48 logarithmically spaced frequency bins and the directional space is divided into 72 evenly spaced direction bins. For stability reasons, these bins are increased from the default of 36 and 24 bins respectively. The spectral and directional space of model 2 is kept default. Furthermore, the direction of incoming waves at the boundary are varied with wave conditions coming from 0 degrees shore-normal and -45 degrees shore-normal (oblique waves), depending on the simulation described in chapter 3.2. The water level in model 1 will consist of an M2 tidal constituent with a tidal range of 1.5 meters. The waves in model 1 are forced with shore-normal mild wave conditions.

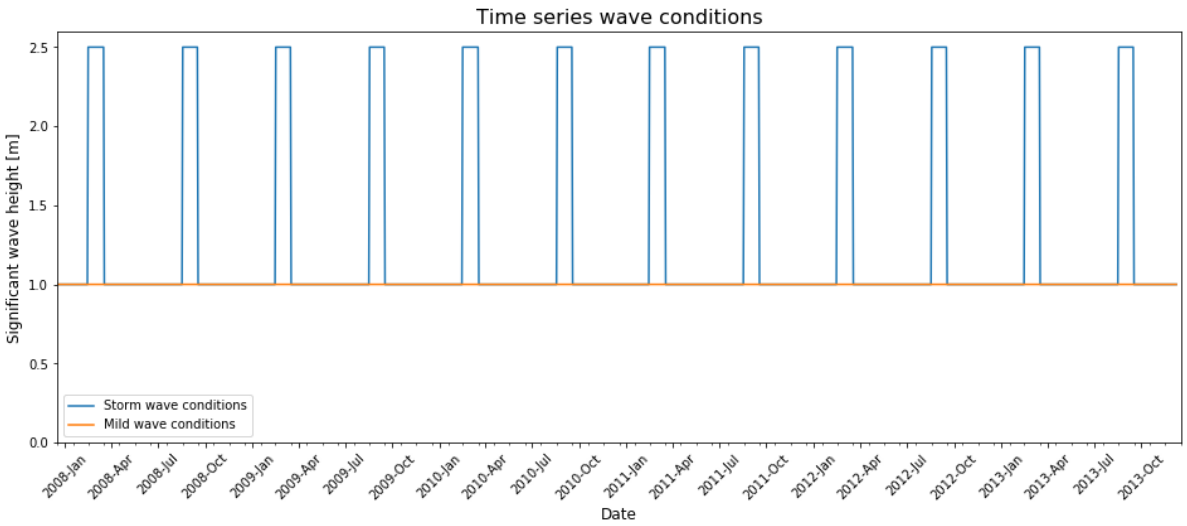

Figure 3.4: Time series of the significant wave height used in the simulations. The blue line shows the significant wave height for the stormy wave conditions and the orange line shows the significant wave height for the mild wave conditions.

3.1.4. Parameters used in the models which are different from the default

Each model has the same hydrodynamical and morphological parameters. These parameters make sure that Delft3D simulates physically reasonable results. Most of the parameters are kept default unless we have reason or data to suggest changes.

There are several sediment transport formulations in the Delft3D FLOW module. The Van Rijn 2007 formulation [van Rijn et al., 2007] yields the best results for simulating the evolution of a mega-nourishment at other sites, specifically the Sand Engine in the Netherlands [Luijendijk et al., 2017]. The wave heights were calculated by using the roller model [Reniers, 2004]. The roller model improved the performance in the surf zone, even though the computation time increased as well. Without the roller model, new beaches were formed in the ebb-tidal delta, which is physically not correct. The breaker parameter in the roller model (Gamdis) was changed to 0.45 and the calibration factor Betaro was changed to 0.05. According to Luijendijk et al. [2017], the default wave-related suspended and bedload transport factors overestimates the erosion and sedimentation and are therefore tuned down to 0.2 for both parameters. The default current-related suspended and bedload transport are also overestimated, hence these are tuned down to 0.5 for both parameters. The aforementioned parameters and other parameters are shown in table 3.1.

Table 3.1: Model parameters which are changed in this thesis from default values. The first column indicates in which module the parameter can be found. The Parameter column indicates the ASCII parameter code as read by the Delft3D FLOW/WAVE/sediment modules.

Module	Parameter	Value	Unit	Description
Roller	Betaro	0.05	[-]	Calibration factor (default = 0.1)
	Gamdis	0.45	[-]	Breaker parameter (default = 0.55)
	CstBnd	Yes	[-]	Helps to avoid the formation of artificial boundary layers along the domain boundaries.
Morphology	Sus	0.5	[-]	Current related suspended load transport factor (default = 1.0)
	Bed	0.5	[-]	Current related bedload transport factor (default = 1.0)
	SusW	0.2	[-]	Wave related bedload transport factor (default = 1.0)
	BedW	0.2	[-]	Wave related bedload transport factor (default = 1.0)
	Tresh	0.2	[m]	Threshold sediment thickness for transport and erosion reduction (default = 0.05)
	RWave	1.0	[-]	Multiplication factor estimated ripple height (default = 2.0)
	SedThr	0.3	[m]	Minimum depth for sediment calculations (default = 0.1)
	ThetSD	1.0	[-]	Factor for erosion of adjacent dry cells (dafault = 0.0)
Van Rijn 2007	TraFrm	-2	[-]	Sediment transport formula (default = -1)
Flow	Dt	0.5	[min]	Time step in minutes (default = 1)
	Vicouv	10.0	[m²/s]	Horizontal eddy viscosity (default = 1.0)
	Dicouv	10.0	[m²/s]	Horizontal eddy diffusivity (default = 1.0)
	Rhow	1025	[kg/m³]	Water density (default = 1000)
	Roumet	Manning	[-]	Roughness formula (default = Chézy)
	Ccofu	0.02	[s/m^1/3]	Manning value in u direction (default = 0.02)
	Ccofv	0.02	[s/m^1/3]	Manning value in v direction (default = 0.02)
	Drycrt	0.1	[m]	Drying criterium (default = not used)

3.2. Scenarios

The research question will be answered by looking at different scenarios. The wave height, wave direction and tidal range will vary to investigate their effects on a mega-feeder nourishment. The distance of the mega-feeder nourishment to the tidal inlet will also vary. The first model will make sure that the ebb-tidal delta is formed and the overall bathymetry is better shaped towards an equilibrium. The second simulation will make use of the bathymetry results of the first simulation. Hence, the initial bathymetry of the second simulation includes the ebb-tidal delta and the mega-feeder nourishment.

3.2.1. Simulation to create an ebb-tidal delta

The aim is to capture the largest morphological change of the ebb-tidal delta. Therefore, a morphological time-span of 30 years is selected to capture the most important morphological features. This includes the ebb-tidal delta and to some extent the flood channels. However, the ebb-tidal delta, tidal inlet and tidal basin are still far from an equilibrium, which might take up to several millennia [van der Wegen, 2010]. The ebb-tidal delta simulation is setup using one simplified hydrodynamic condition, which is shore-normal mild wave conditions with a tidal range of 1.5 meters (chapter 3.1.3). This will make sure that the simulations of model 2 will have the same initial bathymetry, hence allowing for a better absolute comparison.

To speed up the calculations, a morphological acceleration factor (Morfac) of 60 is used. For every hydrodynamical time-step, the bed level change is multiplied by a factor of 60, effectively allowing for longer time-spans to be modelled with the same computational effort. The morphological changes are the largest in the first morphological time-step but do not become unstable.

3.2.2. Simulations of the mega-feeder nourishment

The second set of simulations will include the mega-feeder nourishment. The resulting bathymetry of model 1 is used as the initial bathymetry of the second simulations (model 2). The mega-nourishment is included in the bathymetry at two consecutive locations. The first one is located where the centroid of the mega-feeder nourishment is 2 kilometers away, in the alongshore direction, from the tip of the barrier island. The second location of the mega-feeder nourishment is 5 kilometers from the tip of the barrier island. For each location a simulation is done where the tidal inlet is open, allowing for tidal currents to form, and a simulation where the tidal inlet is closed. The ebb-tidal delta is preserved in all simulations, allowing for the wave breaking to be captured in both simulations. Hence, the only difference is the closure of the tidal inlet and the absence of tidal flow in the tidal inlet.

This results in four sets of grid structures and bathymetries for every hydrodynamic conditions (Figure 3.5). By closing the tidal inlet the effect of the tidal inlet on the mega-feeder nourishment can be investigated. A total of four hydrodynamic conditions will be used for the simplified simulations. This will yield a total of 16 simulations (table 3.2). Simulations with the ID $Nour\_Run\_1.x$ are also referred to as mild wave conditions (where x varies from 1 to 4). Simulations with the ID $Nour\_Run\_2.x$, $Nour\_Run\_3.x$ and $Nour\_Run\_4.x$ are referred to as oblique wave conditions, storm wave conditions and high tidal range respectively. These terms and the ID's are used interchangeably.

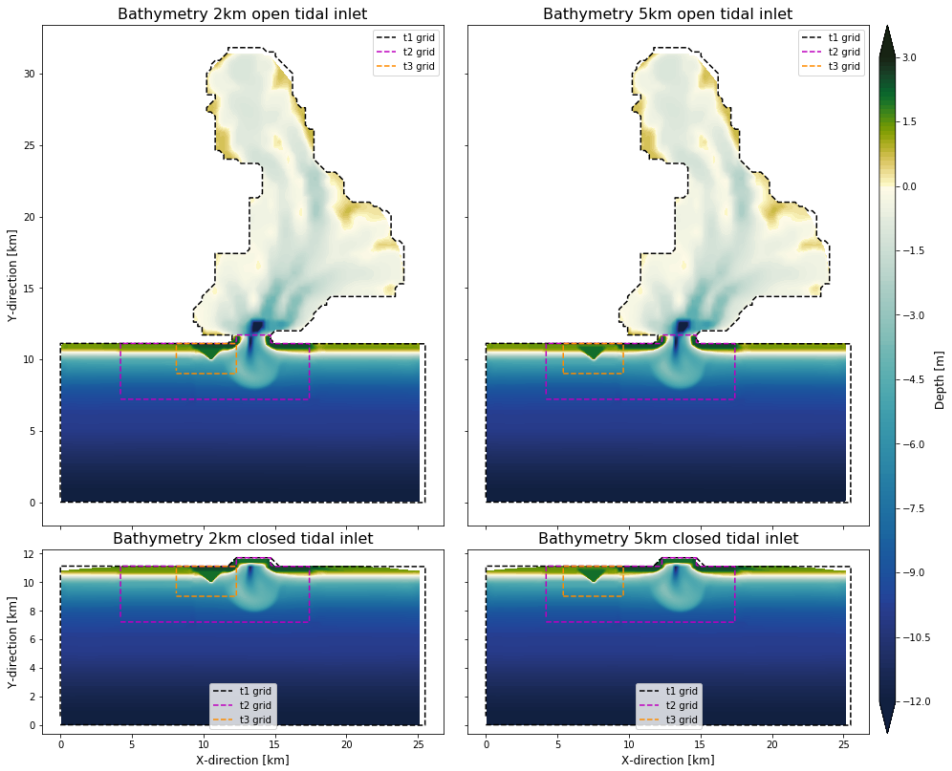

Figure 3.5: The grid and bathymetry used in all simulations of model 2, the development of a mega-feeder nourishment. The black, purple and orange dashed lines shows the boundary of the course outer grid, intermediate grid and fine inner grid. The location of the fine inner grid (orange line) will vary depending on the alongshore location of the mega-nourishment. All figures show the initial bathymetry for a given simulation. The top left figure corresponds with simulations $Nour\_Run\_x.1$ where x varies from 1 to 4 (see table 3.2). The bottom left figure corresponds with simulations $Nour\_Run\_x.3$, the top right figure corresponds with simulations $Nour\_Run\_x.2$ and the bottom right figure corresponds with simulations $Nour\_Run\_x.4$.

Table 3.2: Simulations conducted for the mega-feeder nourishment (model 2). Where the variable parameters are **1.** Significant Wave height (Hs) **2.** Peak wave direction relative to shore-normal (Dp) **3.** Tidal range (η) **4.** The alongshore distance of the centroid of the mega-feeder nourishment to the tip of the barrier island (Dist.). **5.** Indication of whether the tidal inlet is closed or open. At last, each simulation has been given an unique ID (Run ID) which will be referred to throughout the thesis.

Run ID	Hs [m]	Dp [Dir]	η [m]	Dist. [km]	Inlet
Nour_Run_1.1	1.0	0	1.5	2.0	Open
Nour_Run_1.2	1.0	0	1.5	5.0	Open
Nour_Run_1.3	1.0	0	1.5	2.0	Closed
Nour_Run_1.4	1.0	0	1.5	5.0	Closed
Nour_Run_2.1	1.0	-45	1.5	2.0	Open
Nour_Run_2.2	1.0	-45	1.5	5.0	Open
Nour_Run_2.3	1.0	-45	1.5	2.0	Closed
Nour_Run_2.4	1.0	-45	1.5	5.0	Closed
Nour_Run_3.1	Storm	0	1.5	2.0	Open
Nour_Run_3.2	Storm	0	1.5	5.0	Open
Nour_Run_3.3	Storm	0	1.5	2.0	Closed
Nour_Run_3.4	Storm	0	1.5	5.0	Closed
Nour_Run_4.1	1.0	0	3.0	2.0	Open
Nour_Run_4.2	1.0	0	3.0	5.0	Open
Nour_Run_4.4	1.0	0	3.0	2.0	Closed
Nour_Run_4.4	1.0	0	3.0	5.0	Closed

Morphological Acceleration factor

The morphological acceleration factor (Morfac) is a non-physical parameter to scale-up the bathymetric changes in every hydrodynamic time-step. This means that one hydrodynamic time-step may represent a morphology time-step equal to the hydrodynamic time-step times the morfac. This will reduce the computational time, provided that the morfac is low enough to still represent the actual morphology. A morfac that is too high may lead to unphysical results. The diffusion of sediment of the mega-feeder nourishment and the interaction with the tidal current in the ebb-tidal delta owing to the tidal inlet must be represented reasonably well in the model. Therefore, the simulations including the mega-feeder nourishment (table 3.2) need a much lower morfac than the simulation of the ebb-tidal delta (morfac of 60). Thus a morfac of 12 is used in the mega-feeder nourishment simulations (referred to as morfac12). A morfac of 12 will result in a similar behavior as if a morfac of 1 (referred to as brute force) is used (Figure 3.6).

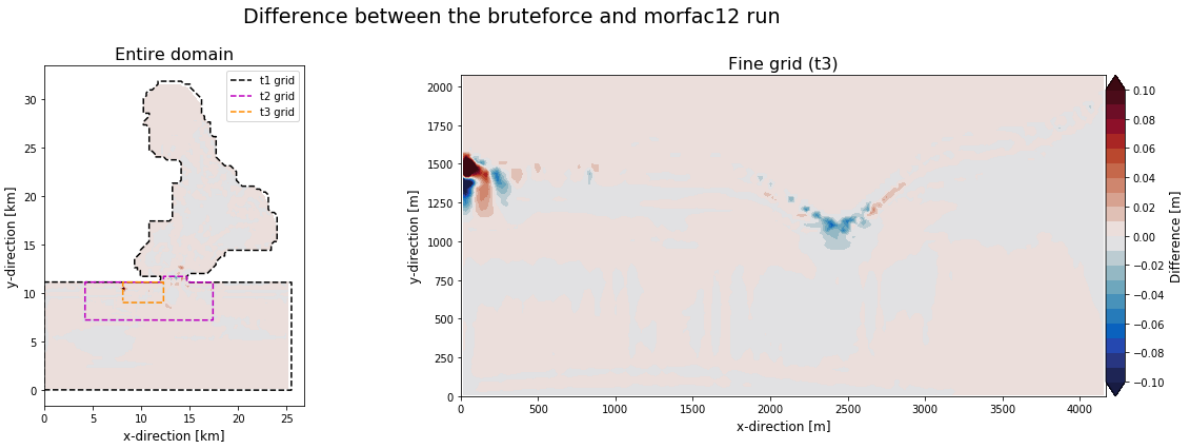

Figure 3.6: The difference in bed level after 1 year between brute force (morfac of 1) and a run with a morfac of 12 is depicted in both figures. The left figure shows the difference in the entire domain. The right figure shows the difference zoomed into the fine t3 grid. Simulation $Nour\_Run\_11$ is used as a basis for the brute force and morfac12 runs (table 3.2).

The model to validate the use of the morfac is run for one morphological year. The difference between the morfac12 and the brute force is very low (Figure 3.6). The highest difference on the left of the fine grid (t3 grid, see right figure) is about 0.10 meter. A commonly used measure to quantify the effectiveness of a morphodynamic model is to utilize the Brier Skill Score (Sutherland et al. [2004]). The Brier Skill Score (BSS) is given as:

$$BSS = 1 - \frac{\langle (Y - X)^2 \rangle}{\langle (B - X)^2 \rangle} \tag{3.1}$$

X Observation data (Brute Force)
Y Prediction data (Morfac 12)
B Baseline prediction data (Initial bathymetry)

A BSS score close to 1 yields a perfect prediction score and a BSS score close to 0 yields a poor prediction score. Filling in equation 3.1 yields a Brier Skill Score of 0.99. This score is very close to 1 and as a result the chosen morfac of 12 will be a good representation of the Brute Force simulation.

3.3. Model with real hydrodynamic forcing

The simplified simulations are highly schematized and set up using ideal hydrodynamic forcing. Therefore making use of time-varying hydrodynamic forcing, which can be found in real-life, can give insight into whether the system will behave similarly or completely differently. It has been hypothesized that the residual currents owing to the tidal inlet will have a large impact on the mega-nourishment (see the hypothesis in chapter 2.4). Moreover, the waves will also influence the diffusion of the sediment from the mega-nourishment. Therefore the time-varying hydrodynamic conditions found in nature will be by means of a realistic tide and a realistic wave time series.

3.3.1. Model setup

The models will be set up similarly as model 2 (described in chapter 3.1.2) and will be referred to as model 3. The only difference between model 2 and model 3 will be the water level for the first set of simulations and the wave time series for the second set of simulations.

For the first set of simulations (referred to as real tide), the water levels will be forced with the water levels found at Myrtle Beach, South Carolina, United States of America. The tidal range is about 1.3 meters (NOAA) which is close to the desired 1.5 meters used in model 2. The tidal constituents are obtained from the TPXO 7.2 Global Inverse Tide Model. TPXO is a series of fully-global models of ocean tides, which best-fits, in a least-squares sense, the Laplace Tidal Equations and altimetry data (Egbert et al. [2010]). The waves will be forced with a spatially uniform, stationary mild wave conditions (H_s = 1.0 m; T_p = 5s) as described in chapter 3.1.3. Therefore, the real tide conditions best represent the mild wave conditions of model 2.

The second set of simulations (referred to as real wave) has the same M2 tide as used in model 2 (as described in chapter 3.1.3). This will result in a tidal range of 1.5 meters. The waves in the second set of simulations will describe the waves found at Myrtle Beach, South Carolina, United States of America. The wave data is obtained from WaveWatch III (WW3). WW3 solves the random phase spectral action density balance equation for wavenumber-direction spectra (Tolman [2009]). The significant wave height time series is compressed with the same factor as the morfac of 12 (Li et al. [2018] cited in Luijendijk et al. [2019], without filtering). The compressed wave time series is taken uniform over the domain (Figure 3.7).

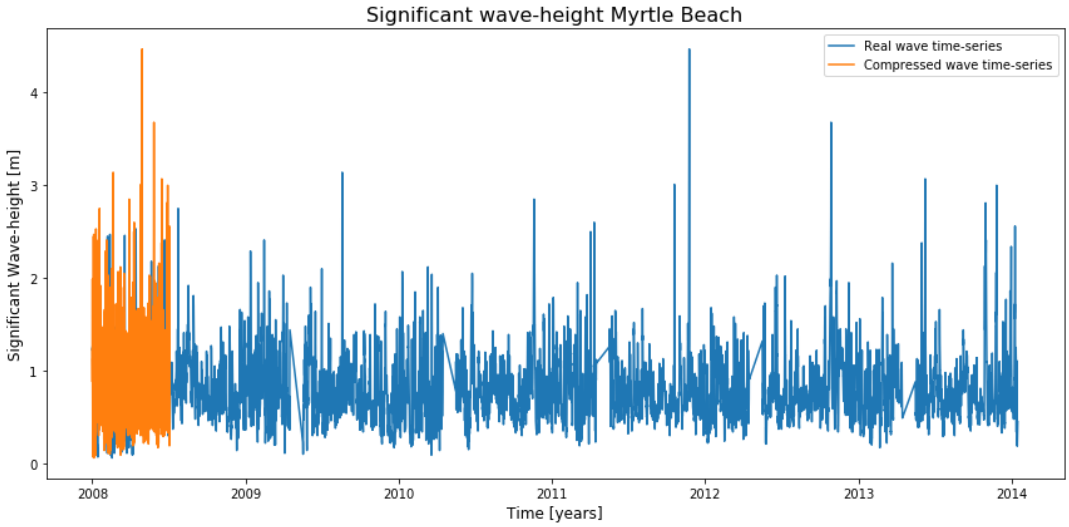

Figure 3.7: Time series of the significant wave height used in the realistic wave model. The blue line shows the uncompressed significant wave height time series as found in Myrtle Beach. The orange line shows the compressed significant wave height time series used in the hydrodynamics of the realistic model runs.

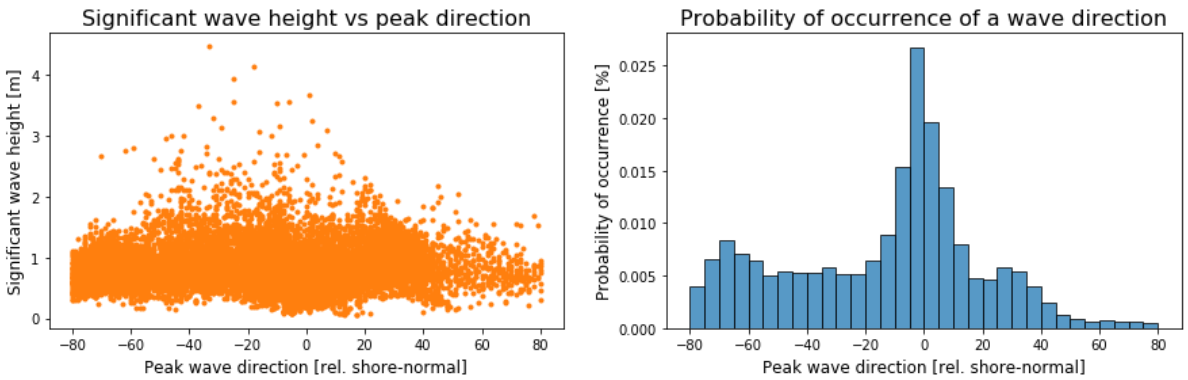

Figure 3.8: The left figure shows the significant wave height vs peak wave direction. Each dot represents one condition in the compressed wave data set used in the models. The right figure shows the probability of occurrence of a peak wave direction for the real waves.

The obtained wave data from Myrtle Beach is briefly analyzed to get insight in the overall characteristics of the wave climate (Figure 3.8). First, most of the waves come from -80 to 0 degrees relative to shore-normal (right figure in Figure 3.8). The average peak wave direction is about -15 degrees relative to shore normal. Furthermore, not only do most of the waves come from -80 to 0 degrees relative to shore normal, also the highest wave comes from this range (left figure in Figure 3.8). The averaged significant wave height for the compressed data set is 0.8 meters. Therefore, the real wave conditions (model 3) represent the hydrodynamic conditions of the mild wave conditions (model 2) best with a slightly oblique wave direction.

3.3.2. Scenarios of the model with real hydrodynamic forcing

The simulations of the realistic model runs are set up in the same way as in model 2 (Chapter 3.2.2). The simulations in model 3 will have different unique ID's. Namely, simulations with the ID $Real\_Run\_5x$ represent the simulations of model 3 with a real tidal range (referred to as real tide) found at Myrtle Beach (where x varies from 1 to 4). The simulations with the ID $Real\_Run\_6x$ represent simulations with a real wave time series found at Myrtle Beach (referred to as real wave).

Table 3.3: All simulations of model 3 using real hydrodynamic conditions. Where the variable parameters are **1.** Significant Wave height (Hs) **2.** Peak wave direction relative to shore-normal (Dp) **3.** Tidal range (η) **4.** The distance of the centroid of the mega-feeder nourishment to the tip of the barrier island (Dist.). **5.** Indication of whether the tidal inlet is closed or open. At last each simulation has been given a unique ID (Run ID) which will be referred to throughout the thesis.

Run ID	Hs [m]	Dp [Dir]	η [m]	Dist. [km]	Inlet
Real_Run_5.1	1.0	0	Variable	2.0	Open
Real_Run_5.2	1.0	0	Variable	5.0	Open
Real_Run_5.3	1.0	0	Variable	2.0	Closed
Real_Run_5.4	1.0	0	Variable	5.0	Closed
Real_Run_6.1	Variable	Variable	1.5	2.0	Open
Real_Run_6.2	Variable	Variable	1.5	5.0	Open
Real_Run_6.3	Variable	Variable	1.5	2.0	Closed
Real_Run_6.4	Variable	Variable	1.5	5.0	Closed

3.4. Post-processing methodology

The data of the simulations must be processed to obtain valuable information, which can be used to answer the sub-questions and consequently the research question.

3.4.1. Residual currents

It has been hypothesized that a net residual current, owing to gyres, is an important process nearby a tidal inlet (chapter 2.4). Therefore, it is also important to show that residual currents owing to the tidal flow are in fact present in the domain. The residual currents can be obtained by averaging the currents over one or multiple tidal cycles. The current output of the simulations are discrete and have an output frequency of once every 3 hours. Therefore, at least 7 tidal cycles are required to create a closed tidal cycle as the M2 tide has a period of 11 hours and 25 minutes. Furthermore, by taking 7 tidal cycles errors owing to the output being discrete are mitigated. Moreover, no significant bathymetry changes occur during the first 7 tidal cycles.

Owing to the way the models have been setup, the residual currents will have different contributions. With an open tidal inlet, the residual currents include currents owing to the tidal flow and alongshore currents owing to the waves. With an closed tidal inlet the residual currents will only include the alongshore currents owing to waves. The residual currents vectors of the tidal inlet being open are subtracted from the tidal inlet being closed. By doing so, the residual currents owing to the tidal flow generated by the tidal inlet is shown and the alongshore currents owing to the waves are mostly filtered out. The filtered residual currents owing to the tidal flow will be referred to as **RTF currents**. The RTF currents are a combination of RTF currents owing to the tidal flow, wave-current interactions and changed waves due to a change in the bathymetry between the simulation with the tidal inlet being open and closed.

3.4.2. Total alongshore sediment transport

The first goal is to analyze the total alongshore sediment transport (referred to as TAST) along multiple cross-sections at and near the mega-feeder nourishment. This method will give insight in the alongshore varying total sediment transport. The hypothesis (see chapter 2.4) is that the residual currents owing to the tidal inlet will increase the TAST towards the tidal inlet. Therefore, one would expect an increase in TAST with the tidal inlet being open and the mega-nourishment closest to the tidal inlet, compared to a closed inlet. The TAST owing to the tidal currents over the ebb-tidal delta must be filtered out of the cross-sections as this sediment is not necessarily from the mega-nourishment. Therefore, the cross-sections are taken from the shore to a depth contour (Figure 3.9). This depth contour is where most of the TAST takes place. A depth-contour of -4.0 m below MSL will allow for only the effects of the residual currents to be included, whereas the effects of the TAST owing to the ebb-tidal delta is excluded (see Figure 3.9).

Along every cross-section, the total sediment transport vector components (tt_x is the total sediment transport component in the alongshore(x) direction and tt_y is the total sediment transport component in the cross-shore(y) direction) are first integrated over time. This will give a vector field with the total sediment transport over 6 years (see Figure 3.9). After which, the total transport vector components are integrated over the cross-section (the active depth, red line in Figure 3.9 to most shore-wards grid point in the y-direction). At last, the magnitude of the total sediment transport vector integrated over time and the cross-section is taken. This will result in an alongshore varying total sediment transport (equation 3.2), referred to as the total alongshore sediment transport (TAST) in $m^3/6y/m$.

$$tt = \sqrt{\left(\int_{shore}^{depth-contour}\left(\int_{0}^{6years} tt_x dt\right)dy\right)^2 + \left(\int_{shore}^{depth-contour}\left(\int_{0}^{6years} tt_y dt\right)dy\right)^2} \qquad (3.2)$$

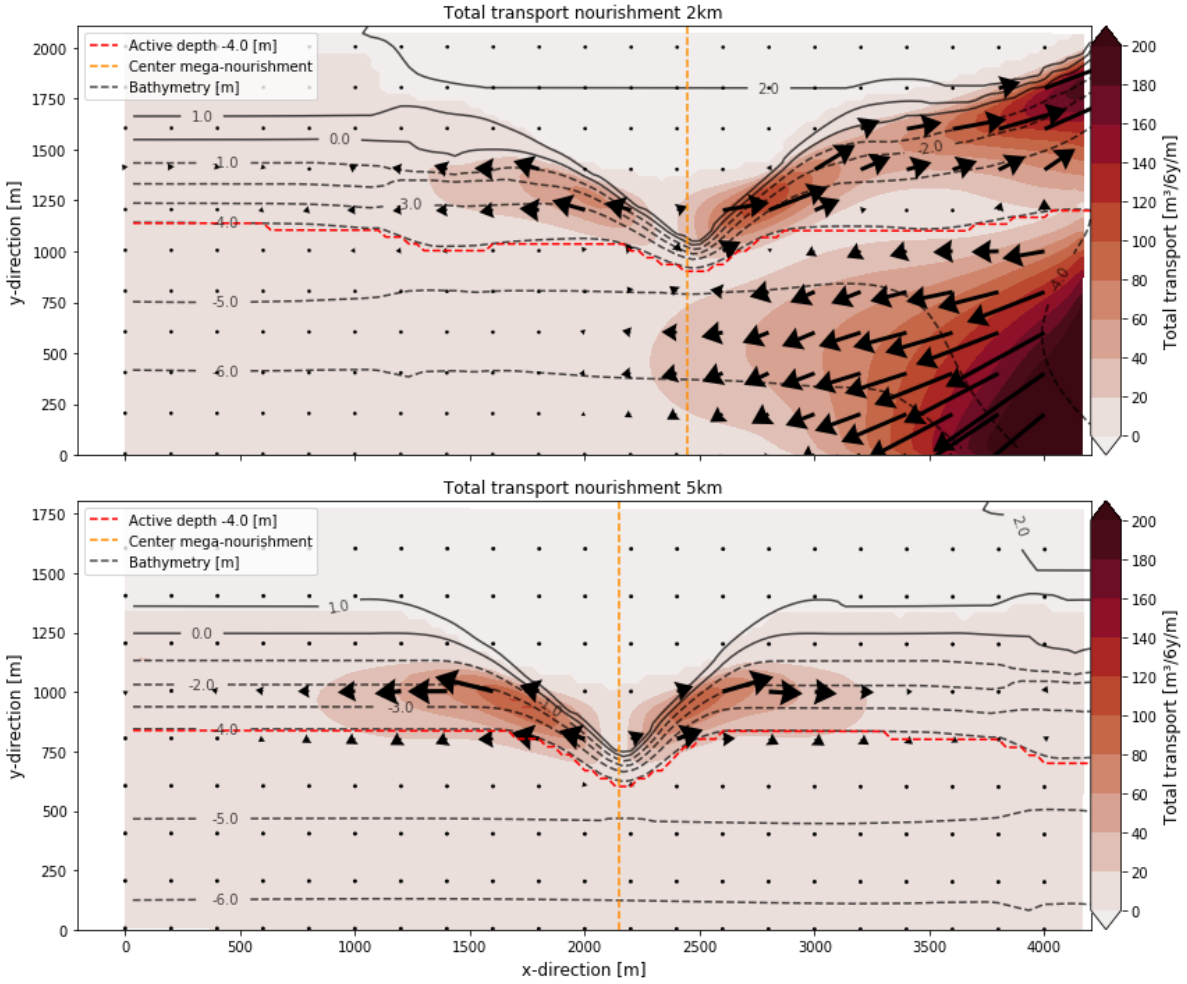

Figure 3.9: Methodology to derive the total sediment transport estimates. The total sediment transport is taken from the shore to the active depth (red dashed line). The top figure includes the initial bathymetry with the mega-nourishment 2km from the tidal inlet. The colors indicate the 6 year integrated total sediment transport from $Nour\_Run\_41$ (see table 3.2). The active depth is represented with a red dashed line and has a depth of -4.0 meter. The bottom figure includes the initial bathymetry with the mega-nourishment 5km from the tidal inlet and the 6 year integrated total transport from $Nour\_Run\_12$ (see table 3.2). The arrows in both figures represent the magnitude and direction of the total sediment transport integrated over 6 years.

The TAST will be compared with an open tidal inlet and a closed tidal inlet. By comparing the TAST a measure can be given to how much sediment has been transported through each cross-section in the alongshore direction over the duration of the simulation. If a tidal inlet being open, will result in higher sediment transport at a given cross-section compared to with the tidal inlet being closed, then this will indicate whether the development of a mega-feeder nourishment is influenced by the tidal inlet. Therefore, the absolute difference between the TAST with an open tidal inlet and closed tidal inlet (referred to as **RTF TAST**) will quantify the effect the tidal inlet flow has on the development of the mega-feeder nourishment.

The influence (reach) of the tidal inlet will be defined as the distance where the RTF TAST is more than 50 $m^3/6y/m$ from the tip of the barrier island (start of the tidal inlet). This threshold will make sure that most of the noise is not included in the quantification of the reach of the tidal inlet. However, when noise does exceed this threshold value, the distance is chosen based on the trend of the the RTF TAST line.

3.4.3. Development of the mega-nourishment over time

The second goal is to analyze the change in the shoreline over time. The 0-meter depth contour is used to analyze how the mega-nourishment and the adjacent coast develop over time. The 0-meter depth contour at any given time is compared to the initial 0-meter depth contour at time t=0. As a result, the distance the mega-nourishment and adjacent shoreline has gained (accretion) or retreated (eroded) at any given time is visualized. A time-stack of this distance is made to give insight into where most shoreline is gained or lost and how these accretion or erosion patterns develop over time.

Terminology used in the figures

The results will make use of certain words (terms) to describe a given location in the figures used in primarily the results. The approximate locations of these terms are shown in Figure 3.10. The exact location of these terms may vary slightly per simulation.

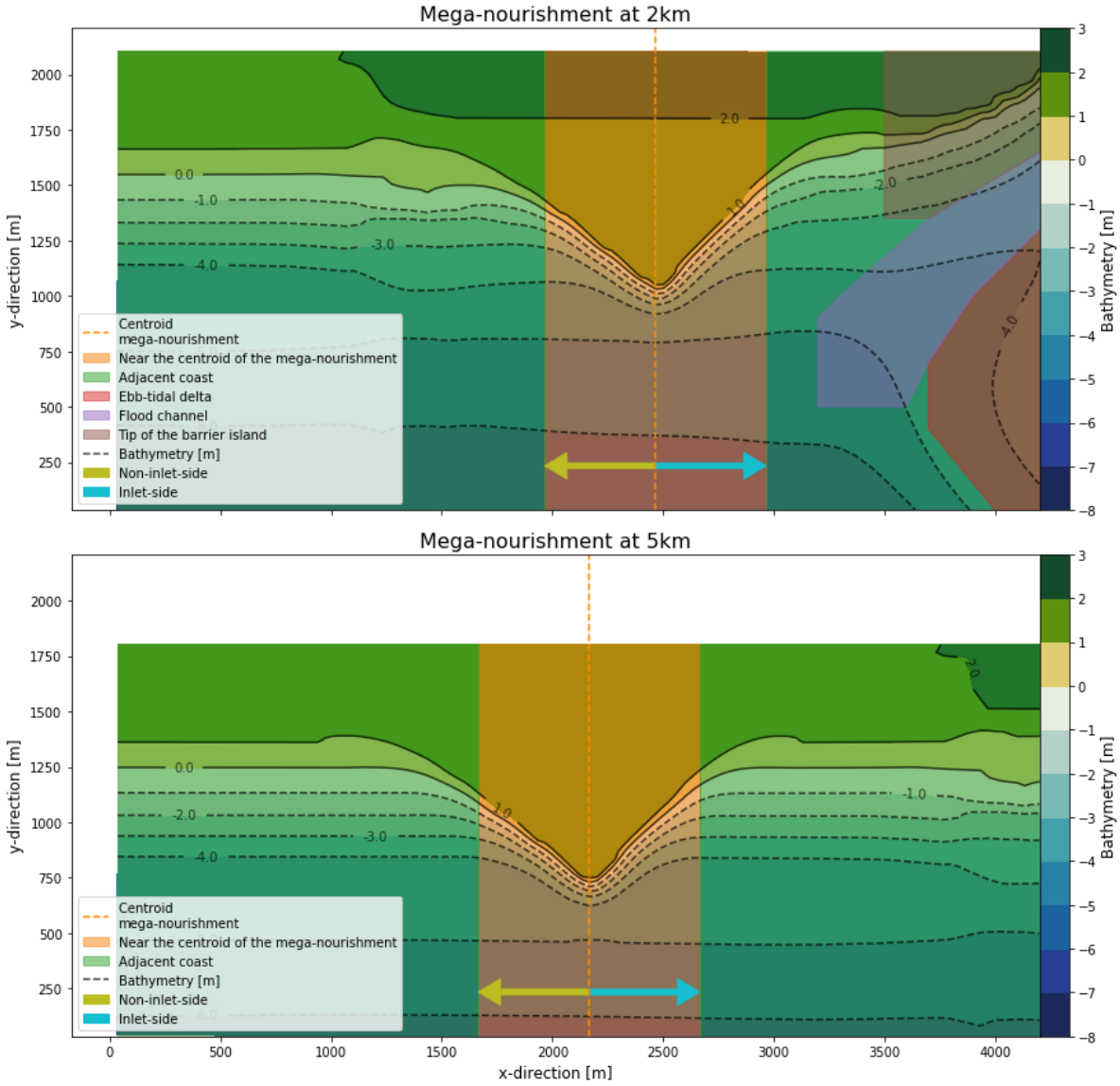

Figure 3.10: Approximate location of the terminology used in this thesis. The top figure shows the bathymetry and terms used with the mega-nourishment at a distance of 2km from the tidal inlet. The bottom figure shows the bathymetry and terms used with the mega-nourishment at a distance of 5km from the tidal inlet. The bathymetry shown is the initial bathymetry of the nourishment and realistic model runs.

3.5. Hydrodynamic validation

The hydrodynamic forcing should be roughly correct. The forcing at the boundary will generate currents in the model domain. These currents are the main driver behind sediment transport. Therefore, if the hydrodynamic forcing is correct then the morphology will roughly follow the correct patterns.

The hydrodynamics of the model are validated by creating a model that represents the simplified model well. The parameters related to the hydrodynamics are kept the same for the simplified models as well as for the models used to validate these models. First the tidal interaction with the tidal basin and ebb-tidal delta is validated by comparing a model, with observed data (see Appendix A). This is achieved by modelling Grand Isle, Louisiana, USA. Grand Isle is a barrier island located in the Mississippi delta and has a complex tidal system. The currents and water levels were measured in the tidal inlet in 2005 [Hartman Engineering, 2007]. Furthermore, the waves, water levels and currents at a relatively straight coast are validated by comparing a model with observed data at Myrtle Beach, South Carolina, USA (see Appendix A).

The modelled water level and currents at Grand Isle are almost identical to the observed ones (Figure 3.11). The r-squared values for the water level and current magnitude between the modelled and observed values are 0.83 and 0.80 respectively, which is close to one. Furthermore, the waves, water levels and currents also have the right order of magnitude at Myrtle Beach (see Appendix A). Therefore, the hydrodynamics of the simplified models are validated by means of the hydrodynamical models used in Appendix A.

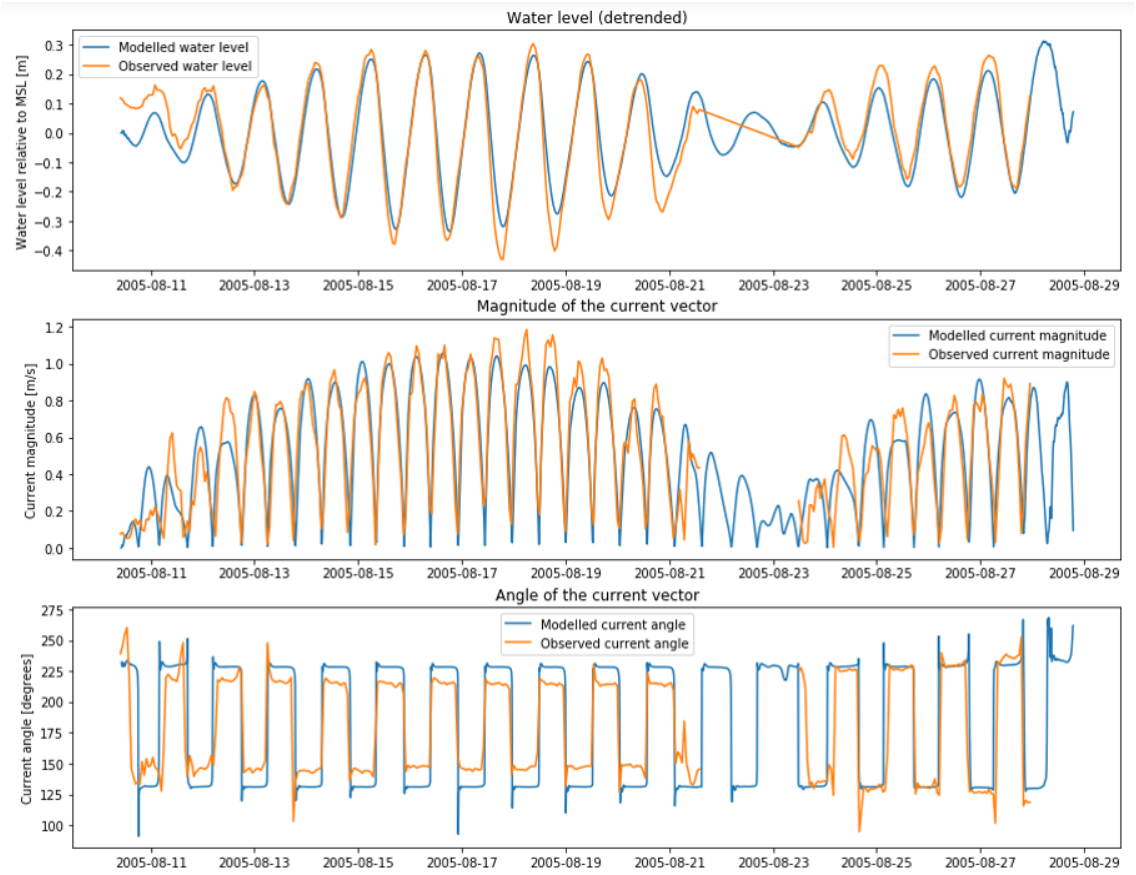

Figure 3.11: Modelled and observed hydrodynamics at Grand Isle, Louisiana, USA. The modelled currents are depicted in blue and the observed currents (Hartman Engineering [2007]) are shown in orange. The top figure shows the water levels compared to MSL. The middle figure shows the magnitude of the currents vector and the bottom figure shows the direction angle of the current vector relative to North.

4

Model results

In the previous chapter the model setup as well as the methods of post processing have been described in detail. This chapter will show the results of the models using the described methodology to process the data. First it is briefly shown that using real time-varying hydrodynamic conditions (model 3), represent the simpler non time-varying hydrodynamics well (model 2). Thereafter, the results using simpler hydrodynamic conditions are presented.

4.1. Real hydrodynamic conditions

Using real hydrodynamic conditions represent the hydrodynamics and morphodynamics of model 2 well. The hydrodynamic forcing used in this thesis is a simplified forcing compared to reality (chapter 3.3). Simplifying the wave and tide forcing might result in a completely different behavior of the tidal inlet system and the mega-feeder nourishment. The results of using real tidal constituents and a real time-varying wave series are consistent with the representative simplified hydrodynamic forcing (the mild wave conditions, which is described in detail in appendix B). Therefore, the decision is made to stick with the simplified hydrodynamic conditions to better explain the results.

4.2. Residual currents

It has been hypothesized that residual currents owing to the tidal flow in the tidal inlet (RTF currents) will cause a net transport of sediment towards the tidal inlet (see chapter 2.4). Therefore, it is important to examine if RTF currents do exist. However, first the contribution of the waves in the RTF currents is investigated to examine their effects on the RTF currents. This is done by investigating whether wave characteristics, such as the significant wave height, wave peak period and wave peak direction change between the tidal inlet being open and closed.

Importance of the wave-current interactions

There is a small wave-current interaction. This will not impact the RTF currents during the first 7 tidal cycles. The RTF currents will have other processes contributing to this flow which are not entirely created by only the tidal flow owing to the tidal inlet or which are artifacts generated by using the method as described in chapter 3.4.1. In the RTF current flow field, there might be flows owing to wave-current interactions and owing to the method used. The wave-current interaction will decrease or increase the significant wave height, wavelength and/or the wave direction (Appendix C shows the change in significant wave height, wavelength and peak wave direction, between the tidal inlet being open and closed, for all simulations). The change in any wave parameter during the first 7 tidal cycles describe

the wave-current interactions, as the bathymetry has not changed much in this time-span. The change over the entire simulation is a combination of wave-current interactions and differences in the bathymetry. In the relative change (second row in the Figures in Appendix C), the large changes at the beach are ought to be ignored as the values of the significant wave height and wavelength are small in general. Thus increasing the relative change without any significant meaning.

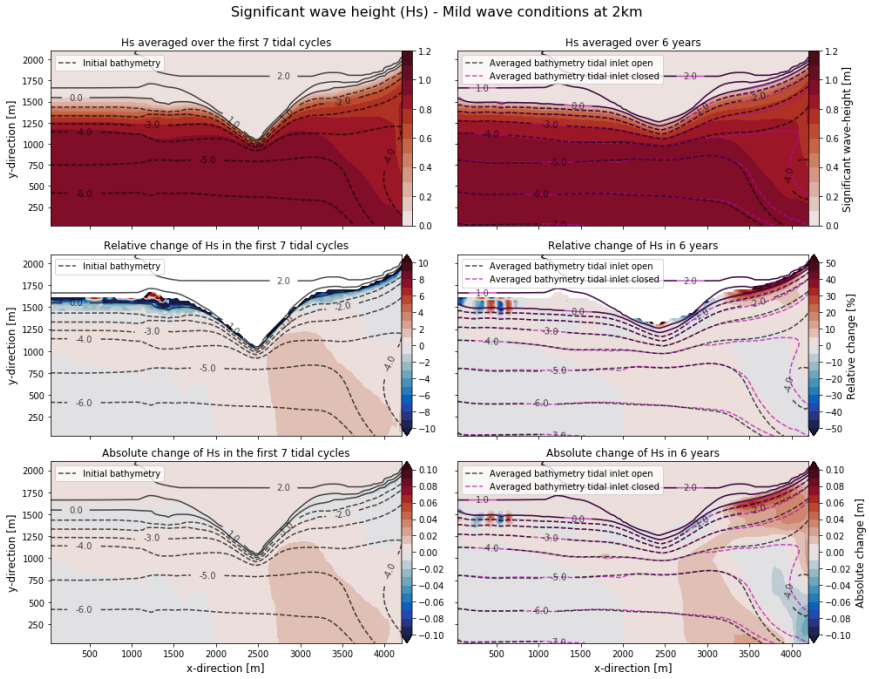

Figure 4.1: Significant wave height (hs) for the mild wave conditions at 2km from the tidal inlet. The first column shows the significant wave height averaged over the first 7 tidal cycles and the second column shows the hs averaged over 6 years. The first row shows the averaged hs, the second row shows the relative difference in hs between the tidal inlet being open and closed. The third row shows the absolute difference in hs between the tidal inlet being open and closed.

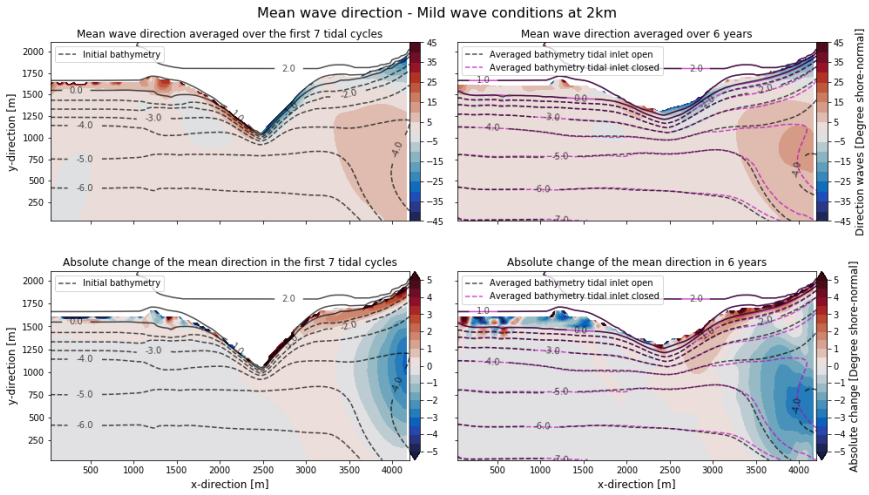

Figure 4.2: Peak wave direction for the mild wave conditions at 2km from the tidal inlet. The first column shows the peak wave direction averaged over the first 7 tidal cycles and the second column shows the peak wave direction averaged over 6 years. The first row shows the averaged peak wave direction and the third row shows the absolute difference in the peak wave direction between the tidal inlet being open and closed.

Waves do not change much owing to wave-current interactions for the mild wave conditions

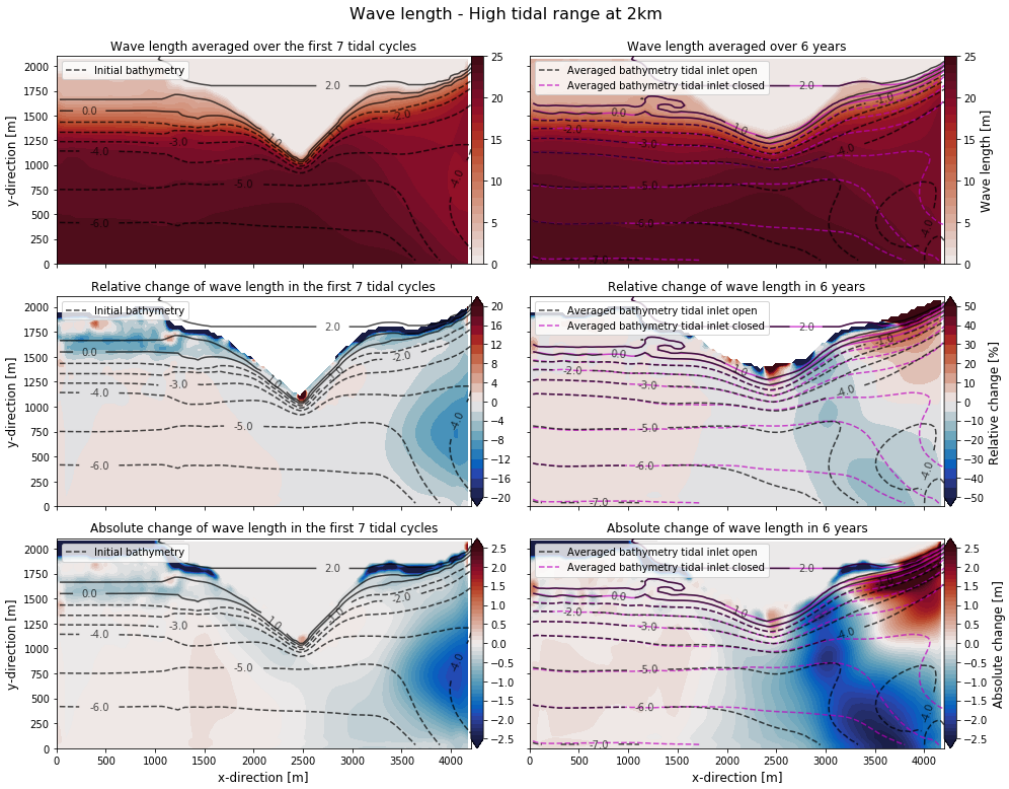

Figure 4.3: Wavelength for the high tidal range at 2km from the tidal inlet. The first column shows the wavelength averaged over the first 7 tidal cycles and the second column shows the wavelength averaged over 6 years. The first row shows the averaged wavelength, the second row shows the relative difference in the wavelength between the tidal inlet being open and closed. The third row shows the absolute difference in the wavelength between the tidal inlet being open and closed.

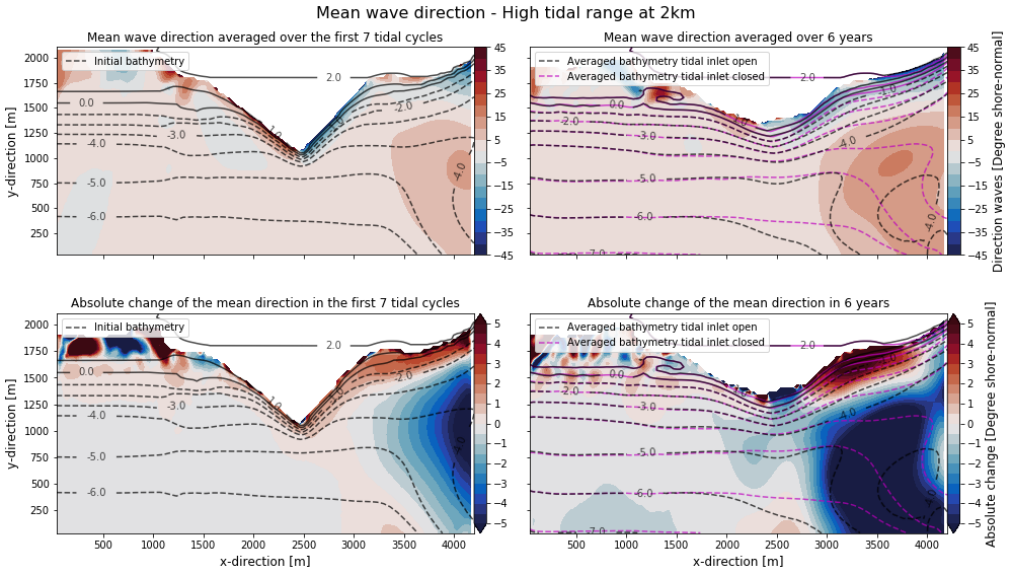

Figure 4.4: Peak wave direction for the high tidal range at 2km from the tidal inlet. The first column shows the peak wave direction averaged over the first 7 tidal cycles and the second column shows the peak wave direction averaged over 6 years. The first row shows the averaged peak wave direction and the third row shows the absolute difference in the peak wave direction between the tidal inlet being open and closed.

during the first 7 tidal cycles (left column in Figures 4.1 and 4.2). The significant wave height does not change by more than 2% in the domain. In general, it can be seen that for none of the simulations the significant wave height changes by more than 3% (Appendix C). The wavelength does not change by more than 5% in the t3 domain, with the largest values found over the ebb-tidal delta. However, the wavelength does increase by about 10% over the ebb-tidal delta for the high tidal range simulation (center right figure in Figure 4.3). The mean direction of the waves may differ by up to 3.5 degrees anti-clockwise at the ebb-tidal delta and clockwise near the shore to the inlet-side of the mega-nourishment (bottom right figure in Figure 4.2). For the high tidal range, the mean wave direction differs by slightly over 5 degrees (Figure 4.4). To summarize, there is a small wave-current interaction. This wave-current interaction will most likely not impact the RTF currents.

Importance of the difference in the bathymetry between tidal inlet being open and closed

The waves do change averaged over the entire simulation as a result of the difference in the bathymetry, between the simulations where the tidal inlet is open and closed. The difference in wave height and wavelength are higher averaged over 6 years than over 7 tidal cycles (right column in Figures 4.1 and 4.3, and in Appendix C). This change is for all wave parameters most noticeable near the tidal inlet (last column in the figures in appendix C). The change is also largest for the high tidal range. A large tidal range increases the RTF currents (high tidal range in Figure 4.6) over the ebb-tidal delta and at the tips of the barrier islands. This increases the size of the ebb-tidal delta relative to the tidal inlet being closed (chapter 2.1.1). The increased size of the ebb-tidal delta will, in general, reduce the wave height and wavelength over the ebb-tidal delta. The location of the shoal (-4.0 m depth contour in the ebb-tidal delta) is different for the tidal inlet being open and closed. The ebb-tidal delta is larger for the tidal inlet being open which results in the shoal being located further away from the tidal inlet than for the tidal inlet being closed. The location of the shoal will lower the significant wave height and wavelength over it but increase the significant wave height and wavelength next to it, all the way up to the shore (right column in Figure 4.3).

Residual currents

The tide averaged flow in the simulations mainly consists of two parts, namely the flow generated by waves which are predominantly alongshore currents, and flow generated by the tidal inlet (Figure 4.5 and Figure 4.6). The flow generated by the tidal inlet is referred to as RTF currents, where closed tidal inlet simulations will not include RTF currents and an open tidal inlet does include RTF currents. Therefore, the contribution of the wave generated alongshore flow is filtered out by subtracting the tide averaged flow field of the closed tidal inlet simulation (center column in Figures 4.5 and 4.6) from that of the open tidal inlet (left column in Figures 4.5 and 4.6). Effectively resulting in the flow (RTF currents) owing to the tidal inlet (right column in Figures 4.5 and 4.6).

Overall, there is a tide averaged current at the tip of the barrier island in all simulations (Figures 4.5 and 4.6). The tidal currents have high magnitudes (order of several meters per second) at the center of the tidal inlet. The tidal current cannot spread out fast enough owing to the momentum of the tidal current (chapter 2.2). This generates a flow towards the tidal inlet at the adjacent barrier island tips. However, it can be seen that there is a flow towards the location of the tidal inlet with the tidal inlet being closed too. This suggests that the tide averaged currents with the tidal inlet being closed, are generated by waves. Owing to the orientation of the shore with respect to the waves an alongshore flow is generated at the tips of the barrier islands.

In all hydrodynamic conditions, the RTF currents are directed towards the tidal inlet at the tips of the barrier island (right column in Figures 4.5 and 4.6). There also is a flow from the center of the tidal inlet spreading outwards into the ocean. This flow does not reach the mega-nourishment and is therefore not of interest in the analysis.

The magnitude of the RTF currents seems to diminish fairly quickly (order several hundreds of meters to a few kilometers) from the tidal inlet towards the mega-nourishment. In general, the RTF current owing to the tidal inlet does reach the centroid of the mega-nourishment at 2km from the tidal inlet. However, it does not reach further than the centroid of the mega-nourishment. One exception is the RTF currents for the high tidal range, which does reach further than the mega-nourishment at 2km from the tidal inlet, which is about 3km from the tidal inlet (Figure 4.6). There is no difference in the flow field between an open and closed tidal inlet, with the mega-nourishment at an alongshore distance of 5km from the tidal inlet.

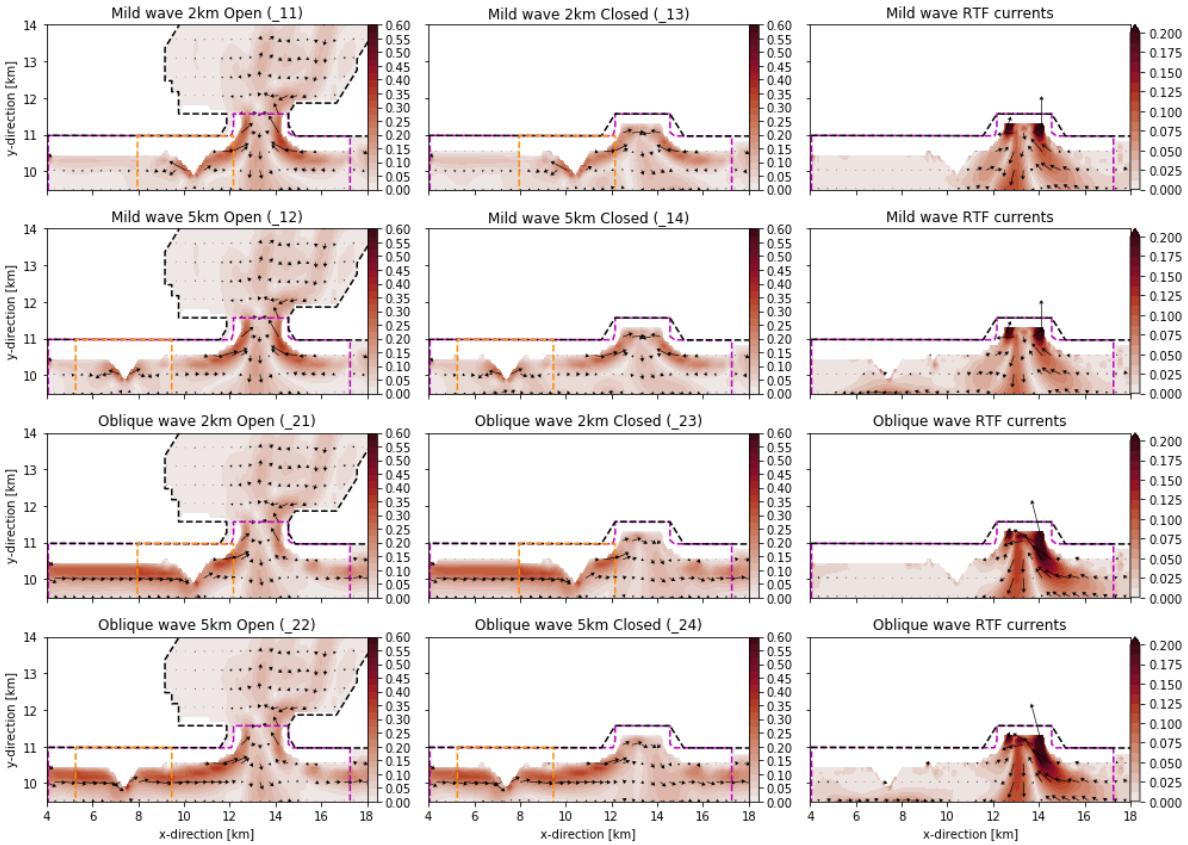

Figure 4.5: Tide averaged and RTF currents in m/s for shore-normal mild wave conditions and oblique wave conditions (see Table 3.2). The rows are alternating with the mega-nourishment at an alongshore distance of 2 kilometers and 5 kilometers from the mega-nourishment. The left column shows the tide averaged currents with an open tidal inlet. The center column shows the tide averaged currents with the tidal inlet being closed and the right column shows the difference in the tide averaged currents between the tidal inlet being open and closed. The latter are the residual currents owing to the tidal inlet (RTF currents).

The alongshore directed tide-averaged flow is blocked by the mega-nourishment for the oblique wave conditions (see Figure 4.5). This effect is owing to the wave shadowing (see Figure C.2 in appendix C for the significant wave height of the oblique wave conditions simulation) caused by the mega-nourishment. The wave shadowing in the tidal inlet becomes noticeable when analyzing simulation _21. The currents are weaker than compared to the mild conditions (simulation _11), emphasizing the effect of wave shadowing. Furthermore, the RTF currents do not reach as far (about 800 meters) compared to the mild wave conditions.

The tide-averaged flow for the storm wave conditions show similar behavior compared to the mild wave conditions. There is no storm during the first 7 tidal cycles of the simulations (Figure 3.4). Therefore, the forcing is similar to that of the mild wave conditions. As a result, the flow patterns are the same as for the mild wave conditions during the first 7 tidal cycles.

The high tidal range with an open tidal inlet (_41 and _43) increased the tide averaged currents significantly (see first column in Figure 4.6). On the contrary, the closed tidal inlet (_42 and

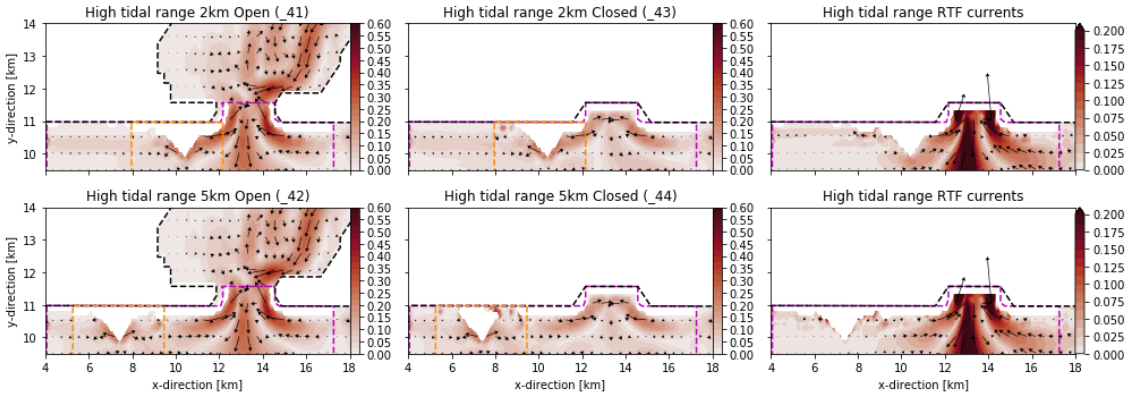

Figure 4.6: Tide averaged and RTF currents in m/s for the high tidal range (see Table 3.2). The rows are alternating with the mega-nourishment at an alongshore distance of 2 kilometers and 5 kilometers from the mega-nourishment. The left column shows the tide averaged currents with an open tidal inlet. The center column shows the tide averaged currents with the tidal inlet being closed and the right column shows the difference in the tide averaged currents between the tidal inlet being open and closed. The latter are the residual currents owing to the tidal inlet (RTF currents).

_44 in Figure 4.6) shows a somewhat similar behavior as the closed tidal inlet for the mild wave conditions (_12 and _14 in Figure 4.5). As a result, the RTF currents (right column in Figure 4.6) owing to the tidal inlet have increased significantly. The RTF currents do reach further than the centroid of the mega-nourishment and are directed towards the tidal inlet.

4.3. Total alongshore sediment transport

As discussed in the methodology, only the transport owing to the mega-nourishment and the tidal inlet is of interest. Therefore the transport as a result of the ebb-tidal delta is discarded. Moreover, the results are shown inside the t3 grid only. The mild wave conditions simulations act as the basis for all other simulations. Similarities between the mild wave conditions and the other hydrodynamic conditions are presented in the mild wave conditions and are referred to as in general. The differences between the mild wave conditions and the other hydrodynamic conditions are individually addressed per hydrodynamic condition. Detailed figures and explanations for all simulations are given in Appendix D.

Mild wave conditions

The influence of the tidal inlet does not reach the mega-nourishment located at an alongshore distance of 5km from the tidal inlet for all hydrodynamic conditions. The total alongshore sediment transport (TAST) for the tidal inlet being open and closed are similar (Figure 4.7). As a result, the absolute difference in TAST between the tidal inlet being open and closed is zero (referred to as RTF TAST). This suggests that the flows owing to the tidal inlet does not reach up to the mega-nourishment located at 5km from the tidal inlet, which is also shown in chapter 4.2.

Furthermore, the wave angle relative to the shoreline orientation is an important process in the magnitude of the TAST with the mega-nourishment at an alongshore distance of 5km from the tidal inlet. For all simulations, with the mega-nourishment at 5km from the tidal inlet, the TAST line follows the shoreline orientation line (Figure 4.7). The largest TAST is located where there is a maximum in the absolute shoreline orientation (right column in Figure 4.7). Moreover, for all simulations, except for the oblique wave conditions, the TAST approaches zero towards the boundary of the t3 grid (Appendix D). This is also consistent with the orientation of the shoreline, which slowly reduces to zero. For the oblique wave angle simulation, the wave angle is -45 degrees relative to shore-normal. This means that the TAST is already maximum with a zero degrees shoreline orientation when the wave angle

is -45 degrees. Consequently, the wave angle relative to the orientation of the shoreline (incident wave angle) is the governing process with the mega-nourishment at an alongshore distance of 5km from the tidal inlet and the currents owing to the tidal inlet have no impact in the sediment transport.

The incident wave angle is also an important process for the mild wave conditions with the mega-nourishment at an alongshore distance of 2km from the tidal inlet. The TAST is not symmetrical around the mega-nourishment (Figure 4.7). Towards the non-inlet-side, the TAST first increases in magnitude after which it gradually reduces towards a zero TAST. Again the TAST line follows the orientation of the shoreline (Figure 4.7). The non-inlet-side has a similar shape and magnitude as the TAST found with the mega-nourishment at 5km from the tidal inlet. However, there is a difference in the TAST towards the inlet-side. The TAST first increases towards a local maximum, after which it gradually decreases and then increases towards a maximum TAST at the boundary of the t3 grid. Contrary to the mega-nourishment at an alongshore distance of 5km from the tidal inlet, the shoreline orientation, with the mega-nourishment at a distance of 2km from the tidal inlet, does not approach zero. Instead, the shoreline orientation increases towards the tidal inlet. As a result, the TAST also increases. Therefore, the TAST follows the shoreline orientation.

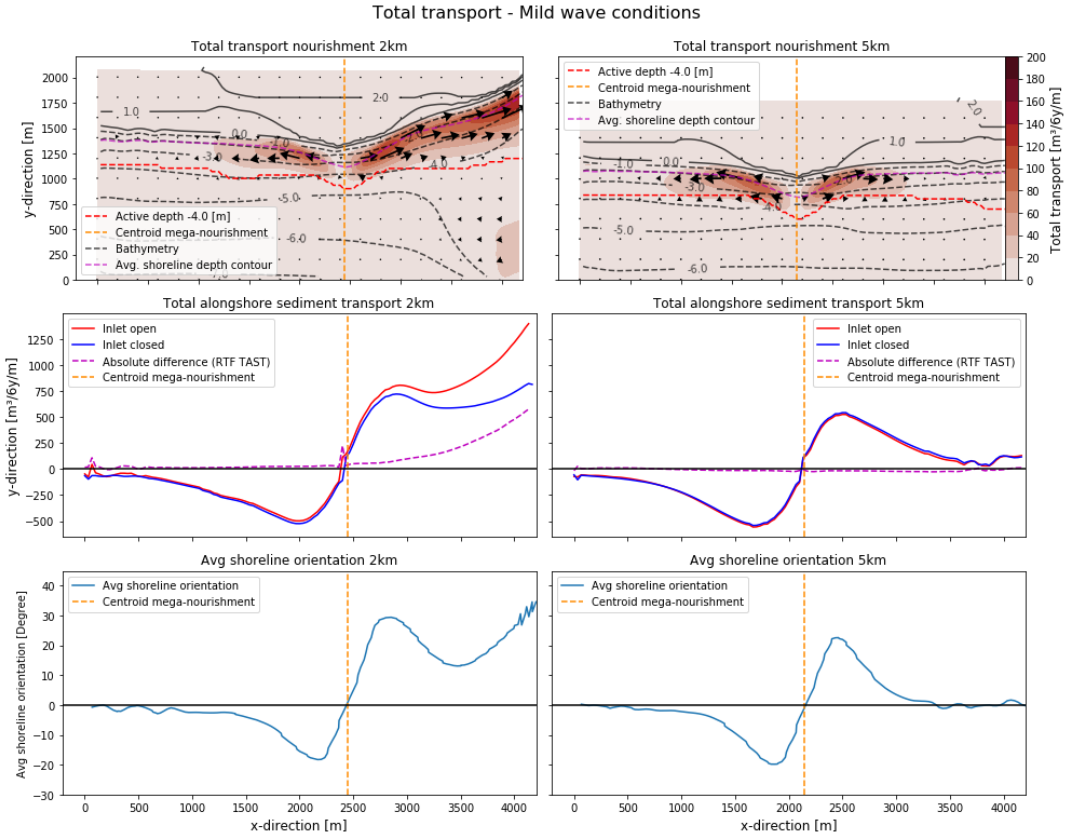

Figure 4.7: Total alongshore sediment transport mild wave conditions over 6 years. The top, center and bottom row show the total sediment transport, total alongshore sediment transport (TAST) and average shoreline orientation respectively. The left and right column shows this for the mega-nourishment at 2km and 5km from the tidal inlet. The centroid of the mega-nourishment at t=0 is shown with the orange dashed line, where the inlet side is to the right of this line and the non-inlet side is to the left of this line. The red and blue lines in the center row figures show the TAST for the tidal inlet being open and closed. The purple dashed line shows the absolute difference between the former and latter.

The RTF TAST increases in magnitude towards the tidal inlet for all simulations with the mega-nourishment at an alongshore distance of 2km from the tidal inlet at the inlet-side. The maximum RTF TAST for the mild wave conditions is about 580 $m^3/6y/m$. This does not

reach further than 2200 meter from the tidal inlet for the mild wave conditions, which is the same location as the centroid of the mega-nourishment. The RTF TAST increases towards the tidal inlet (Figure 4.7) as the RTF currents increase towards the tidal inlet as well (Figure 4.5).

Oblique waves conditions

The TAST for the oblique wave conditions, on average, is much higher than for the mild wave conditions. The wave angle is -45 degrees relative to shore-normal. This will result in an average TAST along the non-perturbed shore to be non-zero. In fact, the TAST is almost maximum at the boundary at the non-inlet-side with an average TAST of about 1200 $m^3/6y/m$. Whereas, for the mild wave conditions, the TAST at the non-inlet-side boundary was zero (Figure 4.7). This further emphasizes that the wave angle relative to the shoreline orientation is an important process (incident wave angle). The $s-\phi$,curve dictates that the maximum transport takes place with a wave angle of 45 degrees relative to shore-normal (chapter 2.2). The wave angle for the oblique wave conditions is 45 degrees. Hence, the TAST is maximum near the boundary where the incident wave angle is also about 45 degrees. The TAST on the non-inlet-side first decreases after which it increases again. This is owing to the incident wave angle decreasing and then also increasing. The same applies to the inlet-side for the tidal inlet being closed.

For the oblique wave conditions, the magnitude and reach of the RTF TAST is smaller than for the mild wave conditions. The magnitude of the RTF TAST as a result of the RTF currents is about 370 $m^3/6y/m$. This is lower than for the mild wave conditions which is about 580 $m^3/6y/m$. Moreover, the influence owing to the tidal inlet diminishes faster (1070 meters) than compared to the mild wave conditions (2200 meters). This is also consistent with the reduction in RTF currents as seen in Figure 4.5. The maximum RTF TAST is 370 $m^3/6y/m$, which is lower than the maximum RTF TAST (580 $m^3/6y/m$) of the mild wave conditions. The RTF TAST for the oblique wave conditions also slowly increases towards the tidal inlet. Consequently, the most important processes for oblique wave conditions are the incident wave angle and RTF currents.

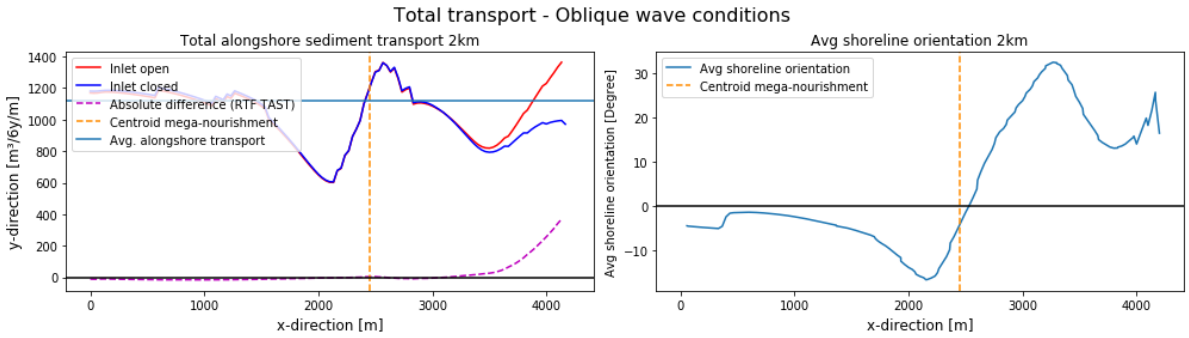

Figure 4.8: Total alongshore sediment transport oblique wave conditions over 6 years with the mega-nourishment at 2km from the tidal inlet. The left figure shows the TAST for the tidal inlet being open (blue), closed (red) and the RTF TAST (purple). The right figure shows the average shoreline orientation.

Storm wave conditions

The occurrence of storms increases the magnitude of the TAST for both the tidal inlet being open and closed (Figure 4.9). Similarly to the mild wave conditions (Figure 4.7), the TAST is not symmetric around the centroid of the mega-nourishment. At the non-inlet-side, the TAST first increases in magnitude after which it gradually decreases towards a zero TAST. At the inlet-side, the TAST first increases towards a local maximum after which it gradually decreases and then increases towards a maximum TAST at the boundary of the t3 grid, again following the shoreline orientation. The TAST is proportional to the significant wave height

to the power 2.5 ($H_s^{2.5}$) (chapter 2.2). This means that during storm conditions the TAST is significantly higher. Therefore, the TAST for the tidal inlet being open and closed has increased over the entire domain.

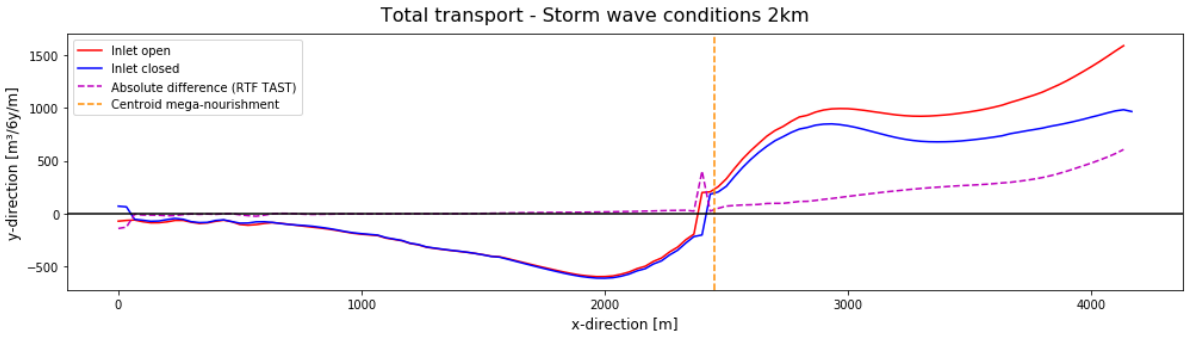

Figure 4.9: Total alongshore sediment transport storm wave conditions over 6 years with the mega-nourishment at 2km from the tidal inlet, in which the TAST for the tidal inlet being open (blue), closed (red) and the RTF TAST (purple) are shown.

The RTF TAST, however, remained virtually unchanged compared to the mild wave conditions. The reach (2200 meters), as well as the magnitude of the RTF TAST (600 m³/6y/m), is similar for both the storm and mild wave conditions. Moreover, the RTF TAST increases towards the tidal inlet as the RTF currents also increases towards the tidal inlet (see Figure 4.6)

High tidal range

The TAST for the tidal inlet being closed is similar for the high tidal range compared to the mild wave conditions (Figure 4.10). The magnitude of the TAST at the right-most boundary is 750 m³/6y/m for the tidal inlet being closed. The TAST with an open tidal inlet (2310 m³/6y/m) is significantly higher compared to the closed tidal inlet and compared to the mild wave conditions (Figure 4.7).

The RTF TAST has significantly increased for the high tidal range, just as well as the magnitude and reach of the RTF current (Figure 4.6). This increased magnitude and range is owing to the increased tidal range and thus an increased tidal prism. The reach of the RTF currents for the high tidal range is further than the centroid of the mega-nourishment (Figure 4.6). Consequently, the reach of the RTF TAST has increased to 3100 meters from the tidal inlet. The maximum magnitude of the RTF TAST at the right boundary of the t3 grid is 1590 m³/6y/m. This means that the maximum RTF TAST is much larger than compared to the mild wave conditions. Moreover, the RTF TAST has a higher contribution compared to the TAST owing to the waves (blue line in Figure 4.10).

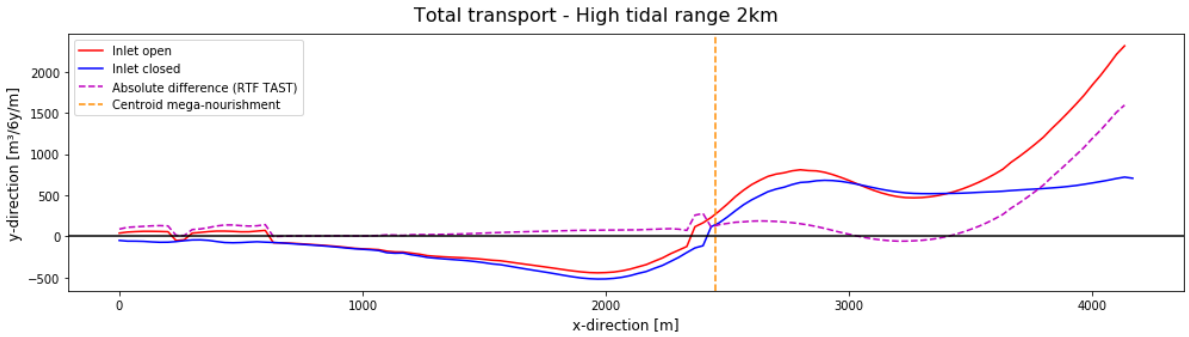

Figure 4.10: Total alongshore sediment transport high tidal range over 6 years with the mega-nourishment at 2km from the tidal inlet, in which the TAST for the tidal inlet being open (blue), closed (red) and the RTF TAST (purple) are shown.

4.4. Morphological development of the mega-feeder nourishment

The research question regarding the development of the mega-nourishment nearby a tidal inlet, over time, will be investigated in this chapter. As described in the methodology, the change over time compared to the initial shoreline is analyzed. Moreover, the results are shown inside the t3 grid only. The mild wave conditions simulations act as the basis for all other simulations. Similarities between the mild wave conditions and the other hydrodynamic conditions are presented in the mild wave conditions and are referred to as in general. The differences between the mild wave conditions and the other hydrodynamic conditions are individually addressed. Detailed figures and explanations for all simulations are given in Appendix E.

Mild wave conditions

In general, the shoreline development (difference in shoreline development between the tidal inlet being open and closed) over 6 years is not influenced by the tidal inlet with the mega-nourishment at an alongshore distance of 5km from the tidal inlet. The tip of the mega-nourishment erodes the same amount for both the tidal inlet being open and closed (top row in Figure 4.11b). This tip erodes quickly at first (2008 to 2010) but slows down as time progresses. The shoreline retreat at the tip for the mild wave conditions are 150, 70 and 55 meters from 2008 to 2010, from 2010 to 2012 and from 2012 to 2014 respectively. For the other hydrodynamic conditions the tip develops slightly differently, this is shown in more detail in Appendix E. The adjacent coast of the mild wave conditions gains up to 100 meters of shoreline during the first two years on both sides of the mega-nourishment. The magnitude in shoreline gain reduces significantly after the first two years. As a result of the gained shoreline around the 0m depth contour, the slope of the beach has become steeper.

Moreover, in general, the entire shoreline inside the t3 grid is not influenced by the tidal inlet over time, with the mega-nourishment at an alongshore distance of 5km from the tidal inlet (Figure 4.11b). For all hydrodynamic conditions there is an uniform accretion pattern on both or either side of the mega-nourishment (bottom row in figure 4.11b). After about two years, for the mild wave conditions, an accretion pattern spreads out from the centroid of the mega-nourishment. Furthermore, over time, there is no pattern evolving in the difference between the gained shoreline of the tidal inlet being open and closed. This is the same for all hydrodynamic conditions, there merely is some noise.

The development of the tip of the mega-nourishment is influenced by the curvature of the shoreline owing to the tidal inlet, however, not owing to the flow, for the mild wave conditions with the mega-nourishment at an alongshore distance of 2km from the tidal inlet. The tip of the mega-nourishment again erodes quickly during the first 2 years but slows down as time progresses. The shoreline retreat from 2008 to 2010, from 2010 to 2012 and from 2012 to 2014 are 150, 70 and 55 meters respectively for the tidal inlet being open and closed. Indicating that the tip is not influenced by the tidal inlet flow, as the shoreline retreat is similar for the mega-nourishment at 5km from the tidal inlet. As a result, the tip of the mega-nourishment propagates slowly towards the non-inlet-side. This effect can be seen for both the tidal inlet being open and closed (Figure 4.11a).

The adjacent shoreline on the inlet-side, with the mega-nourishment at 2km from the tidal inlet, erodes more owing to the RTF currents. At the last time-step, the shoreline has lost more shoreline for the tidal inlet being open than closed (Figure 4.11a). The maximum difference in shoreline is 33.3 meters. Whereas, the total gained shoreline of the tidal inlet being closed is 0 meters relative to the initial shoreline. This means that the RTF currents have a significant effect on the gained shoreline for the mild wave conditions close to the tidal inlet. There is an accretion pattern on the non-inlet-side spreading out from the centroid of the mega-nourishment, after the first two years (bottom row in Figure 4.11a). This pattern is not visible on the inlet-side. Moreover, the inlet-side with the mega-nourishment at a distance of 5km from the tidal inlet (Figure 4.11b), shows an accretion pattern similar to the non-inlet-side. Furthermore, there is no uniform accretion pattern during the first two years

on the inlet-side of the mega-nourishment. This indicates that not only the tidal flow has an impact on the shoreline development on the inlet-side of the mega-nourishment, but also the incident wave angle.

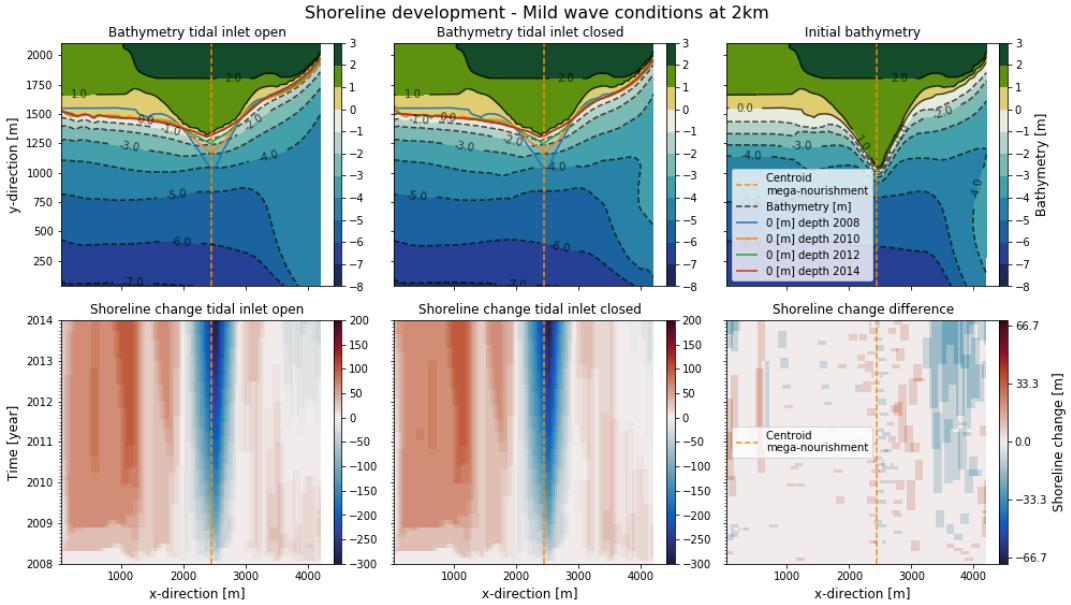

(a) Shoreline development mild wave conditions at 2 km from the tidal inlet

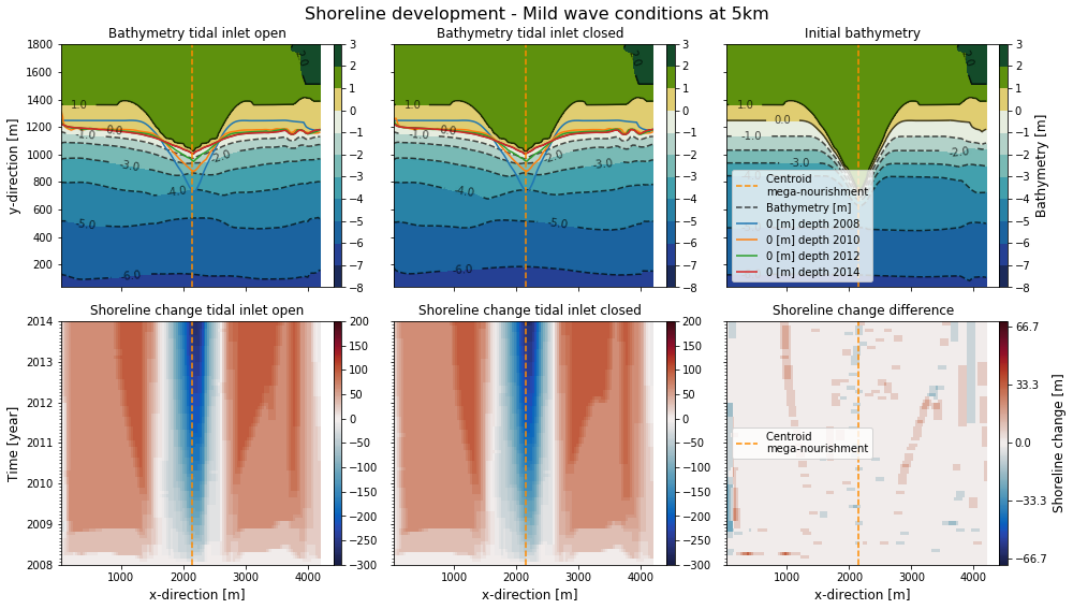

(b) Shoreline development mild wave conditions at 5 km from the tidal inlet

Figure 4.11: Shoreline development for the mild wave conditions. The top figure shows the mega-nourishment located at an alongshore distance of 2km from the tidal inlet and the bottom figure shows this at 5km from the tidal inlet. The first row shows the bathymetry and the shoreline over time. The blue, orange, green, red and dashed orange lines show the zero meter depth contour at the years 2008, 2010, 2012, 2014 and centroid of the mega-nourishment respectively. The second row shows the gained or lost shore with respect to the initial shoreline. Red shades indicate the gained shore compared to the first time step (2008) and blue shows shore being lost. Furthermore, the first column shows the results for the tidal inlet being open. The second column shows the results for the tidal inlet being closed. At last the top right figure shows the initial bathymetry and the bottom left figure shows the difference in gained shoreline between the tidal inlet being open and closed.

Oblique wave conditions

The mega-nourishment diffuses its sediment towards the inlet-side for the oblique wave conditions. The inlet-side directed diffusion is in most part owing to the angle of the waves, which generates a spit. The oblique wave conditions is the only hydrodynamic condition where a spit is formed (top row in Figure 4.12). This spit is also found with the mega-nourishment at an alongshore distance of 5km from the tidal inlet (Figure E.2b in Appendix E). This means that the diffusion of the sediment towards the tidal inlet and the formation of the spit is not owing to the tidal inlet.

Over time there is a difference in shoreline gain/retreat between the tidal inlet being open and closed, increasing in magnitude towards the tidal inlet, with the mega-nourishment at an alongshore distance of 2km from the tidal inlet. For both the tidal inlet being open and closed there is a strong accretion pattern just on the inlet-side of the mega-nourishment (see Figure 4.12). This accretion pattern is the spit. Towards the tidal inlet, just on the inlet-side of the spit, shoreline is being lost for both the tidal inlet being open and closed. However, more shoreline is lost for the tidal inlet being open. This extra shoreline retreat of a maximum magnitude of 66.7 meters after 6 years is owing to the RTF currents.

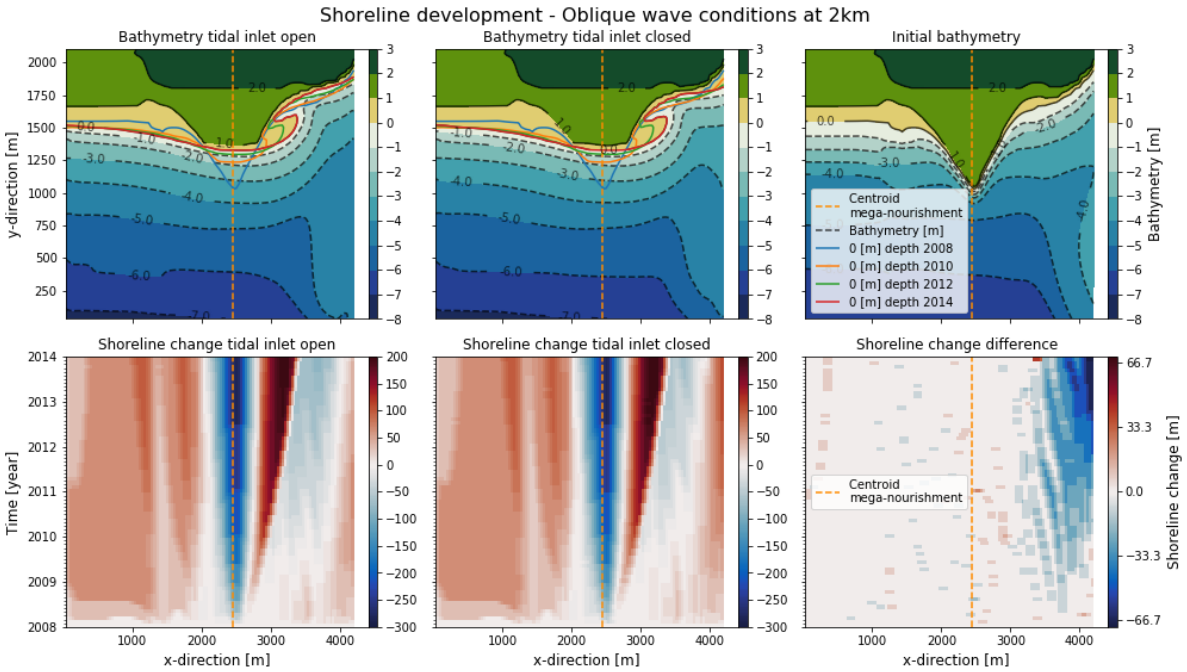

Figure 4.12: Shoreline development for oblique wave conditions at 2km from the tidal inlet. The first row shows the bathymetry and the shoreline over time. The blue, orange, green, red and dashed orange lines show the zero meter depth contour at the years 2008, 2010, 2012, 2014 and centroid of the mega-nourishment respectively. The second row shows the gained or lost shore with respect to the initial shoreline. Red shades indicate the gained shore compared to the first time step (2008) and blue shows shore being lost. Furthermore, the first column shows the results for the tidal inlet being open. The second column shows the results for the tidal inlet being closed. At last the top right figure shows the initial bathymetry and the bottom left figure shows the difference between the gained shoreline between the tidal inlet being open and closed.

Storm wave conditions

The shoreline development of the storm wave conditions is similar to that of the mild wave conditions (Figure 4.13). However, the difference in the change in shoreline between the tidal inlet being open and closed is similar for the mild wave conditions (Figure 4.11a) and the storm wave conditions (Figure 4.13). With the tidal inlet being open there is more shoreline being lost compared to the closed tidal inlet. Therefore, the RTF currents erodes the shoreline inlet-side of the mega-nourishment more than with the closed tidal inlet. The maximum difference between the tidal inlet being open and closed is 33.3 meters. Whereas, the gained

shoreline of the tidal inlet being closed is 0 meters relative to the initial shoreline. This means that the RTF currents have a significant effect on the gained shoreline on the inlet-side of the mega-nourishment.

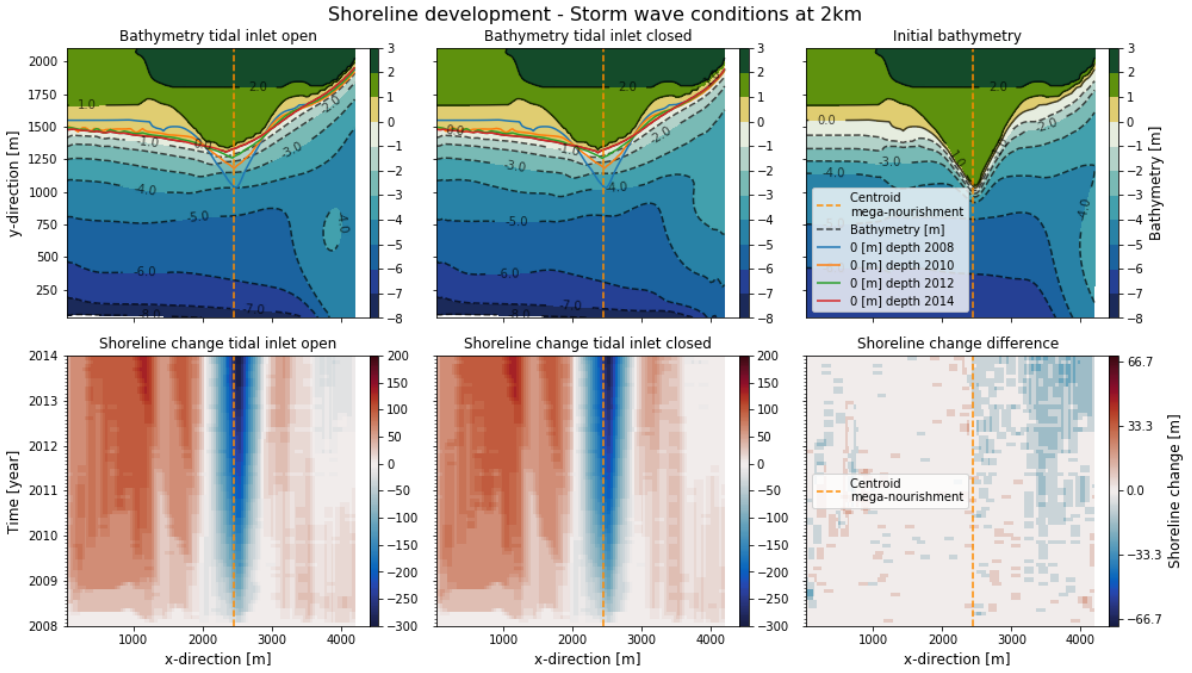

Figure 4.13: Shoreline development for storm wave conditions at 2km from the tidal inlet. The first row shows the bathymetry and the shoreline over time. The blue, orange, green, red and dashed orange lines show the zero meter depth contour at the years 2008, 2010, 2012, 2014 and centroid of the mega-nourishment respectively. The second row shows the gained or lost shore with respect to the initial shoreline. Red shades indicate the gained shore compared to the first time step (2008) and blue shows shore being lost. Furthermore, the first column shows the results for the tidal inlet being open. The second column shows the results for the tidal inlet being closed. At last the top right figure shows the initial bathymetry and the bottom left figure shows the difference between the gained shoreline between the tidal inlet being open and closed.

High tidal range

There is a large difference in the shoreline between the tidal inlet being open and closed with the mega-nourishment at an alongshore distance of 2km from the tidal inlet. Not only has the shoreline changed significantly, the bathymetry at the ebb-tidal delta is very different with the tidal inlet being open and closed (Figure 4.14). A flood channel is formed with an open tidal inlet. This flood channel is located close to the shoreline. As a result, the shoreline has retreated more with a open tidal inlet than a closed tidal inlet. The tip of the mega-nourishment has retreaded by 150, 70 and 55 meters from 2008 to 2010, from 2010 to 2012 and from 2012 to 2014 respectively. This is about the same as for the mild wave conditions. However, the tip has prograted more to the non-inlet-side compared to a closed tidal inlet (top row in Figure 4.14), as the inlet-side erodes more. For the high tidal range, the 1-meter depth contour seems to accrete more than the 0-meter depth contour. Whereas, the 0-meter depth contour accreded more for the mild wave conditions. This suggests that the high tidal range moves the sediment higher into the beach profile compared to the mild wave conditions.

The gained shoreline over time is smaller for the high tidal range compared to the low tidal range of the mild wave conditions. However, the difference in shoreline between the open tidal inlet and closed tidal inlet is much larger for the high tidal range. At the inlet-side, for a closed tidal inlet, the shoreline has gained a maximum of 66.7 meters. This is smaller than the gained shoreline for the mild wave conditions (Figure 4.11a). There is no difference in shoreline gained/lost between the tidal inlet being open and closed at the non-inlet-side. However, on the inlet-side there is a significant difference. This difference increases towards

the tidal inlet. There is significantly more shoreline retreat with the tidal inlet being open. This retreat has a maximum of 100 meters after 6 years. With a closed tidal inlet, the shoreline gain was about 0 meters towards the tidal inlet. Therefore, the RTF currents have a significant effect on the adjacent shoreline at the inlet-side of the mega-nourishment.

However, the TAST (Figure 4.10) stated that there still is sediment being transported at the non-inlet-side of the mega-nourishment towards the tidal inlet. This pattern is not seen in the development of the shoreline. Therefore, the transported sediment at the non-inlet-side of the mega-nourishment must come from a deeper contour line.

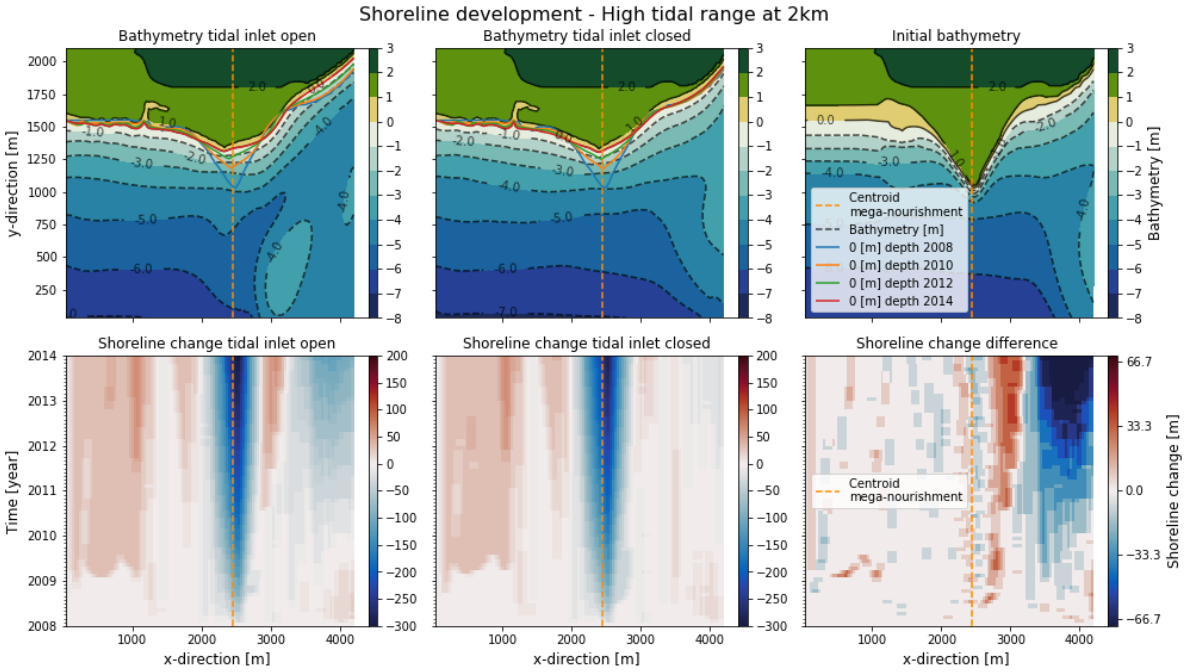

Figure 4.14: Shoreline development for a high tidal range at 2km from the tidal inlet. The first row shows the bathymetry and the shoreline over time. The blue, orange, green, red and dashed orange lines show the zero meter depth contour at the years 2008, 2010, 2012, 2014 and centroid of the mega-nourishment respectively. The second row shows the gained or lost shore with respect to the initial shoreline. Red shades indicate the gained shore compared to the first time step (2008) and blue shows shore being lost. Furthermore, the first column shows the results for the tidal inlet being open. The second column shows the results for the tidal inlet being closed. At last the top right figure shows the initial bathymetry and the bottom left figure shows the difference between the gained shoreline between the tidal inlet being open and closed.

4.5. Chapter summary

Residual currents

Overall, there is a tide averaged current at the tip of the barrier island in all simulations. The tidal currents have a high magnitude (order of several meters per second) at the center of the tidal inlet. This flow is directed towards the tidal inlet at both sides of the tidal inlet. With a closed tidal inlet there is also a flow towards the tidal inlet. This suggests that the tide averaged currents with the tidal inlet being closed, are generated by waves. Owing to the incident wave angle, an alongshore flow is generated at the tips of the barrier islands. Furthermore, it is also important to note that the ebb-tidal delta is present in all simulations, for the tidal inlet being open as well as closed. This will make sure that the flow owing to waves over the ebb-tidal delta remains the same.

There are also residual currents owing to the tidal inlet (RTF currents) near the tip of the barrier islands directed towards the tidal inlet. The magnitude and reach of these RTF currents depend on the hydrodynamic condition. For the mild, storm and oblique wave conditions and high tidal range the reach is 2200m, 2200m, 1070m meters and 3100m from the banks of the tidal inlet respectively. This means that an increased tidal range and consequently an increased tidal prism will increase the range and magnitude of the RTF currents. Moreover, the wave direction decreased the range of the RTF currents.

Total alongshore sediment transport

For simplified models including a mega-nourishment, it was shown that the incident wave angle is an important process in the magnitude of the TAST. The largest TAST is located where the incident wave angle approached 45 degrees relative to shore-normal. Moreover, for all simulations except for the oblique wave conditions, the TAST approaches zero towards the boundary of the t3 grid. This is also consistent with the incident wave angle, which slowly reduces to zero degrees. For the oblique wave conditions the angle of the waves are -45 degrees relative to shore-normal. This means that the TAST is already maximum with a zero degrees shoreline orientation when the wave angle is -45 degrees. Consequently, the incident wave angle is the governing process with the mega-nourishment. This is in agreement with the s,ϕ-curve.

Total alongshore sediment transport owing to the tidal inlet

There is virtually no TAST owing to the tidal inlet flow (RTF TAST, absolute difference in TAST between an open and closed tidal inlet) with the mega-nourishment at 5km from the tidal inlet. The RTF TAST is about zero over the entire x-direction (Figure 4.15). This means that the RTF currents do not influence the mega-nourishment located at an alongshore distance of 5km from the tidal inlet. The total transported RTF TAST (integral of the RTF TAST over the x-direction) is therefore insignificant (O(10,000 m^3/6y), table 4.1).

The RTF TAST does become important with the mega-nourishment at 2km from the tidal inlet. The magnitude of the RTF TAST increases towards the tidal inlet for all simulations (Figure 4.15). Furthermore, the RTF TAST for the mild wave conditions and the storm wave conditions are almost similar. The RTF TAST for the oblique wave condition is considerably lower than the mild wave. On the contrary, the RTF TAST for the high tidal range first decreases after which it increases to a magnitude much higher than that of the other hydrodynamic conditions. The maximum RTF TAST (at x=4166 meter) is 580, 390, 625 and 1590 m^3/6y/m for the mild wave conditions, oblique wave conditions, storm wave conditions and high tidal range respectively.

The total transported RTF TAST is highest for the high tidal range and lowest for the oblique wave conditions (Table 4.1). Furthermore, the total transported RTF TAST for the mild and storm wave conditions are about the same, the storm wave conditions are about 15% larger than the mild wave conditions. The total transported RTF TAST for the high tidal range is

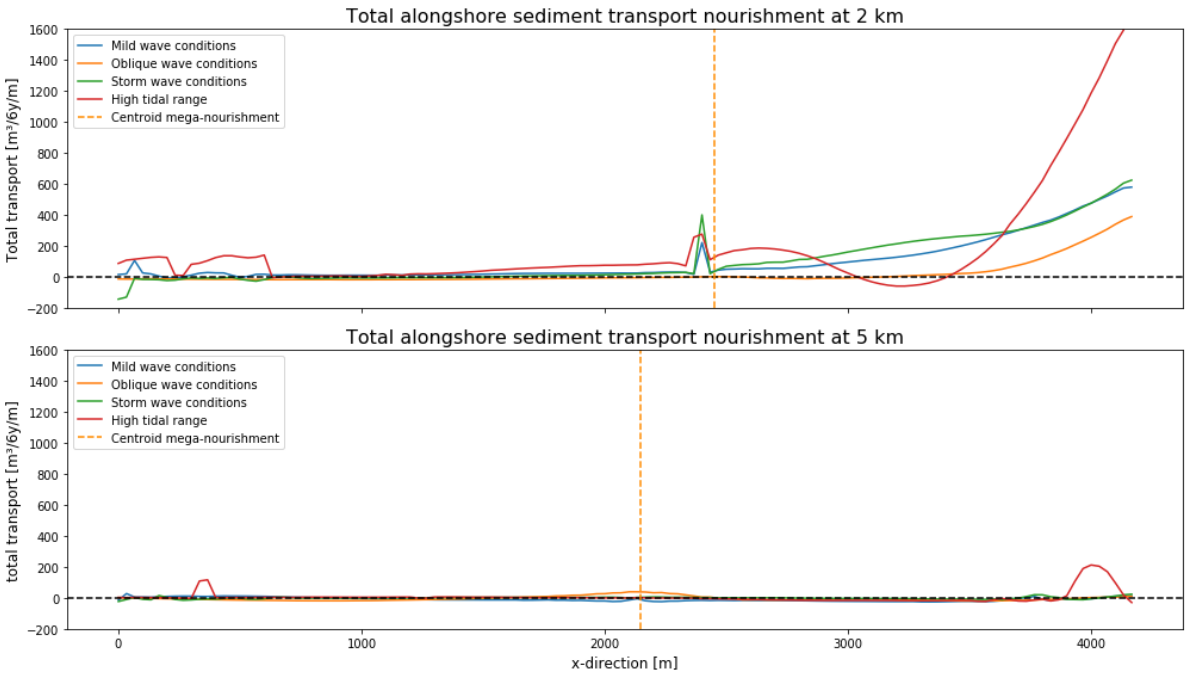

Figure 4.15: Total alongshore sediment transport owing to the tidal flow (RTF TAST) in the tidal inlet for all simulations over 6 years. The top figure shows the RTF TAST owing to the RTF current caused by the tidal inlet, with the mega-nourishment at 2km from the tidal inlet. The bottom figure shows the RTF TAST with the mega-nourishment at 5km from the tidal inlet. In both figures the blue, orange, green and red lines show the RTF TAST for the mild wave conditions, oblique wave conditions, storm wave conditions and high tidal range respectively.

Table 4.1: Total transported total alongshore sediment transport owing to the tidal flow in the tidal inlet for simplified simulations (integral of the RTF TAST over the x-direction). The columns show the referred hydrodynamic conditions, RTF TAST with the mega-nourishment at 2km from the tidal inlet and RTF TAST at 5km from the tidal inlet.

Condition	RTF TAST 2km [m³/6y]	RTF TAST 5km [m³/6y]
Mild wave condition	402,200	42,680
Oblique wave condition	131,120	34,040
Storm wave condition	459,040	6,510
High tidal range	729,430	18,620

about 81% larger than the mild wave conditions. At last the total transported RTF TAST for the oblique wave conditions is about 205% smaller than the mild wave conditions.

Furthermore, it can be seen that the RTF TAST reduces in magnitude and approaches 0 m³/6y/m at the centroid of the mega-nourishment. However, the RTF TAST for the high tidal range does not approach 0 m³/6y/m at the centroid of the mega-nourishment. Instead it decreases to 0 m³/6y/m about 1000 meter further to the non-inlet-side.

Morphological development of the mega-feeder nourishment

There is no difference in the development of the shoreline between the tidal inlet being open and closed with the mega-nourishment at an alongshore distance of 5km from the tidal inlet. Hence, the tidal inlet does not influence the shoreline development at the location of the mega-nourishment. Moreover, for all simulations, the centroid of the mega-nourishment (the tip of the mega-nourishment) erodes fast in the first two years (2008 to 2010) and then slows down over time.

In general, an open tidal inlet will increase the shoreline retreat for all simulations towards the tidal inlet, with the mega-nourishment at an alongshore distance of 2km from the tidal

inlet (Figure 4.16). The difference in the shoreline retreat between the tidal inlet being open and closed is the largest for the oblique wave conditions (maximum of 66.7 meters) and high tidal range (maximum of 100 meters). A high tidal range will increase the RTF currents owing to the tidal flow and therefore the RTF TAST. This is in line with the hypothesis (chapter 2.4) which states that increasing the tidal range will increase the tidal prism and therefore increase the RTF currents owing to tidal jetting.

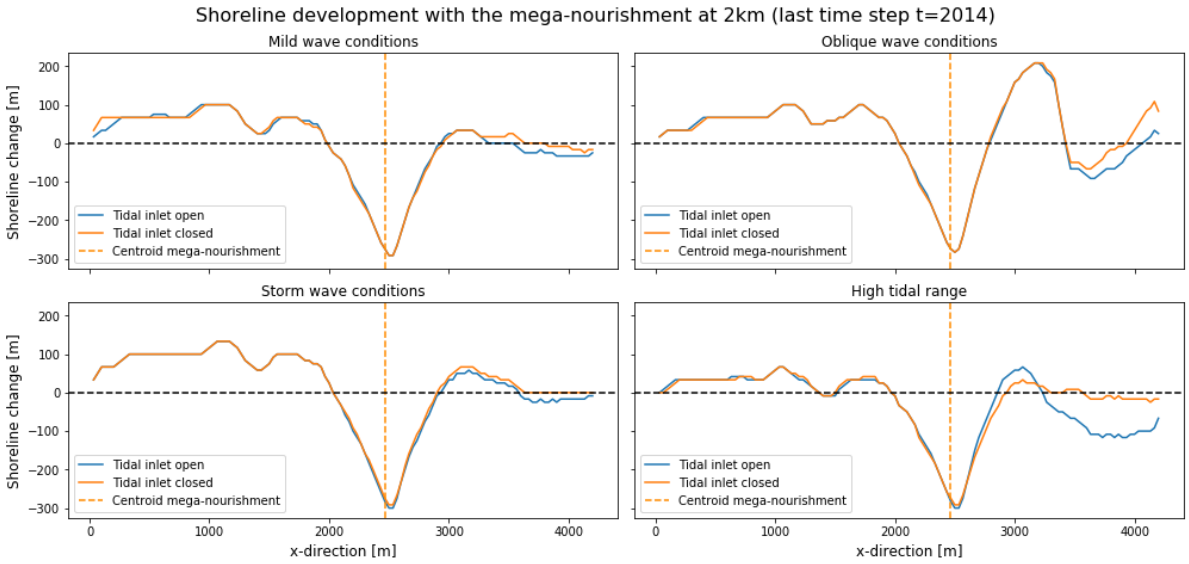

Figure 4.16: The change in shoreline at the last time-step (t=2014) for all simulations with the mega-nourishment at 2km from the tidal inlet. The change in shoreline (0-meter depth contour) is the difference between the shoreline at t=2014 and the initial shoreline at t=2008. Where a negative number indicates a shoreline retreat and a positive number indicates a shoreline gain.

5

Discussion

5.1. Interpreting the results

The mega-nourishment was not affected by the presence of a tidal inlet, with the mega-nourishment at an alongshore distance of 5km from the tidal inlet. This is one of the findings in the results. The total alongshore sediment transport (TAST) for the tidal inlet being open and closed were similar at the location of the mega-nourishment and the adjacent coast for all hydrodynamic conditions investigated in this thesis. Moreover, the difference in the shoreline (0m depth contour) between the tidal inlet being open and closed was similar.

Essentially, the area adjacent to the tidal inlet does not feel the presence of the mega-nourishment, with the mega-nourishment located at 5km from the tidal inlet. Moreover, the mega-nourishment located at 5km from the tidal inlet does not feel the presence of the tidal inlet. Therefore, the simulations with the mega-nourishment an alongshore distance of 5km from the tidal inlet can be seen as if there was no mega-nourishment at all near the tidal inlet. Consequently, the simulations with the mega-nourishment at an alongshore distance of 5km from the tidal inlet is considered as a base case, where there is no influence of a mega-nourishment. This assumption is valid until a location of approximately 2700 meters from the tidal inlet, which is the location of the inlet-side most boundary of the fine grid where the mega-nourishment is located at an alongshore distance of 5km from the tidal inlet. Moreover, at this location the TAST has approached a zero transport, which means that the tidal inlet has no effect on the sediment transport from the mega-nourishment.

Not only can the simulations with the mega-nourishment at 5km from the tidal inlet be seen as if there is no tidal inlet at all. The simulations with an open tidal inlet with the mega-nourishment at an alongshore distance of 5km from the tidal inlet can be seen as a situation including effect of the tidal inlet and the flow owing to the tidal inlet close to the tidal inlet. The closed tidal inlet simulations with the mega-nourishment located at an alongshore distance of 2km from the tidal inlet can be seen as a situation including the effect the tidal inlet but without the effect of the flow owing to the tidal inlet.

Sediment balance mega-nourishment

Coastal managers are often interested in whether a sandy solution is losing sediment and how much sediment is lost. Also it is interesting to know where the sediment ends up to see whether the solutions are effective. Therefore, the area of the mega-nourishment is investigated to see how much sediment the mega-nourishment loses, where the area of the mega-nourishment is defined as the area where sediment for the mega-nourishment is placed on top of the initial bathymetry (chapter 3.1.2). In this area the gross sediment erosion and accretion is investigated where there is no tidal inlet, for the open tidal inlet and for the closed

tidal inlet. This will give an idea of what the effect is of the tidal inlet owing to its bathymetry (curvature of the coast) and owing to the flow in the tidal inlet.

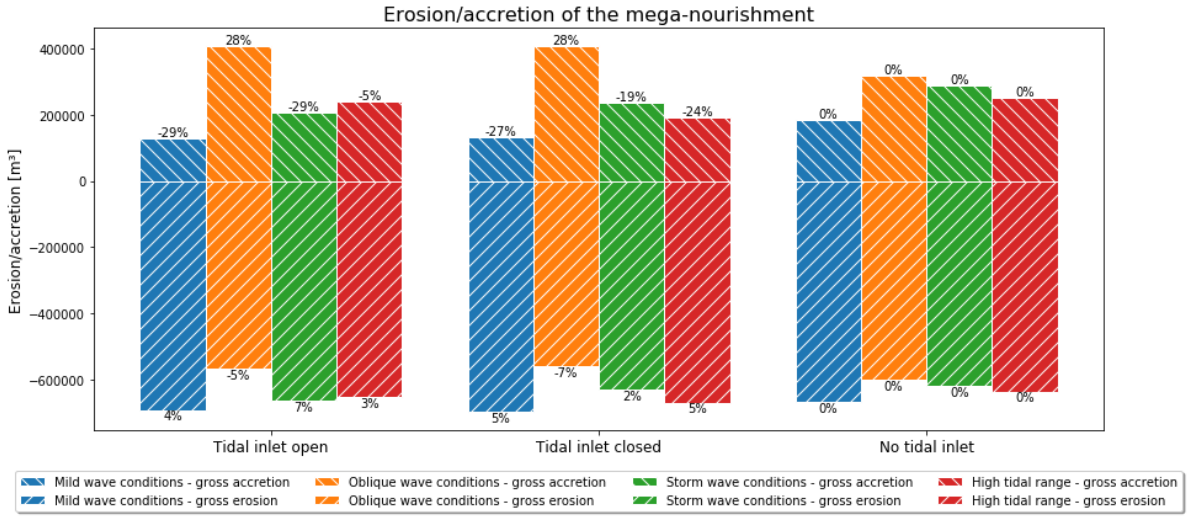

Figure 5.1: Gross erosion and accretion volumes of the mega-nourishment in m³ at the last time-step (t=6y). Values larger than zero indicate accretion and values lower than 0 indicate erosion. The blue, orange, green and red bars represent the erosion or accretion of the mild wave conditions, oblique wave conditions, storm wave conditions and high tidal range simulations respectively. The percentage given is the relative difference between a simulation for the open/closed tidal inlet and with no tidal inlet.

The mega-nourishment loses sediment for all simulations. The magnitude of the gross accretion and erosion differs per hydrodynamic condition (Figure 5.1). In general, the mega-nourishment erodes more than it gains for all simulations, which means that there is a net erosion. The mega-nourishment has a nourished volume of about 2.1 million m³ (chapter 3.1.2). This means that after 6 years about 20% of the sediment supplied has eroded and consequently about 80% is still within the contours of the supplied nourishment, except for the oblique wave conditions where this is about 10% (Figure 5.1). This means that for every scenario the sediment which is located within the depth contours of the mega-nourishment are similar to the findings of de Schipper et al. [2016], which did not have a tidal inlet.

Furthermore, there is not much difference in the gross volume of sediment being lost between an open tidal inlet, closed tidal inlet and no tidal inlet (percentages in Figure 5.1). Therefore, the hydrodynamic condition and the state (open or closed tidal inlet) of the tidal inlet does not seem to effect the volume of eroded sediment in the grid cells where there is erosion, as the difference is at most 7% compared to the equivalent scenario without a tidal inlet. This is contrary to the volume of sediment being accreded, where there are large differences in the volume of sediment being accreded, these differences are up to -29% compared to no tidal inlet. Therefore, the hydrodynamic condition and the state (open or closed tidal inlet) of the tidal inlet does impact the volume of sediment being accreded in the area of the mega-nourishment.

There are some surprising differences between some simulations. First the oblique wave conditions simulations eroded considerably less and accreded more than all other simulations. This is owing to more sediment being accreded within the area of the mega-nourishment. Whereas, for the other hydrodynamic conditions, the sediment diffuses more to outside the area of the mega-nourishment. This can also be seen when investigating the volume of sediment being accreded, which is larger compared to the other hydrodynamic conditions (Figure 5.1).

Secondly, the mild wave conditions had the most erosion in the area of the mega-nourishment, while it had the least energetic hydrodynamic forcing (chapter 3.2.2). It also had the least accretion relative to the other hydrodynamic conditions (Figure 5.1). This means

that less sediment is accreded inside the area of the mega-nourishment compared to the other hydrodynamic conditions.

At last, the accretion volume for the storm wave conditions and high tidal range were different for the tidal inlet being open and closed compared to no tidal inlet (Figure 5.1). For the storm wave conditions, with an open tidal inlet, the mega-nourishment accreded less than compared to a closed tidal inlet. Possibly more sediment is mobilized and transported outside of the area of the mega-nourishment.

The high tidal range is the only scenario where the volume accreded is higher for an open tidal inlet than for a closed tidal inlet. This could be owing to the tidal inlet attracting more sediment towards the tidal inlet. However, it is also not unlikely that the change in bathymetry owing to the ebb-tidal delta not being in equilibrium with the increased tidal range has major contribution in the extra volume of sediment in the area of the mega-nourishment (chapter 4.2).

Sediment pathway

In the previous section it was shown that within the area of the mega-nourishment more sediment has eroded than was gained. Therefore, it is important to investigate where this sediment ends up and how much is, if any sediment is lost to the tidal basin. This can be visualized by investigating the difference in the final bathymetry after 6 years for the mega-nourishment at an alongshore distance of 2km and 5km from the tidal inlet with the tidal inlet being open, and the difference in the initial bathymetry (Equation 5.1). This can be done under the assumption that no sediment of the 5km scenario ends up to the inlet-side of the mega-nourishment located at 2km from the tidal inlet. The difference in the initial bathymetry is subtracted to remove the effect of the mega-nourishment being included in one of the bathymetry but not in the other one. These differences in bathymetry will result in the erosion/accretion patterns owing the the mega-nourishment (Figure 5.2).

$$\Delta bathymetry_{t=6yr} - \Delta bathymetry_{t=0} \tag{5.1}$$

Most sediment eroded from the mega-nourishment is accreded outside the area of the mega-nourishment (Figure 5.2). For the mild and storm wave conditions it becomes clear that the non-inlet-side accreded more than the inlet-side of the mega-nourishment. However, there is strong accretion band at the shoreline on the inlet-side of the mega-nourishment. This indicates that sediment is potentially being ”pulled” towards the tidal inlet owing to the tidal inlet. However, the erosion pattern just ocean-wards of this accretion pattern indicates that part of this pattern is caused by a mismatch in grid-size between the two simulations (mega-nourishment at 2km and 5km from the tidal inlet) but not all as there is more accretion than erosion.

For the oblique wave conditions it can clearly be seen that more sediment is diffused to the inlet-side of the mega-nourishment compared to the non-inlet side (the strong accretion pattern on the non-inlet-side outside of the area of the mega-nourishment should be ignored as this is an artifact of the method used and is, in fact, an erosion pattern owing to the mega-nourishment located at 5km from the tidal inlet, Figure 5.2). This accretion pattern causes a strong erosion pattern more to the inlet-side.

For the high tidal range, the accretion and erosion patterns in the ebb-tidal delta changed owing to the presence of the mega-nourishment (Figure 5.2). The accretion in the ebb-tidal delta is not sediment from the mega-nourishment but rather a changed flow pattern owing to the presence of the mega-nourishment. However, it can still be seen that there is more accretion to the non-inlet-side than the inlet-side of the mega-nourishment.

Sediment does end up into the tidal basin for the mega-nourishment located at an alongshore distance of 2km from the tidal inlet and an open tidal inlet (Figure 5.2). Most of the accretion owing to the mega-nourishment takes place at the deepest contours in the tidal basin.

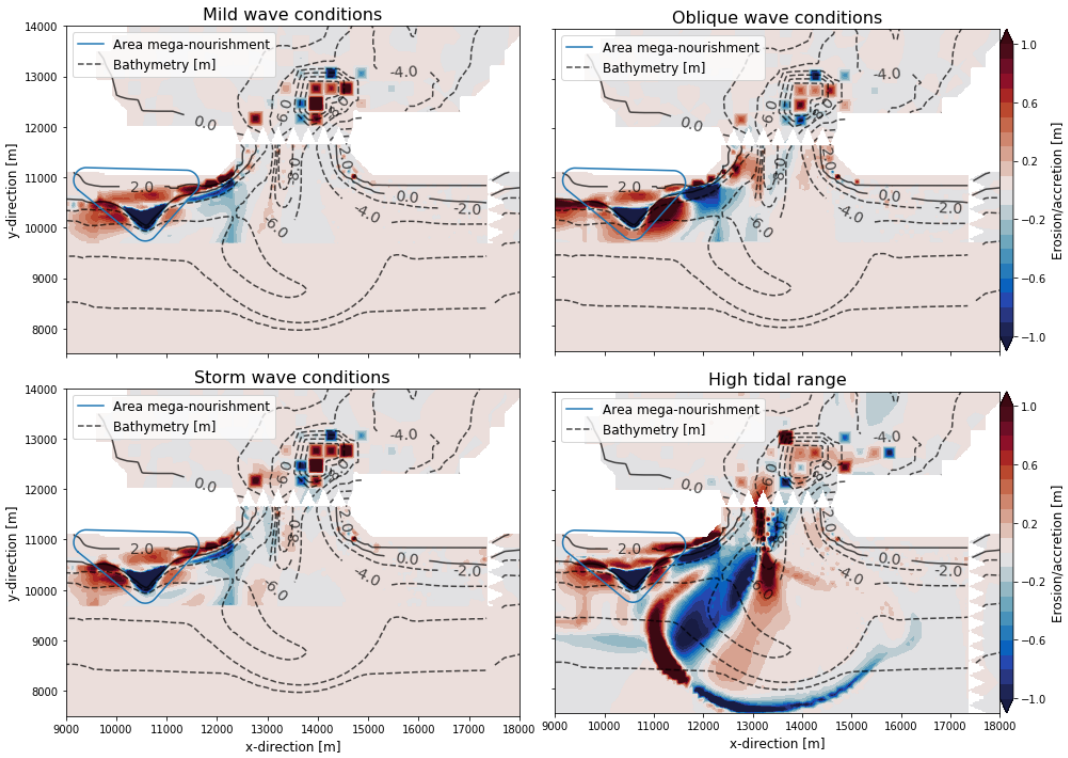

Figure 5.2: Erosion and accretion patterns owing to the mega-nourishment at the last time-step. Where the red shades indicate accretion and the blue shades indicate erosion compared to a scenario without a mega-nourishment. The blue line shows the boundary of the mega-nourishment. The erosion and accretion patterns are obtained by looking at the difference in bathymetry between the mega-nourishment located at 2km and 5km from the tidal inlet with the tidal inlet being open, and subtracting the difference in the initial bathymetry of both simulations to remove the effect of the difference in the initial bathymetry.

However, not only is sediment accreded, there are erosion patterns as well. This means that the presence of the mega-nourishment causes accretion which most likely caused erosion elsewhere in the tidal basin, compared to no mega-nourishment.

Table 5.1: Volume of accretion owing to the mega-nourishment inside the tidal basin. The percentage of the net erosion is percentage of the volume in the tidal basin relative to the net erosion (net erosion is the gross erosion plus the gross accretion in Figure 5.1). The max accretion is the grid cell where the change in bathymetry owing to the mega-nourishment inside the tidal basin is the largest (dark red cells in Figure 5.2). The last column shows the percentage of the max accretion over the water depth found in the cell of the max accretion, which gives an quantitative measure on how much such a grid cell is impacted by the mega-nourishment.

Scenario	Volume in basin [m³]	Percentage of the net erosion	Max accretion [m]	Percentage of the local depth
Mild wave condition	166,285	30%	3.35	25%
Oblique wave condition	-34,090	-20%	0.89	10%
Storm wave condition	173,181	38%	3.54	27%
High tidal range	113,460	27%	2.46	61%

For the mild and storm wave conditions about 30% to 40% percent of the net erosion of the mega-nourishment was lost to the tidal basin (Table 5.1). The grid cell with the most accretion, had its bed level gain about 25% of the local water depth in that grid cell. This is a significant gain considering that the most accreded grid cell is located in the deepest depth contours (the channel). The accumulation of sediment in mainly the deepest depth contours could mean that the deepest depth contours should be nourished if it is a navigation channel.

The oblique wave conditions had volume being lost owing to the mega-nourishment (Ta-

ble 5.1). However, it is not possible that a negative volume is coming from the mega-nourishment. This method cannot distinguish between the sand actually coming from the mega-nourishment and accretion/erosion patterns owing to the change in flow due to the presence of the mega-nourishment. Therefore, the negative volume must be owing to the tidal basin exporting more sediment, which is demanded near the ebb-tidal delta, tidal inlet or near the mega-nourishment. Also, the volume of sediment in the basin (Table 5.1) as well as the net erosion (Figure 5.1) is much lower than for the other scenarios. Furthermore, the location of the most accretion is located at the deepest depth contours (Figure 5.2), similar to the mild and storm wave conditions. However, the magnitude and percentage of the local depth is smaller compared to the mild and storm wave conditions (Table 5.1). One could argue that the magnitude of the sediment volume lost is insignificant compared to noise.

The volume of sediment accreded in the tidal basin relative to the net erosion of the mega-nourishment is about 30% for the high tidal range (Table 5.1). As described in the previous paragraph, this method cannot distinguish between the sand actually coming from the mega-nourishment and accretion/erosion patterns owing to the change in flow due to the presence of the mega-nourishment. Therefore, it is questionable how much of this volume is actually coming from the mega-nourishment, as the ebb-tidal delta changes significantly owing to the presence of the mega-nourishment (Figure 5.2). The change in the sediment and erosion patterns owing to the existence of the mega-nourishment most likely has a big impact on the development of the ebb-tidal delta and the adjacent coast of the mega-nourishment.

5.2. Modeling approach and post-processing methods

From the previous sections it becomes apparent that there are limitations in the results owing to the methods used. These limitations are described to show the focus of the study and what to take into account when using the results.

One of the most important considerations to take into account is the fact that the ebb-tidal delta is not in an equilibrium. The ebb-tidal delta was modelled for 30 years using the hydrodynamic conditions similar to the one used in the mild wave conditions scenario. After 30 years of morphological development, the largest changes had occurred. However, to reach an equilibrium of the ebb-tidal delta several centuries to millennia should be modelled instead of decades [van der Wegen, 2010]. As a result, there still is sediment transport in the result owing to the ebb-tidal delta not being in equilibrium. However, real tidal inlet systems are often very dynamic and never in an equilibrium, such as the cyclic behavior of the Ameland inlet system [Cheung et al., 2007, Elias et al., 2019].

Moreover, the ebb-tidal delta has developed in a certain way for the given bathymetry, tidal basin, tidal inlet and hydrodynamic forcing. The forcing used to build the ebb-tidal delta was similar to that of the mild wave conditions. This means that for the other scenarios, using different hydrodynamic conditions, the ebb-tidal delta is more out of equilibrium. This allowed for a better comparison in the absolute difference between the simulations using an open and closed tidal inlet. However, the ebb-tidal delta was not in equilibrium, which is most apparent for the high tidal range simulations. In these simulations there was a significant increase in the magnitude of the tidal currents in the tidal inlet, which changed the bathymetry in the ebb-tidal delta (Chapter 4.2), between an open and closed tidal inlet. The currents patterns were similar for the high tidal range compared to the other scenarios (Figure 4.5 and 4.6). Which means that the erosion and accretion patterns are most likely correct. However, it is questionable how much of the sediment transport and morphological development is owing to the tidal inlet system readjusting to the increased tidal range. In the previous section is was shown that there is accretion in the tidal basin but also that the mega-nourishment caused a change in the sediment and erosion patterns in the ebb-tidal delta.

Another important consideration is the fact that a numerical model called Delft3D has been used. The use of numerical models imposes limitations of its own. Besides the standard

limitations of a numerical model, the set up model had important limitations as well. One of which are boundary artifacts, which could not be removed. In all of the simulations, the roller model was used to allow for better results. At the breaker zone, waves generate a surface roller which temporally stores the momentum. The surface roller will dissipate its energy by the production of turbulence. However, in Delft3D the roller model has only been tested and validated for a single grid. In this thesis the grids were domain decompositioned, hence the application of the roller model was not validated for these grids. Although not being validated for domain decompositioned grids, the roller model did improve the results and prevented the creation of a new beach in the ebb-tidal delta by transporting some of the moment towards the tidal inlet. Furthermore, the roller model produced an artificial current at all boundaries parallel to the shore. The size of the grid has been chosen as such that the artificial currents do not reach the mega-nourishment. Moreover, the artificial current does not impact the waves propagating towards the mega-nourishment. As a result, the artifacts do not significantly impact the mega-nourishment or the nearshore transport of sediment.

5.3. Implications for mega-nourishments near a tidal inlet

This thesis focused on the hydrodynamics of a mega-nourishment nearby a tidal inlet system. Therefore, the results are only applicable to this particular system with a fairly large and elongated tidal basin, a shore-normal channel orientation and the size and location of the mega-nourishment. However, it can be explored what the results could mean for other tidal inlet systems.

Dimensions and location of the mega-nourishment

The dimensions of the mega-nourishment used in this thesis are about half the size of the one used in the Sand Engine. The nourished volume is 10 times smaller compared to the Sand Engine (2.1 million in this thesis compared to 21 million in the Sand Engine [Stive et al., 2013]). Nevertheless it was found in this chapter that about 80% of the sediment supplied is still located within the depth contours of the mega-nourishment for all scenarios but the oblique wave condition. This is consistent with the findings for the Sand Engine [de Schipper et al., 2016]. Therefore, it is expected that scaling the mega-nourishment will not significantly affect the erosion rate of the mega-nourishment itself.

The location of the mega-nourishment matters in how much sediment is lost owing to the tidal inlet and the flow of the tidal inlet (Chapter 4.3). It was concluded that the a mega-nourishment located at an alongshore distance of 5km from the tidal inlet will not be effected by the tidal inlet, for the hydrodynamic conditions and the morphological setup used in this thesis. The mega-nourishment located at an alongshore distance of 2km from the tidal inlet does not erode more owing to the tidal inlet. However, the accretion pattern on the inlet-side of the mega-nourishment is reduced relative to the non-inlet-side. Moreover, sediment is transported into the tidal basin owing to the presence of the mega-nourishment near (2km) a tidal inlet. Therefore, it expected that the if the mega-nourishment is placed even closer to the tidal inlet, the mega-nourishment will be affected by the tidal inlet. Also, it is expected that if the mega-nourishment is located within the reach of the tidal inlet (Chapter 4.3 and 4.5), then sediment owing to the mega-nourishment will end up into the tidal basin.

Influence of the tidal range

The tidal range increases the transport owing to the tidal flow inside the tidal inlet. This increased transport will enhance the total alongshore sediment transport (TAST) towards the tidal inlet. Although, the mega-nourishment did not erode more for the high tidal range scenario compared to the other scenarios with a lower tidal range (Figure 5.1), the adjacent coast did erode more for the high tidal range owing to the tidal range (Figure 4.14 and 4.16). Moreover, the increased tidal range increased the magnitude and reach of the residual currents owing to the tidal inlet (RTF current in Figure 4.6) and the reach and magnitude of the

absolute difference in the TAST owing to the tidal inlet (RTF TAST, Figure 4.15). The mega-nourishment not eroding more and the absolute difference in the total alongshore sediment transport (RTF TAST) reaching to the non-inlet-side of the mega-nourishment, suggests that sediment is transported from depth contours outside the area of the mega-nourishment. Therefore, it is expected that an increased tidal range will increase the erosion of the mega-nourishment if it is located closed to the mega-nourishment, where RTF TAST is large relative to the TAST without an closed tidal inlet.

Influence of the wave angle

An oblique wave angle increased the accretion in the area of the mega-nourishment (Figure 5.1). This is owing to more sediment staying within the area of the mega-nourishment. Sediment which diffused to the non-inlet-side of the mega-nourishment in all other scenarios but the oblique wave conditions, has now diffused to the inlet-side. Therefore, an incident wave angle will diffuse sediment down-drift. This in agreement with the alongshore sediment transport being proportional to the incident wave angle ($S \propto H_s^{2.5} * sin(2 * \phi_{incident-wave-angle})$, chapter 2.2 [Bosboom and Stive, 2015]). However, the presence of the tidal inlet seems to erode the coast more towards the tidal inlet. A spit was formed for both the mega-nourishment located at an alongshore distance of 2km and 5km from the tidal inlet. The spit reattaches to the coast after 6 years of morphodynamic change (Figure E.2b) for the mega-nourishment located at 5km from the tidal inlet. At this location the mega-nourishment does not feel the presence of the tidal inlet. However, the spit does not reattach for the mega-nourishment located at 2km from the tidal inlet. Therefore, it is expected that the tidal inlet will pull more sediment towards the tidal inlet. Moreover, the coast just to the inlet-side of the spit erodes more owing to the tidal inlet. However, the time span of 6 years is too short to be certain that more sediment is being pulled towards and into the tidal inlet.

In the results it was shown that the absolute difference in the total alongshore sediment transport between the tidal inlet being open and closed (RTF TAST), is lowest compared to all other hydrodynamic conditions. This means that an oblique wave angle reduces the reach and magnitude of the RTF current and RTF TAST. The gyres(eddies) at the adjacent coast of the tidal inlet are caused by a flow separation due to momentum of the flow in the tidal inlet, when the water is flowing into the ocean. van Heijst and Wells [2004] modelled the gyre(vortex) using a dipole potential flow element, which can propagate away from the tidal inlet. Moreover, a sink potential flow element is used to simulate the flow going into the tidal basin. By time-averaging these flow elements over a tidal cycle will result in a residual current at the adjacent coast.

It is hypothesized that by adding a uniform potential flow element to represent the alongshore current owing to the waves, in combination with a dipole potential flow element, will result in a deflected flow field (downstream directed) compared to as if there was no uniform flow element. This effectively increases the horizontal length scale of the eddy on the updrift side and ”squeezes” the eddy on the downstream side of the tidal inlet. Increasing the horizontal length scale of the eddy will reduce the magnitude of the residual currents.

Hence, it is expected that a positive wave angle (mega-nourishment at the downdrift side of the tidal inlet) will increase the magnitude of the total alongshore sediment transport owing to the tidal inlet. Moreover, the alongshore sediment transport is proportional to the incident wave angle ($S \propto H_s^{2.5} * sin(2 * \phi_{incident-wave-angle})$, chapter 2.2 [Bosboom and Stive, 2015]). Which means that the strength of the uniform potential flow element is also proportional to the incident wave angle. Therefore, it is expected that the reach and magnitude of the residual currents have a similar dependency on the incident wave angle.

6

Conclusion

A large-scale feeder nourishment (mega-feeder nourishment) has been constructed along a straight coastal stretch (Sand Engine). In several studies, it was shown that the concept of a mega-feeder nourishment is feasible for an uninterrupted straight coastal stretch. However, approximately 10% of the world's beaches consist of barrier islands. Often, on either or both sides of a barrier island a tidal inlet is located. A mega-feeder nourishment concept has not been applied nor studied near a tidal inlet system. Therefore, this thesis investigates the effect a tidal inlet system has on the development of a mega-feeder nourishment. Consequently, the research question is:

> *How does a nearby tidal inlet system influence the development of a mega-feeder nourishment?*

This thesis aims to investigate the effect different hydrodynamic conditions have on the development of a mega-feeder nourishment, while keeping the morphodynamic features of the tidal inlet, ebb-tidal delta and mega-feeder nourishment fixed. The alongshore distance of the mega-feeder nourishment to the tidal inlet (2km and 5km) is the only morphodynamic feature which is varied. A numerical model called Delft3D is used to investigate the development of a mega-feeder nourishment nearby a tidal inlet. Four distinct hydrodynamical conditions, namely the mild wave conditions, oblique wave conditions, storm wave conditions and the high tidal range, gave insight into the morphodynamic response of the mega-feeder nourishment. These hydrodynamic conditions were simplified, meaning steady wave characteristics and a single M2 tidal constituent. Using real time-varying hydrodynamic conditions yields similar results compared to the simplified hydrodynamic conditions. Therefore, simplifying the hydrodynamic conditions is justified.

Several sub-questions have been formalized in order to answer the research question. The numerical model with the simplified hydrodynamic conditions allows for the sub-questions to be answered. The first sub-question is:

> How does a mega-feeder nourishment nearby a tidal inlet develop over time under various hydrodynamic conditions

The change in the shoreline relative to the initial shoreline (at t=0) is similar for the mega-feeder nourishment located at an alongshore distance of 5km and 2km from the tidal inlet. Moreover, it was shown that a mega-feeder nourishment at an alongshore distance of 5km from the tidal inlet is not influenced by the tidal inlet. However, the adjacent coast to the inlet-side of the mega-feeder nourishment at an alongshore distance of 2km from the tidal inlet, does have more shoreline retreat owing to the tidal inlet. Therefore, a mega-feeder nourishment closer (order several hundreds of meters) to a tidal inlet could develop differently owing to a tidal inlet.

What processes are important in the development of a mega-feeder nourishment owing to the tidal inlet?

The most important process in the development of a mega-feeder nourishment nearby a tidal inlet is the incident wave angle. This process resulted in the highest contribution to the total alongshore sediment transport. The most important process owing to the tidal flow in the tidal inlet are the residual currents caused by gyres at the adjacent coast. The incident wave angle has the highest contribution to the total alongshore sediment transport for low tidal ranges (η < 1.5m) and mild and storm wave conditions (H_s > 1m). The contribution of the residual currents increases with an increasing tidal prism and consequently with an increasing tidal range (η > 3m).

What is the effect of the tidal prism on the development of a mega-feeder nourishment?

An increased tidal prism will increase the erosion of the mega-nourishment and adjacent beach towards the tidal inlet. As found in the literature study (chapter 2.2), the tidal prism is proportional to the surface area of the basin times the tidal range. This means that if the tidal range increases, then so will the tidal prism (assuming a constant basin surface area). An increased tidal prism will increase the currents inside the tidal inlet. Moreover, it has been found that the residual currents will also increase in magnitude with an increased tidal prism. These residual currents will generate a residual total alongshore sediment transport owing to the tidal flow in the tidal inlet. The residual total alongshore sediment transport increases the sediment transport towards the tidal inlet. As a result, there is more erosion to the inlet-side of the mega-feeder nourishment. Hence, an increased tidal prism will increase the erosion at the mega-feeder nourishment and adjacent coast, towards the tidal inlet.

What alongshore distance from the tidal inlet will influence the development of a mega-feeder nourishment?

The results show that the influence the tidal inlet has on the adjacent coast is, in part, caused by the residual currents owing to the tidal inlet. The reach and magnitude these currents have, depend on the tidal prism and the direction of the waves. The reach is defined as the alongshore distance from the tidal inlet where the total alongshore sediment transport is larger than 50 $m^3/6y/m$, this threshold is assumed to be the limit of the noise in the results.

The reach of the mild and storm wave conditions ($\eta = 1.5m$) was similar and resulted in an alongshore distance of 2200 meters from the tidal inlet. The high tidal range ($\eta = 3.0m$) increased the reach to 3100 meters due to the increased magnitude in the residual currents owing to the tidal inlet. At last, the reach of the oblique wave conditions ($d_p = -45\,\mathrm{deg}$) was reduced to 1070 meter. This means that an oblique wave angle, directed towards the tidal inlet, with the mega-nourishment upstream of the tidal inlet, will reduce the reach of the tidal inlet.

To conclude the main research question: *"How does a nearby tidal inlet system influence the development of a mega-feeder nourishment?"*. The tidal inlet has an effect on the development of the mega-feeder nourishment if located inside the influence of the tidal inlet. The residual current owing to the tidal inlet is an important process causing erosion. This erosion increases in magnitude towards the tidal inlet. The tidal range influences the residual currents and hence the erosion nearby a tidal inlet. Including the mega-feeder nourishment if located within the influence of the tidal inlet. However, the incident wave angle is the governing process for small tidal ranges (η <1.5) and mild wave conditions (H_s > 1m). In this study, for a tidal range of 1.5 meters to 3.0 meters, the influence of the tidal inlet extends from 2200 meters up to 3100 meters in the alongshore direction.

7

Recommendations

This thesis investigated the influence of a tidal inlet system on the development of a mega-feeder nourishment. Several recommendations can be formulated based on the findings and methods used in this report.

Modelling

The models set up in this thesis had some numerical artifacts which the author was unable to remove. These artifacts were foremost artificial currents produced at the boundaries parallel to the shore, in all grids. The influence of these artifacts on the area of interest is mitigated by moving the boundary further away from the mega-feeder nourishment. However, it cannot be, with absolute certainty, concluded that the artifacts did not affect the results. The artificial currents may still reach the area of interest, all be it small in magnitude compared to the currents owing to the tide and waves. The cause of the artificial currents is not known, however, it is expected that this is owing to the domain decomposition in combination with the roller model used in the simulations, as the roller model is not validated for domain decompositioned grids. It is recommended to investigate what causes these artificial currents and to remove these.

The initial bathymetry used in all simulations regarding the mega-nourishment were generated by simulating the formation of the ebb-tidal delta for 30 years. This is enough for the formation of the ebb-tidal delta and to some extent the flood channels, however, it is still far from an equilibrium. As a result, changes in the bathymetry still occur in the simulations regarding the mega-feeder nourishment. It is debatable whether an equilibrium will ever be reached. However, it is still recommended to build an ebb-tidal delta closer to an equilibrium. Moreover, include a base run without a mega-feeder nourishment to investigate how much of the sediment transport is owing to the ebb-tidal delta (re)adjusting to an equilibrium.

Further research

The results of this thesis were validated by comparing the hydrodynamic results of the numerical models to observed data. The hypothesis is that if the model produces the hydrodynamics well then forcing used in the morphology will be roughly correct. This means that the morphology is not directly validated. As a result, the simplified morphodynamic results, as well as the morphodynamic results for the realistic time-varying hydrodynamic conditions, are hypothetical. It is recommended to validate the morphological results of the simplified simulations by comparing it to a real case (i.e. case study).

The oblique wave conditions were set up for a wave directed towards the tidal inlet with an angle of -45 degrees relative to shore-normal. In the results, it was clear that the updrift side of the tidal inlet has a lower magnitude of the residual currents than on the downdrift

side. Moreover, the residual currents on the updrift side were lower in reach and magnitude compared to all other hydrodynamic conditions scenarios. In this thesis, it was shown that the residual currents owing to the tidal inlet is an important process. Therefore, it is recommended to also conduct a scenario with a wave angle of 45 degrees relative to shore-normal to better understand the physics of what makes the wave angle matter.

The models were run for 6 years of morphological time-scale. This time-scale is too short to fully diffuse the sediment of the mega-nourishment along the coast. The sediment has diffused but mainly locally and to some extent into the tidal basin. It is recommended to increase the morphological time-scale to further investigate where the sediment will end up, be it in the tidal basin or bypassed around the tidal inlet.

Four simplified hydrodynamic condition scenarios and two more scenarios with real time-varying hydrodynamic conditions were investigated. The results of this thesis can be used to extrapolate to certain hydrodynamic conditions and estimate a parameter space. However, doing more simulations between the used hydrodynamic conditions will allow for better extrapolation of the results.

In this thesis, the hydrodynamics forcing was varied. The models were set up using fixed morphodynamic features, such as the dimensions of the tidal basin, tidal inlet and mega-feeder nourishment, but also the orientation of the tidal inlet. Varying, these morphodynamic features will likely have an impact on the development of a mega-feeder nourishment nearby a tidal inlet. Hence, investigating variable morphodynamic features will lead to valuable insights.

Bibliography

Jasper Bak. Nourishment strategies for Ameland Inlet. page 122, 2017.

D R Basco. *Overview of Beach Engineering in the United States of America: Final Report*. Coastal Engineering Centre, Old Dominion University, 1999. URL https://books.google.nl/books?id=rgV0uAAACAAJ.

Judith Bosboom and Marcel J F Stive. *Coastal Dynamics I*, volume 0.5. Delft Academic Press, Delft, 2015. ISBN 978-90-6562-3720.

T J Campbell and Lindino Benedet. Beach nourishment magnitudes and trends in the U.S. *Journal of Coastal Research*, 2004(39):57–64, 2004.

Kwok Fai Cheung, Franciscus Gerritsen, and Jelmer Cleveringa. Morphodynamics and Sand Bypassing at Ameland Inlet, The Netherlands. *Journal of Coastal Research*, 2007(231): 106–118, 2007. doi: 10.2112/04-0403.1. URL https://doi.org/10.2112/04-0403.1.

J L Davies and C A Moses. *A Morphogenic Approach to World Shorelines*. Coastal processes and coastal management. 1964. URL https://books.google.nl/books?id=jMLIoAEACAAJ.

Richard A. Davis and Miles O. Hayes. What is a Wave-Dominated Coast? *Developments in Sedimentology*, 39(C):313–329, 1984. ISSN 00704571. doi: 10.1016/S0070-4571(08)70152-3.

Matthieu A. de Schipper, Sierd de Vries, Gerben Ruessink, Roeland C. de Zeeuw, Jantien Rutten, Carola van Gelder-Maas, and Marcel J.F. Stive. Initial spreading of a mega feeder nourishment: Observations of the Sand Engine pilot project. *Coastal Engineering*, 111: 23–38, 2016. ISSN 03783839. doi: 10.1016/j.coastaleng.2015.10.011. URL http://dx.doi.org/10.1016/j.coastaleng.2015.10.011.

Deltares. Delft3D - WAVE (Simulation of short-crested waves with SWAN) [User Manual]. Technical report, 2014a.

Deltares. Delft3D 3D-FLOW user manual. Technical report, 2014b.

Deltaris. Achtergronddocument Morfologische berekeningen MER Zandmotor Deltares MER zandmotor. Technical Report November, Deltaris, 2009.

J Douglas Glaeser. Global Distribution of Barrier Islands in Terms of Tectonic Setting. *Journal of Geology*, 86, 1978. doi: 10.1086/649691.

Gary Egbert, Lana Erofeeva, and Laurence Padman. TPXO7.2: Global Inverse Tide Model, 2010. URL http://www.esr.org/polar_tide_models/Model_TPXO62.html.

Edwin P.L. Elias, Ad J.F. Van der Spek, Stuart G. Pearson, and Jelmer Cleveringa. Understanding sediment bypassing processes through analysis of high-frequency observations of Ameland Inlet, the Netherlands. *Marine Geology*, 415(November 2018):105956, 2019. ISSN 00253227. doi: 10.1016/j.margeo.2019.06.001. URL https://doi.org/10.1016/j.margeo.2019.06.001.

F. F. Escoffier. The stability of tidal inlets. *Shore and Beach*, 8(4), 1940.

B.P. Hageman. Development of the western part of the Netherlands during the Holocene. Technical report, 1969.

H. Hanson, A. Brampton, M. Capobianco, H. H. Dette, L. Hamm, C. Laustrup, A. Lechuga, and R. Spanhoff. Beach nourishment projects, practices, and objectives - A European overview. *Coastal Engineering*, 47(2):81–111, 2002. ISSN 03783839. doi: 10.1016/S0378-3839(02)00122-9.

Inc. Hartman Engineering. GRAND ISLE BARRIER SHORELINE STABILIZATION STUDY Preliminary Engineering Report Part 1 : Basis of Engineering. (2512), 2007.

Myles O. Hayes. Barrier Island Morphology as a Function of Tidal and Wave Regime. (July), 1979.

Giles R. Lesser, J. A. Roelvink, J. A.T.M. van Kester, and G. S. Stelling. Development and validation of a three-dimensional morphological model. *Coastal Engineering*, 51(8-9):883–915, 2004. ISSN 03783839. doi: 10.1016/j.coastaleng.2004.07.014.

L. Li, J. E.A. Storms, and D. J.R. Walstra. On the upscaling of process-based models in deltaic applications. *Geomorphology*, 304:201–213, 2018. ISSN 0169555X. doi: 10.1016/j.geomorph.2017.10.015.

Arjen Luijendijk, Gerben Hagenaars, Roshanka Ranasinghe, Fedor Baart, Gennadii Donchyts, and Stefan Aarninkhof. The State of the World's Beaches. *Scientific Reports*, 8(1), 2018. ISSN 20452322. doi: 10.1038/s41598-018-24630-6. URL http://dx.doi.org/10.1038/s41598-018-24630-6.

Arjen P. Luijendijk, Roshanka Ranasinghe, Matthieu A. de Schipper, Bas A. Huisman, Cilia M. Swinkels, Dirk J.R. Walstra, and Marcel J.F. Stive. The initial morphological response of the Sand Engine: A process-based modelling study. *Coastal Engineering*, 119 (September 2016):1–14, 2017. ISSN 03783839. doi: 10.1016/j.coastaleng.2016.09.005. URL http://dx.doi.org/10.1016/j.coastaleng.2016.09.005.

Arjen P. Luijendijk, Matthieu A. de Schipper, and Roshanka Ranasinghe. Morphodynamic acceleration techniques for multi-timescale predictions of complex sandy interventions. *Journal of Marine Science and Engineering*, 7(3), 2019. ISSN 20771312. doi: 10.3390/jmse7030078.

R. J. Nicholls, P.P. Wong, V.R. Burket, J. Codignotto, J.E. Hay, R.F. McLean, S. Ragoonaden, and C.D. Woodroffe. Coastal systems and low-lying areas. *Climate Change 2007: Impacts, Adaptation and Vulnerability.*, (January):315–356, 2007. doi: 10.1017/CBO9781107415379.

NOAA. Tides and Currents. URL https://tidesandcurrents.noaa.gov/.

NOAA National Centers for Environmental Information. Myrtle Beach, South Carolina 1/3 Arc-second MHW Coastal Digital Elevation Model, 2006. URL https://data.noaa.gov/metaview/page?xml=NOAA/NESDIS/NGDC/MGG/DEM/iso/xml/300.xml&view=getDataView&header=none#.

NOAA National Centers for Environmental Information. Southern Louisiana 1/3 arc-second NAVD 88 Coastal Digital Elevation Model, 2012. URL https://data.noaa.gov/metaview/page?xml=NOAA/NESDIS/NGDC/MGG/DEM/iso/xml/1521.xml&view=getDataView&header=none.

Albert Oost, Amrit Cado van der Lelij, Mark de Bel, Gu Oude Essink, and M.A.M. Löffler. De bruikbaarheid van het concept Zandmotor. 2016. URL deltareshttp://www.dezandmotor.nl/uploads/2016/09/rapport-bruikbaarheid-zandmotor-4-juli.pdf.

A. J. H. M. Reniers. Morphodynamic modeling of an embayed beach under wave group forcing. *Journal of Geophysical Research*, 109(C1):1–22, 2004. ISSN 0148-0227. doi: 10.1029/2002jc001586.

J. A. Roelvink and M. F.J. Stive. Bar-generating cross-shore flow mechanisms on a beach, 1989. ISSN 01480227.

Marcel Stive, Matthieu de Schipper, Arjen Luijendijk, Roshanka Ranasinghe, Jaap van Thiel De Vries, Stefan Aarninkhof, Carola van Gelder-Maas, Sierd de Vries, Martijn Henriquez, and Sarah Marx. The Sand Engine: a solution for vulnerable deltas in the 21st century? *Coastal Dynamics*, (June):1537–1546, 2013.

Matthew L. Stutz and Orrin H. Pilkey. Open-Ocean Barrier Islands: Global Influence of Climatic, Oceanographic, and Depositional Settings. *Journal of Coastal Research*, 272 (March 2011):207–222, 2012. ISSN 0749-0208. doi: 10.2112/09-1190.1.

Jas Sutherland, A. H. Peet, and R. L. Soulsby. Evaluating the performance of morphological models. *Coastal Engineering*, 51(8-9):917–939, 2004. ISSN 03783839. doi: 10.1016/j.coastaleng.2004.07.015.

M.D. Taal, M.A.M. Loffler, C.T.M. Vertegaal, J.W.M. Wijsman, L. Van der Valk, and P.K. Tonnon. Samenvattende rapportage over de eerste vier jaar van het Monitoring- en Evaluatie Programma (MEP). Technical report, 2016.

Hendrik L. Tolman. WaveWatch III, 2009. URL `https://polar.ncep.noaa.gov/waves/wavewatch/`.

National Oceanic US Department of Commerce and Atmospheric Administration. National Data Buoy Center, 2013. URL `http://www.ndbc.noaa.gov/`.

Mick van der Wegen. *Modeling morphodynamic evolution in alluvial estuaries*. 2010. ISBN 9780415592741. doi: 10.1201/b10824.

G van Heijst and M Wells. Dipole formation by tidal flow in a channel. *Shallow Flows*, pages 63–70, 2004. doi: 10.1201/9780203027325.ch7.

Leo C. van Rijn, Dirk-Jan R. Walstra, and Maarten van Ormondt. Unified View of Sediment Transport by Currents and Waves. IV: Application of Morphodynamic Model. *Journal of Hydraulic Engineering*, 133(7):776–793, 2007. ISSN 0733-9429. doi: 10.1061/(asce)0733-9429(2007)133:7(776).

John C. Warner, Charlene M. Sullivan, Marinna A. Martini, George Voulgaris, Paul A. Work, Kevin A. Hass, and Daniel Hanes. South Carolina Coastal Erosion Study Data Report for Observations October 2003 - April 2004. Technical report, 2006. URL `https://cmgds.marine.usgs.gov/publications/of2005-1429/`.

Kathelijne M. Wijnberg. Environmental controls on decadal morphologic behaviour of the Holland coast. *Marine Geology*, 189(3-4):227–247, 2002. ISSN 00253227. doi: 10.1016/S0025-3227(02)00480-2.

Provincie Zuid-Holland. Projectnota/MER Aanleg en zandwinning Zandmotor Delflandse kust. Technical report, Provincie Zuid-Holland, 2010.

A

Hydrodynamic validation

Appendix A aim is to validate the hydrodynamics of the simplified models. Two locations with distinct characteristics are chosen which represent the simplified models well. Both locations also have extensive data available which allows for a good validation of the hydrodynamics. The first location is Myrtle Beach, which is used to validate the currents imposed by a tidal range (about 1.5 m) and waves (higher than 1 m). The second location is Grand Isle, which is used to validate the currents in a complex tidal system.

A.1. Myrtle Beach

Myrtle Beach is located at the Atlantic coast in the state South Carolina. Extensive data is available for Myrtle Beach, which allows for the validation of currents, water levels and wave heights.

The observed current, water level and wave data are obtained from the South Carolina Coastal Erosion Study (Warner et al. [2006]). This study made observations at 8 different locations (sites) in Long Bay, South Carolina. The observations were made from October 2003 to April 2004. The site with the shallowest depth is used to compare the hydrodynamics, this is site 2. The observations include water level, current and wave data. Moreover, the data only allows for the model to be run during the time-span of the field campaign. The model is ran for one month during February 2004.

A.1.1. Model setup

Grid and bathymetry

The model at Myrtle Beach is set up using one computational grid. This grid is rectilinear and is about 28 kilometers long in the alongshore direction and extends about 19 kilometers in the cross-shore direction. The grids have a spatially uniform resolution of 200 by 200 meters resulting in 139 by 96 cells. Wave breaking is most likely not captured well with this setup, however, there are no observation points in the breaker zone. The horizontal coordinate system of the model is located in UTM zone 18S. The vertical datum of the models are relative to MSL.

The bathymetry is obtained from NOAA's National Geophysical Data Center (NGDC). This institute is building a high-resolution digital elevation models (DEM) for U.S. coastal regions. The Myrtle Beach bathymetry (NOAA National Centers for Environmental Information [2006]) has a resolution of 1/3 Arc-seconds, which is approximately 10 by 10 meters. The coordinate system used in the bathymetry data is relative to World Geodetic System 1984 (WGS84). Therefore, the bathymetry is first converted to the UTM zone 18S coordinate system. Fur-

thermore, the vertical datum of the bathymetry data is relative to MHW. The model is relative to MSL, therefore the bathymetry is translated downwards by the difference between MSL and MHW at Myrtle Beach, which is -0.762 meter (NOAA).

Initial and boundary conditions and forcing

The water levels are initially set at zero height relative to MSL. These initial conditions induce instabilities in the form of artificial waves propagating through the domain. These waves are dampened out by bottom friction.

The FLOW domain is forced by a water level at the boundary of the FLOW grid. The water level is determined by tidal constituents found at Myrtle Beach. These tidal constituents were obtained from the TPXO 7.2 Global Inverse Tide Model. TPXO is a series of fully-global models of ocean tides, which best-fits, in a least-squares sense, the Laplace Tidal Equations and altimetry data (Egbert et al. [2010]). The WAVE domain is forced by waves at the boundary of the WAVE domain. The wave data is obtained from WaveWatch III (WW3). WW3 solves the random phase spectral action density balance equation for wavenumber-direction spectra (Tolman [2009]).

At last the model is spatially uniformly forced by the wind. The wind data was obtained from measuring station MROS1 Springmaid Pier, Myrtle Beach, South Carolina (US Department of Commerce and Administration [2013]). The wind data during February 2004 is extracted from this measuring station.

A.1.2. Hydrodynamic results

The models are run for one month. This gives sufficient data for different wave conditions and to make a comparison with the available observed hydrodynamic data. The modelled water levels show a good resemblance with the observed water levels (Figure A.1). The currents, in general, have the right order of magnitude. However, the currents are also often not correct. It is hypothesized that wind induced currents are not well captured by Delft3D. Often the model simulated a peak in the magnitude of the currents while that was not observed (for example the peak at 13 February, Figure A.1). These peaks do coincide with peaks in the wind data, suggesting that wind cannot be discarded at Myrtle Beach.

The modelled and observed significant wave height are almost similar (Figure A.2). At 26 February there is a peak in the wave height which again coincides with the peak in the wind speeds. Emphasizing the importance of wind in the generation and growth of wind induced waves. The peak period is often significantly higher than the modelled peak periods. This is most likely due to errors in either the boundary or the measuring devices, since the peak period signal which has been measured is quite wobbly. The peak direction is generally also well captured by the model.

Based on the results from Myrtle Beach it can be concluded that the waves are well captured with the model and the currents are in the right order of magnitude. Therefore it is expected that the simplified model will also capture waves and currents well at the shoreface up to the surf-zone.

Figure A.1: The modelled currents are depicted in blue and the measured currents (US Department of Commerce and Ad-

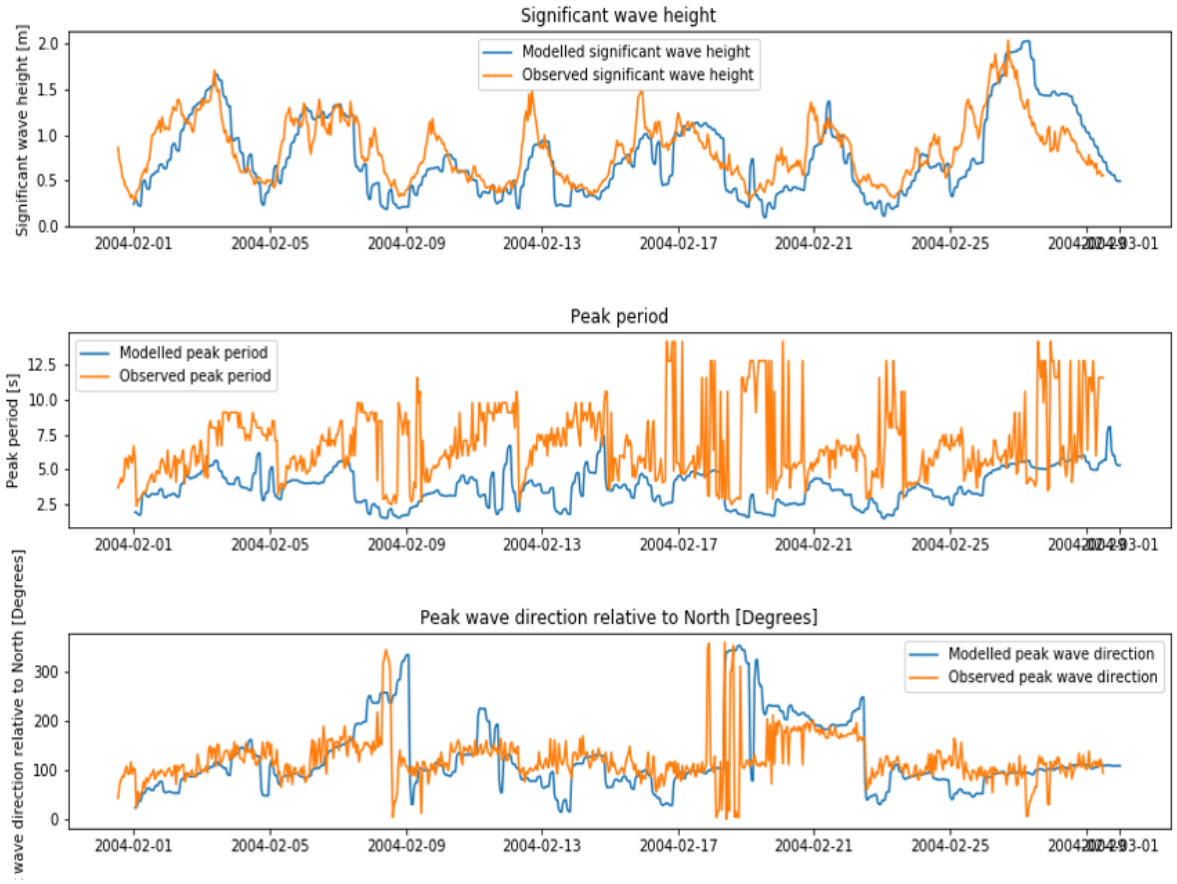

Figure A.2: The modelled waves are depicted in blue and the measured waves (US Department of Commerce and Administration [2013]) are shown in orange. The top figure shows the significant wave height. The middle figure shows the peak period of the waves and the bottom figure shows the peak wave direction relative to North.

A.2. Grand Isle

Grand Isle is located in the Gulf of Mexico, more specifically, in the state Louisiana. Grand Isle is one of the barrier islands in the Mississippi Delta. At Grand Isle many studies have been done. Therefore, extensive data available for Grand Isle. This data includes water level and current data in the tidal inlet.

The observed current and water level data from inside the tidal inlet are obtained from the "Grand Isle Barrier Stabilization Study" (Hartman Engineering [2007]). In this study a field campaign was organized in which at both sides of the Grand Isle barrier island, inside the tidal inlet, currents and water levels were measured. The tidal inlet used for the hydrodynamic validation is called the "Barataria Inlet". This tidal inlet is the largest tidal inlet of Grand Isle. The hydrodynamic data was requested from Hartman Engineering and obtained from the engineering company Mott MacDonald. The data was available from 10-August 2005 to 12-November 2005. However, it was strongly advised to not use the data after 28-August 2005 since the instruments got buried in a layer of sand after hurricane Katrina hit the Mississippi Delta.

A.2.1. Model setup

Grid and bathymetry

The model at Grand Isle consist of two computational grids. Each of these grids are rectilinear. The first grid is the course outer grid, which has a resolution of 250 by 250 meters. This grid has a length of 44 kilometers in the alongshore direction and is about 56 kilometers long in the cross-shore direction. The majority of the 56 kilometers is owing to the large tidal basin. The course outer grid results in 177 cells in the alongshore direction and 250 cells in the cross-shore direction.

The second grid is the fine inner grid. This fine grid captures the hydrodynamics in more detail at the ebb-tidal delta and tidal inlet. These are the locations where the most detailed hydrodynamics are desired. The fine inner grid is nested inside the course outer grid and has a resolution of 50 by 50 meters. The fine inner grid is about 5 kilometers long in the alongshore direction and 7 kilometers long in the cross-shore direction. The coordinate system used in the model is UTM zone 15R. The vertical datum is relative to MSL.

The Grand Isle bathymetry is obtained from NGDC (NOAA National Centers for Environmental Information [2012]) and has a resolution of 1/3 Arc-seconds, which is approximately 10 by 10 meters. The bathymetry coordinate system is relative to WGS84. Therefore, the bathymetry is first converted to the UTM zone 15R coordinate system. Furthermore, the vertical datum of the bathymetry data is relative to MHW. The model is relative to MSL, therefore the bathymetry is translated downwards by the difference between MSL and MHW at Grand Isle, which is -0.159 meter (NOAA).

Initial and boundary conditions and forcing

The water levels are initially set at zero height relative to MSL. These initial conditions induce instabilities in the form of artificial waves propagating through the domain. These waves are dampened out by bottom friction.

The FLOW domain is forced by a water level at the boundary of the FLOW grid. The water level is determined by tidal constituents found at Grand Isle. These tidal constituents were obtained from the TPXO 7.2 Global Inverse Tide Model (Egbert et al. [2010]). The WAVE domain is forced by waves at the boundary of the WAVE domain. The wave data is obtained from WaveWatch III (WW3) (Tolman [2009]).

The model is spatially uniformly forced by the wind. No wind data was available within the model domain. The closest wind data was from the mouth of the Mississippi delta about

50 kilometers from the domain, station BURL1 (28.905N 89.428W) (US Department of Commerce and Administration [2013]). The wind data during August 2005 is extracted from this measuring station.

A.2.2. Hydrodynamic results

The models are run from 10-August 2005 to 28-August 2004. This gives sufficient data and is the maximum range which can be compared to the observed hydrodynamics data found in the tidal inlet. The results of the modelled and observed water levels and current data inside the tidal inlet are shown in Figure A.1. The modelled water levels are almost similar to the observed water levels. Moreover, the currents are also well represented in the model. The magnitude and directions of the currents have similar magnitudes and shapes as the one observed. The r-squared value between the modelled and observed current magnitude is 0.80. Furthermore, the r-squared value between the modelled and observed water level is 0.83. Both values are close to one and therefore the modelled hydrodynamics yield a good representation of the observed hydrodynamics.

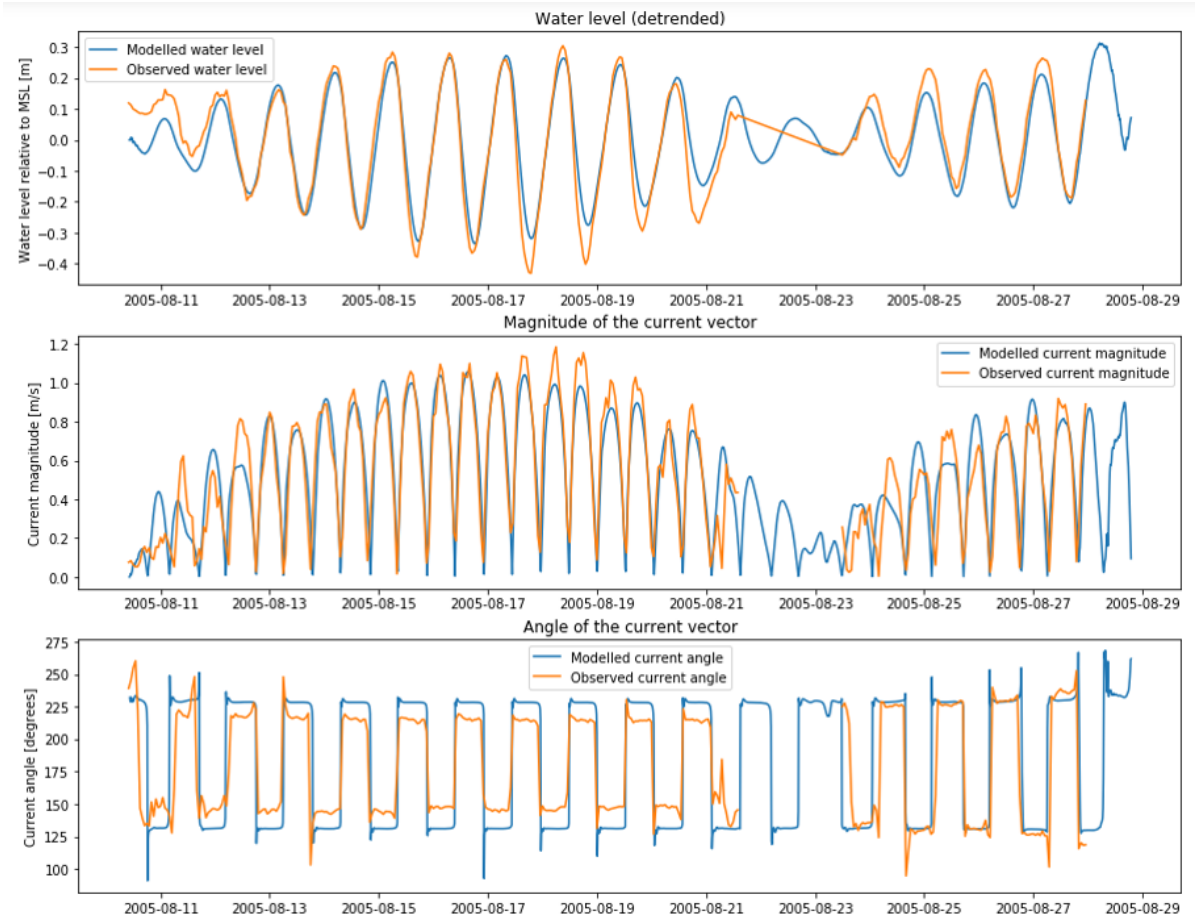

Figure A.3: Modelled and observed hydrodynamics at Grand Isle, Louisiana, USA. The modelled currents are depicted in blue and the measured currents (US Department of Commerce and Administration [2013]) are shown in orange. The top figure shows the water levels compared to MSL. The middle figure shows the magnitude of the currents vector and the bottom figure shows the direction angle of the current vector relative to North.

Based on the results from Grand Isle it can be concluded that the hydrodynamics inside a tidal inlet is captured well by the model. The water levels, as well as the currents, are both almost similar to the observed water levels and currents. Therefore, the hydrodynamics of the model inside a tidal inlet are validated.

B

Realistic model results

B.1. Residual currents

Overall, there is a tide averaged current at the tip of the barrier island in all realistic simulations (see Figure B.1). The tidal currents have a high magnitude (order of several meters per second) at the center of the tidal inlet. The tidal current cannot spread out fast enough due to the momentum of the tidal current. This generates a flow towards the tidal inlet at the adjacent barrier island tips. However, it can be seen that there is a flow towards the tidal inlet with the tidal inlet being closed too. This suggests that the tide averaged currents with the tidal inlet being closed, are generated by waves. Owing to the orientation of the shore with respect to the waves an alongshore flow is generated at the tips of the barrier islands.

The right column shows the tide averaged currents owing to the tidal inlet, which is the difference between the open and closed tidal inlet flow field (RTF currents). In all hydrodynamic conditions, the RTF currents are directed towards the tidal inlet at the tips of the barrier island. The magnitude of the RTF currents seems to diminish fairly quickly (order several hundreds of meters to a few kilometers) from the tidal inlet towards the mega-nourishment. In general, the RTF current owing to the tidal inlet does reach the centroid of the mega-nourishment at 2 kilometers from the tidal inlet. However, does not reach further than the centroid of the mega-nourishment. With the mega-nourishment at 5km from the tidal inlet, the effects of the RTF currents are not present at the mega-nourishment.

The RTF currents are not significantly different from the RTF currents of the mild wave conditions (Figure 4.5). The reach of RTF currents in the real tide and real wave is about the same as for the mild wave conditions. The magnitude of the RTF currents in the real tide is slightly lower than for the mild wave conditions. The magnitude of the RTF currents for the real tide is also lower than for the real wave. This difference is most apparent at the bank on the inlet-side of the tidal inlet, where the magnitude and reach of the RTF currents are larger for the real wave.

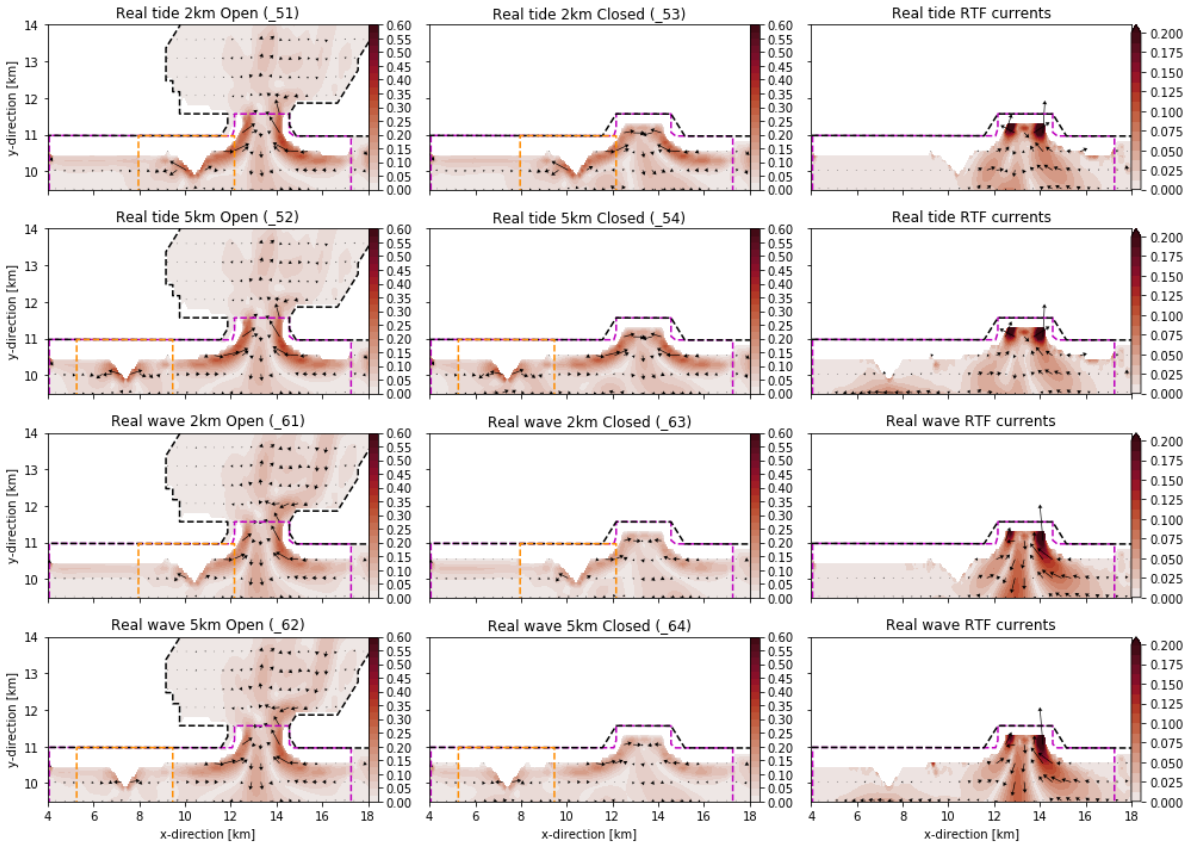

Figure B.1: Tide averaged and RTF currents for the real tide and real waves simulations. The rows are alternating with the mega-nourishment being 2 kilometers and 5 kilometers from the mega-nourishment. The left column shows the tide averaged currents with an open tidal inlet, the center column shows the tide averaged currents with the tidal inlet being closed and the right column shows the difference in the tide averaged currents between the tidal inlet being open and closed, which are called the RTF currents.

B.2. Total alongshore sediment transport

Real tides

The total alongshore sediment transport (TAST) for the real tide is similar to that of the mild wave conditions (see Figure B.2). On the non-inlet-side of the centroid of the mega-nourishment, the TAST first increases in magnitude after which it gradually decreases towards a zero TAST. On the inlet-side of the mega-nourishment, the TAST first increases towards a local maximum, after which it gradually decreases and then increases towards a maximum TAST at the boundary of the t3 grid. The magnitudes of the TAST for both the tidal inlet being open and closed, are similar to the mild wave conditions. The TAST of the tidal inlet being open is slightly lower compared to the mild wave conditions. As a result, the absolute difference in the TAST (RTF TAST) is also slightly lower. The averaged tidal range is 1.3 m for the real tide. This is also slightly lower than the 1.5 meter for the mild wave conditions. As a result, so are the reach and magnitude of the RTF currents and RTF TAST.

Real waves

The TAST of the real wave conditions are shifted upwards (more downstream directed TAST, towards the tidal inlet) compared to the simplified mild wave conditions (see Figure B.3). The average wave angle for the real wave conditions is -15 degrees relative to shore-normal (see chapter 3.3.1). This will result in an average TAST along the non-perturbed shore to be non-zero. The averaged TAST at the non-inlet-side boundary is about 220 $m^3/6y/m$. Whereas,

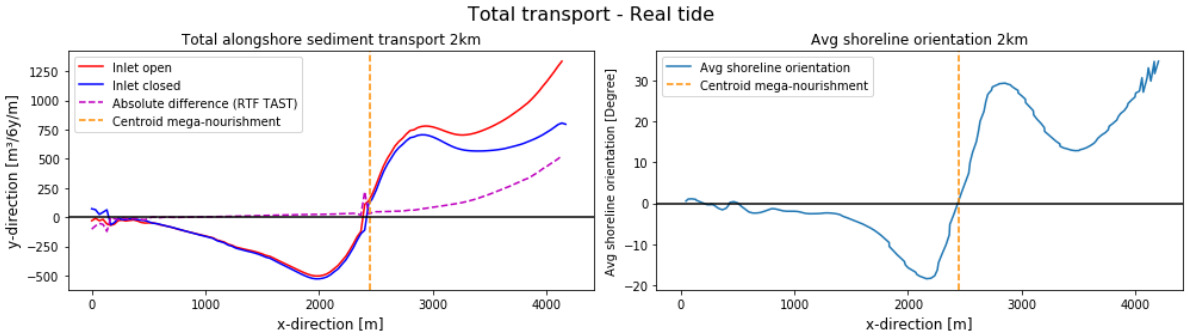

Figure B.2: Total alongshore sediment transport real tide over 6 years with the mega-nourishment at 2km from the tidal inlet. The left figure shows the TAST for the tidal inlet being open (blue) and closed (red) and the RTF TAST (purple). The right figure shows the average shoreline orientation.

for the mild wave conditions the TAST at the non-inlet-side boundary was zero.

The RTF TAST of the real wave conditions is slightly smaller compared to the mild wave conditions. However, it still has the same trend as the RTF TAST of the mild wave conditions. The wave angle does influence the RTF TAST. The magnitude is reduced but the reach is similar to that of the mild wave conditions. As a result, the RTF TAST has characteristics of the RTF TAST found for the oblique wave conditions.

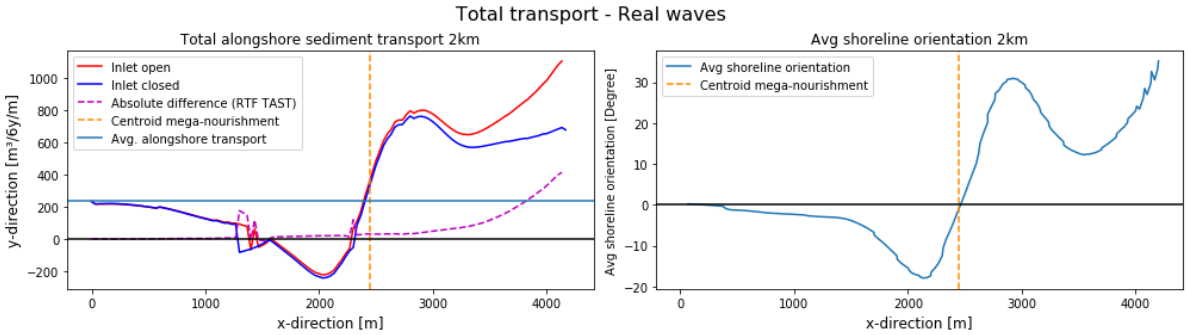

Figure B.3: Total alongshore sediment transport real wave over 6 years with the mega-nourishment at 2km from the tidal inlet. The left figure shows the TAST for the tidal inlet being open (blue) and closed (red) and the RTF TAST (purple). The right figure shows the average shoreline orientation.

B.3. Morphological development of the mega-feeder nourishment

Real tide

The shoreline development of the real tide is similar to that of the mild wave conditions with the mega-nourishment at an alongshore distance of 2km from the tidal inlet. The average tidal range for the real tide is 1.3 meters. Which is slightly smaller than for the mild wave conditions. Therefore, the shoreline development of the real tide should be somewhat similar to the mild wave conditions. Therefore, the tidal inlet does not have an influence on the development of the mega-nourishment, with the mega-nourishment at an alongshore distance of 5km from the tidal inlet (see Appendix E).

However, the tidal inlet does influence the development of a mega-nourishment with the mega-nourishment at an alongshore distance of 2km from the tidal inlet. The mega-nourishment diffuses fast during the first 2 years after which the shoreline retreat at the tip of the mega-nourishment slows down (see Figure B.4). The shoreline retreat is 145, 70 and 55 meters from 2008 to 2010, from 2010 to 2012 and from 2012 to 2014 respectively. This is similar to that of the mild wave conditions. Furthermore, the tip propagates towards the non-inlet-side as the inlet-side side erodes more. This effect can be seen for both the tidal inlet being open and closed. Similarly to the mild wave conditions the coast to the non-inlet-side of the mega-nourishment accretes by up to 100 meters during the first two years after which this slows down. As a result, the beach slope becomes steeper.

The development of the shoreline over time is also similar to that of the mild wave conditions. On the inlet-side of the mega-nourishment, there is a difference in the gained/lost shoreline with the tidal inlet being open and closed. This difference has a maximum of 33.3 meters at the last time-step, which is significant compared to the zero meter change in the shoreline over time for both the tidal inlet being open as well as closed.

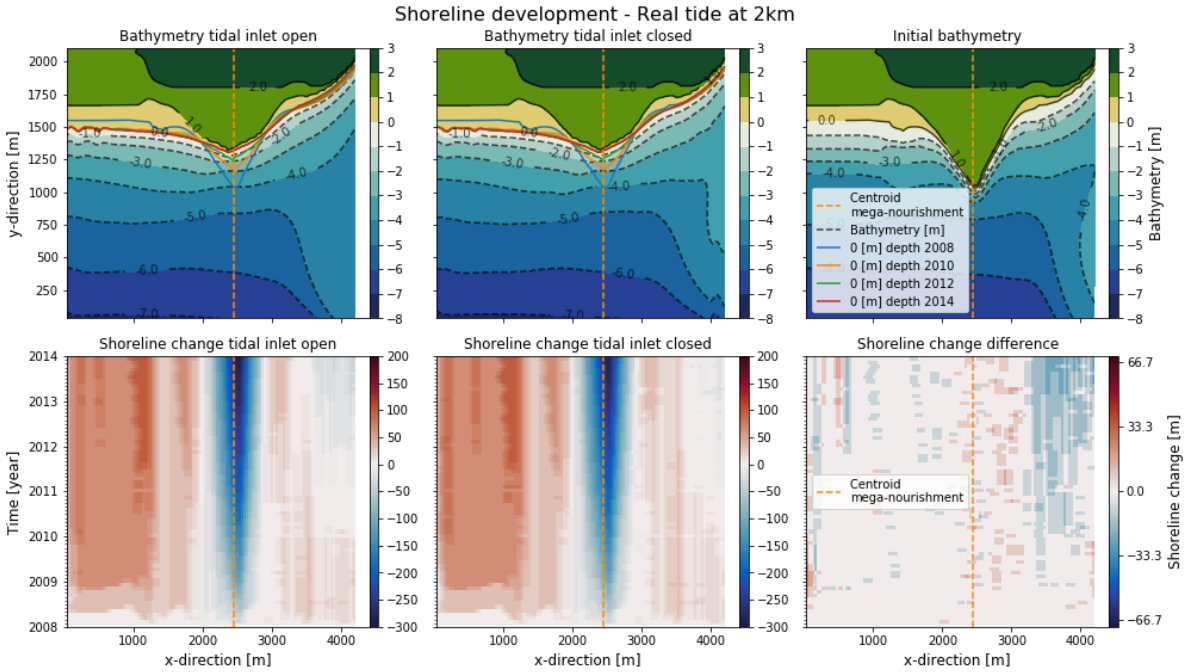

Figure B.4: Shoreline development for real tide. The first row shows the bathymetry and the shoreline over time. The blue, orange, green, red and dashed orange lines show the zero meter depth contour at the years 2008, 2010, 2012, 2014 and centroid of the mega-nourishment respectively. The second row shows the gained or lost shore with respect to the initial shoreline. Red shades indicate the gained shore compared to the first time step (2008) and blue shows shore being lost. Furthermore, the first column shows the results for the tidal inlet being open. The second column shows the results for the tidal inlet being closed. At last the top right figure shows the initial bathymetry and the bottom left figure shows the difference between the gained shoreline between the tidal inlet being open and closed.

Real waves

The shoreline development for the real waves is also similar to that of the mild wave conditions with the mega-nourishment at an alongshore distance of 2km from the tidal inlet. The waves have an average height of 0.8 meters and an averaged direction of -15 degrees relative to shore-normal (see Chapter 3.3.1). Therefore, the hydrodynamic conditions best represents the mild wave conditions. Similarly to the real tide and mild wave conditions, the mega-nourishment is not influenced by the tidal inlet with the mega-nourishment at an alongshore distance of 5km from the tidal inlet (see Appendix E).

Contrary to the mild wave conditions and real tides, there is more shoreline gained on the inlet-side of the mega-nourishment, with the mega-nourishment at 2km from the tidal inlet. This effect is present for both the tidal inlet being open and closed (see bottom row in Figure B.5). However, the difference in gained shoreline between the tidal inlet being open and closed is similar to that of the mild wave conditions and real tide. The maximum difference at the last time-step is 33.3 meters. This caused shoreline retreat with the tidal inlet being open and about a zero net shoreline change with the tidal inlet being closed, towards the tidal inlet. Therefore, the tidal inlet has an effect on the development of the adjacent shoreline over time.

Moreover, the mega-nourishment diffuses fast during the first 2 years after which the shoreline retreat at the tip of the mega-nourishment slows down (see Figure B.4). The shoreline retreat is 165, 60 and 40 meters from 2008 to 2010, from 2010 to 2012 and from 2012 to 2014 respectively. This is slightly different from that of the mild wave conditions. Furthermore, the tip propagates towards the non-inlet-side as the inlet-side erodes more. This effect can be seen for both the tidal inlet being open and closed. Similarly to the mild wave conditions the coast to the non=inlet-side of the mega-nourishment accretes by up to 100 meters during the first two years after which this slows down. As a result, the beach slope becomes steeper.

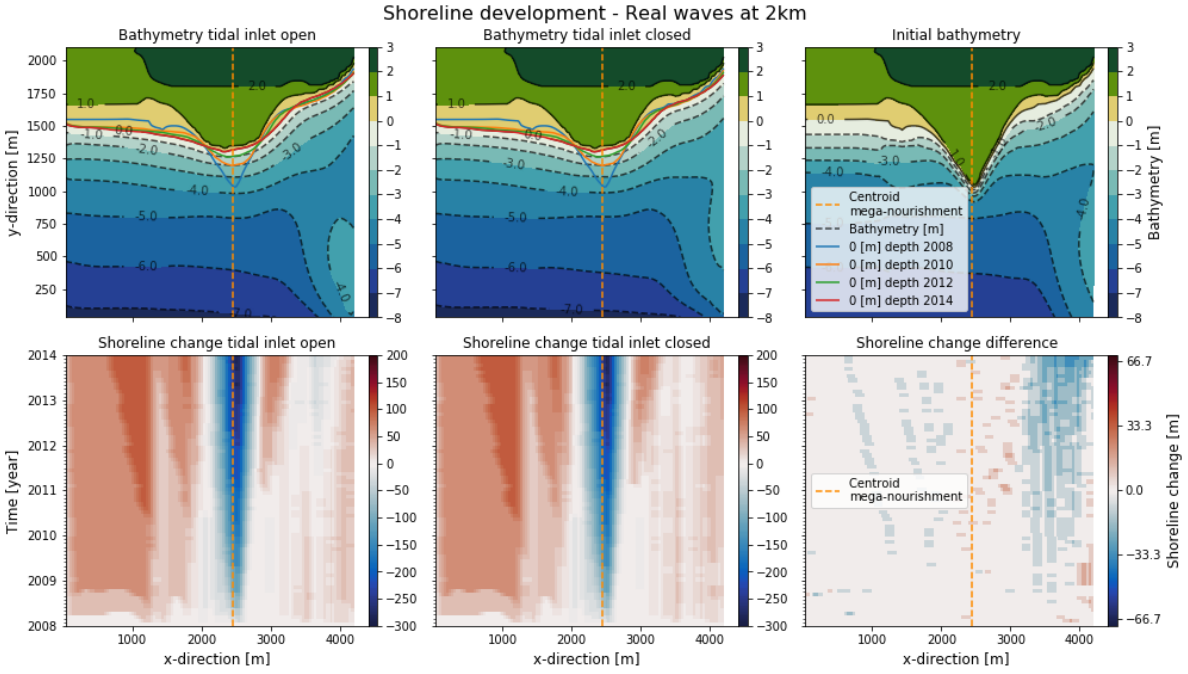

Figure B.5: Shoreline development for real wave. The first row shows the bathymetry and the shoreline over time. The blue, orange, green, red and dashed orange lines show the zero meter depth contour at the years 2008, 2010, 2012, 2014 and centroid of the mega-nourishment respectively. The second row shows the gained or lost shore with respect to the initial shoreline. Red shades indicate the gained shore compared to the first time step (2008) and blue shows shore being lost. Furthermore, the first column shows the results for the tidal inlet being open. The second column shows the results for the tidal inlet being closed. At last the top right figure shows the initial bathymetry and the bottom left figure shows the difference between the gained shoreline between the tidal inlet being open and closed.

B.4. Chapter summary

The realistic simulations use hydrodynamic conditions which are found in reality. The hydrodynamic conditions of the real tide and real wave simulations best represent the mild wave conditions of the simplified models. The results of the simplified models were already summarized in chapter 4.5 and will therefore not be repeated here. However, the similarities and differences will be shown.

Residual currents

The RTF currents are not significantly different from the RTF currents of the mild wave conditions. The reach of RTF currents for the real tide and real wave is about the same as for the mild wave conditions. The magnitude of the real tide is slightly lower than for the mild wave conditions. The magnitude of the RTF current for the real tide is lower than for the real wave as the tidal range of the real tide is lower too.

RTF total alongshore sediment transport

The TAST and RTF TAST of the real tide is similar to the mild wave conditions (see Figure B.6). However, the TAST of the real wave conditions is different from that of the mild wave conditions (see Figure B.6). There is a TAST of 220 $m^3/6y/m$ on average whereas this is 0 $m^3/6y/m$ for the mild wave conditions. Moreover, the RTF TAST of the real wave simulation is slightly lower than for the mild wave conditions. However, the mild wave conditions do still best represent the real wave simulations. But an increased average TAST and reduced RTF TAST means that the real wave also has characteristics from the oblique wave conditions as the average wave angle is -15 degree relative to shore-normal.

There is virtually no RTF TAST with the mega-nourishment at 5km from the tidal inlet. The RTF TAST is about zero over the entire x-direction (see Figure B.6). This means that the tidal inlet does not have an influence on the mega-nourishment at a distance of 5km from the tidal inlet.

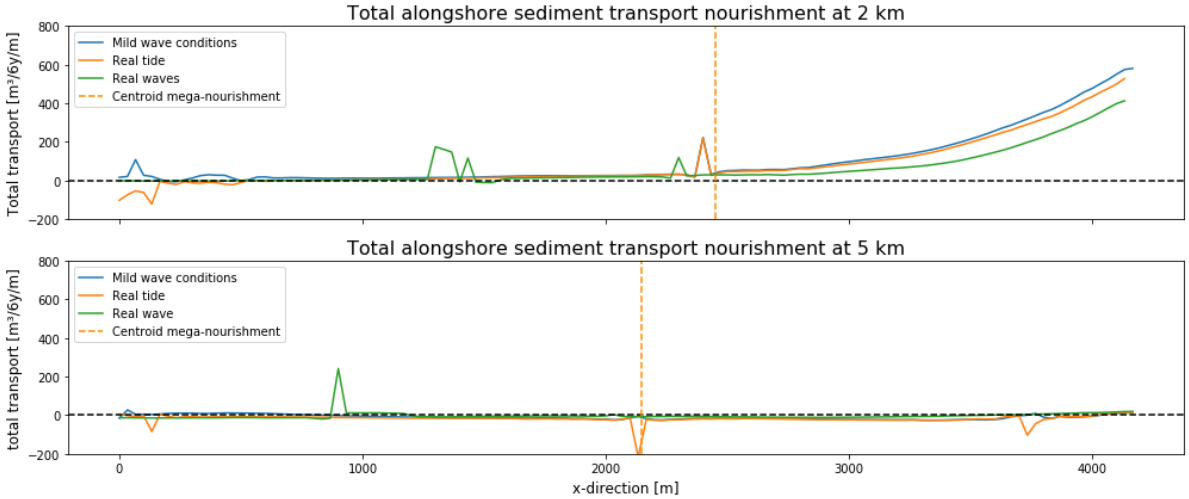

Figure B.6: Total alongshore sediment transport owing to the tidal flow (RTF TAST) in the tidal inlet for all simulations over 6 years. The top figure shows the RTF TAST owing to the RTF current caused by the tidal inlet, with the mega-nourishment at 2km from the tidal inlet. The bottom figure shows the RTF TAST with the mega-nourishment at 5km from the tidal inlet. In both figures the blue, orange, green and red lines shows the total alongshore RTF sediment transport for the mild wave conditions, oblique wave conditions, storm wave conditions and high tidal range.

Morphological development of the mega-feeder nourishment

The development of the shoreline of the real tide conditions are similar to that of the mild wave conditions. Emphasizing that simplifying a real tidal signal represents the real tidal signal well and do not cause a different morphological behavior. The maximum difference between an open tidal inlet and closed tidal inlet is again 33.3 meters.

The development of the shoreline of the real wave conditions is somewhat different from the mild wave conditions and real tide. The adjacent shoreline on the inlet-side of the mega-nourishment gains more shoreline compared to the mild wave conditions and real tide (see Figure B.7). However, the difference between the tidal inlet being open and closed at the last time-step is 33.3 meters. This is again similar to the mild wave conditions. Therefore, the real wave conditions also represent the mild wave conditions well. However, the difference emphasizes that the incident wave angle affects the gained/lost shoreline owing to the tidal inlet.

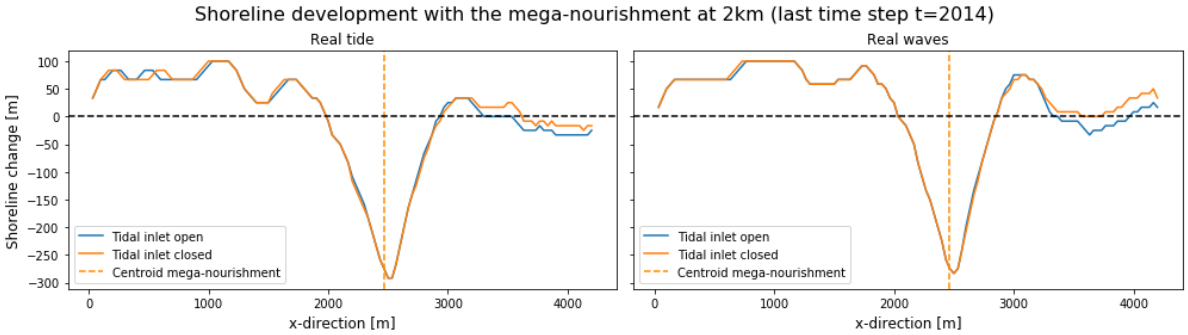

Figure B.7: This figure shows the change in shoreline at the last time-step (t=2014) for all simulations with the mega-nourishment at 2km from the tidal inlet. The change in shoreline (0-meter depth contour) is the difference between the shoreline at t=2014 and the initial shoreline at t=2008. Where a negative number indicates a shoreline retreat and a positive number indicates a shoreline gain.

C

Wave characteristics at the mega-nourishment

C.1. Significant wave height

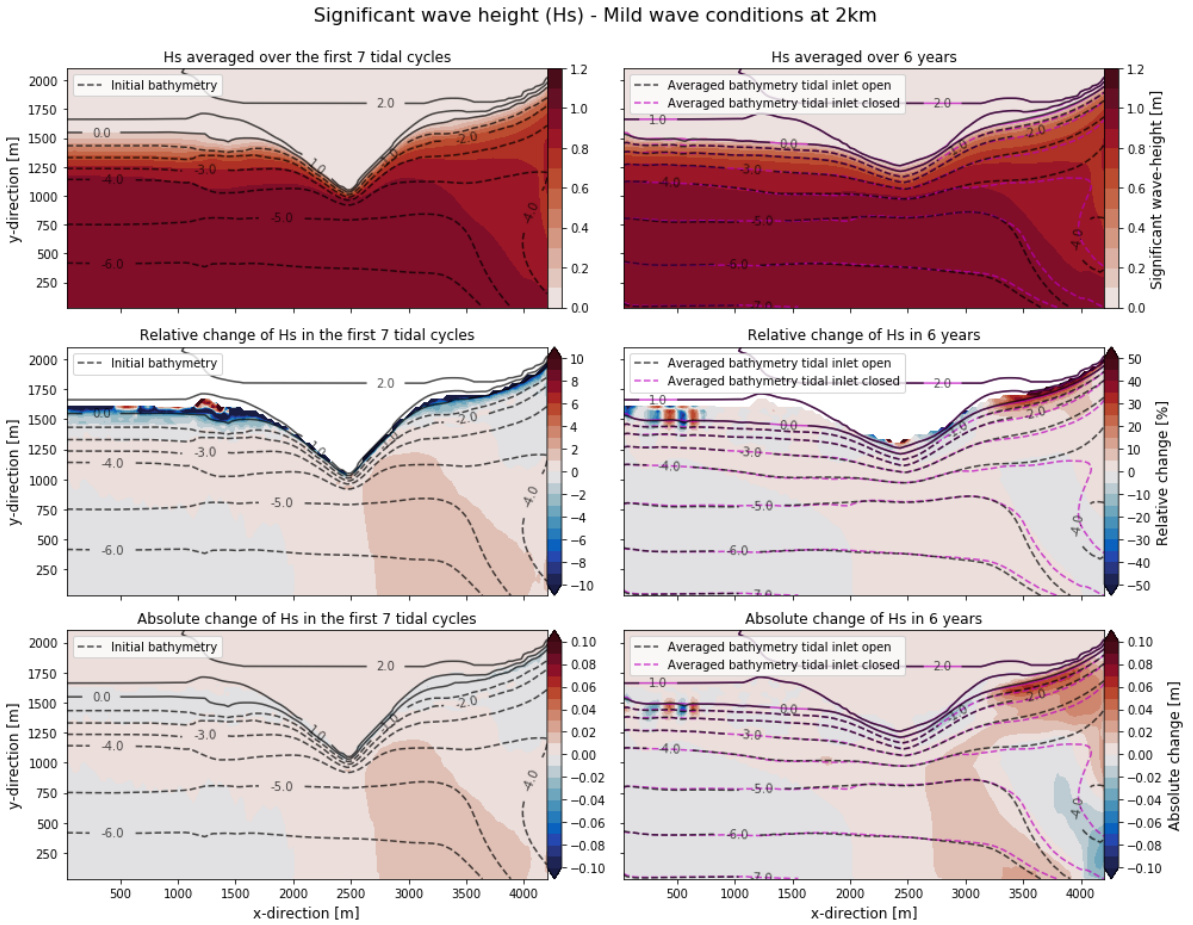

Figure C.1: Significant wave height (hs) mild wave conditions at 2km from the tidal inlet. The first column shows the significant wave height averaged over the first 7 tidal cycles and the second column shows the hs averaged over 6 years. The first row shows the averaged hs, the second row shows the relative difference in hs between the tidal inlet being open and closed. The third row shows the absolute difference in hs between the tidal inlet being open and closed.

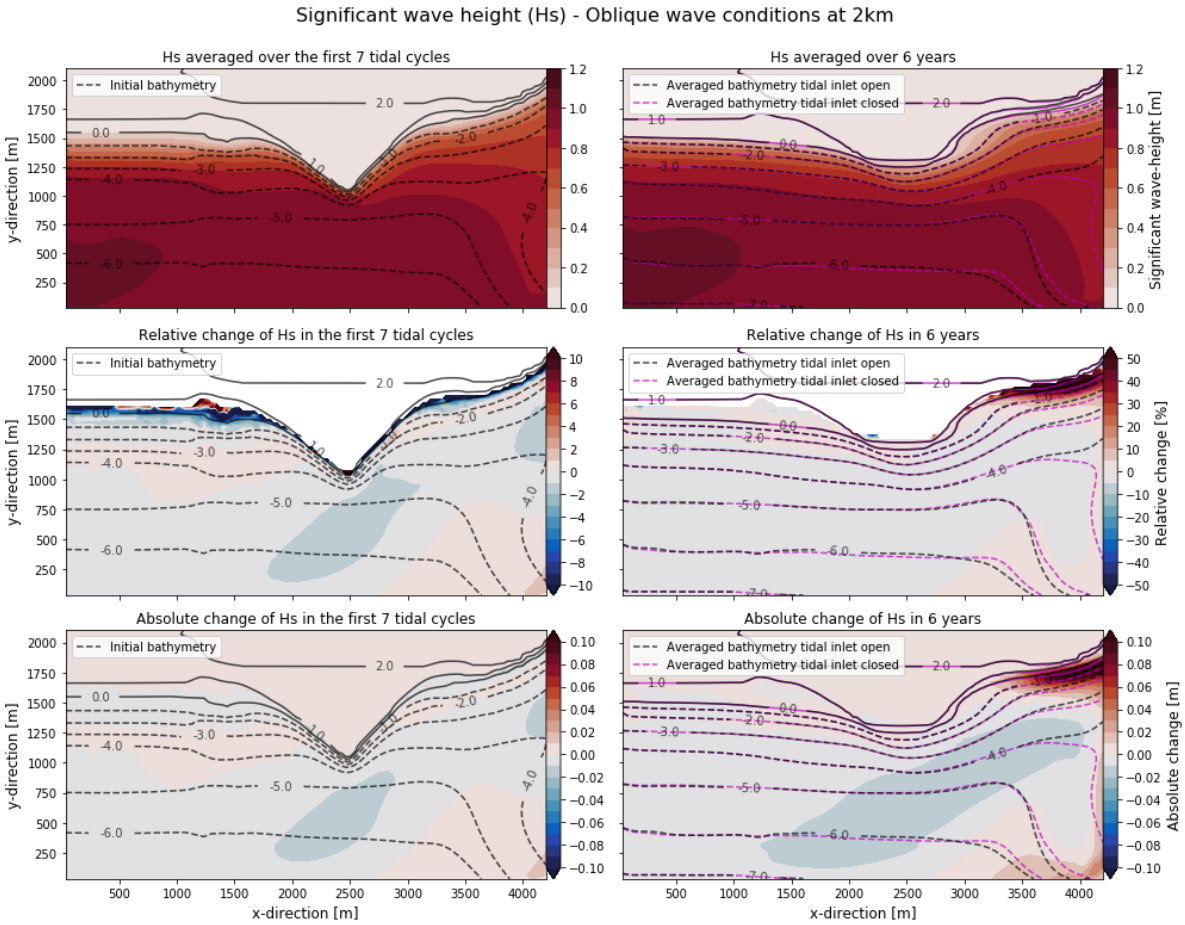

Figure C.2: Significant wave height (hs) oblique at 2km from the tidal inlet. The first column shows the significant wave height averaged over the first 7 tidal cycles and the second column shows the hs averaged over 6 years. The first row shows the averaged hs, the second row shows the relative difference in hs between the tidal inlet being open and closed. The third row shows the absolute difference in hs between the tidal inlet being open and closed.

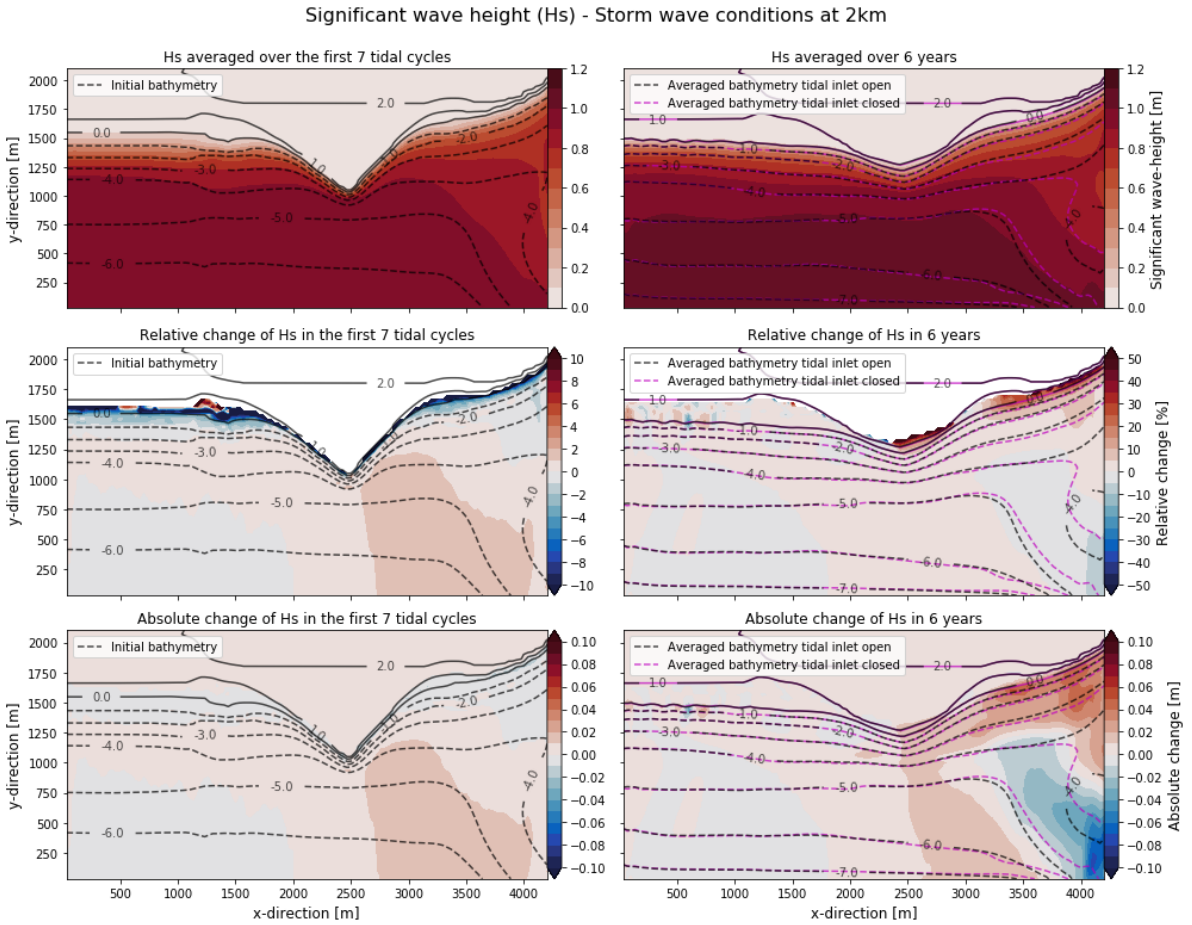

Figure C.3: Significant wave height (hs) storm wave conditions at 2km from the tidal inlet. The first column shows the significant wave height averaged over the first 7 tidal cycles and the second column shows the hs averaged over 6 years. The first row shows the averaged hs, the second row shows the relative difference in hs between the tidal inlet being open and closed. The third row shows the absolute difference in hs between the tidal inlet being open and closed.

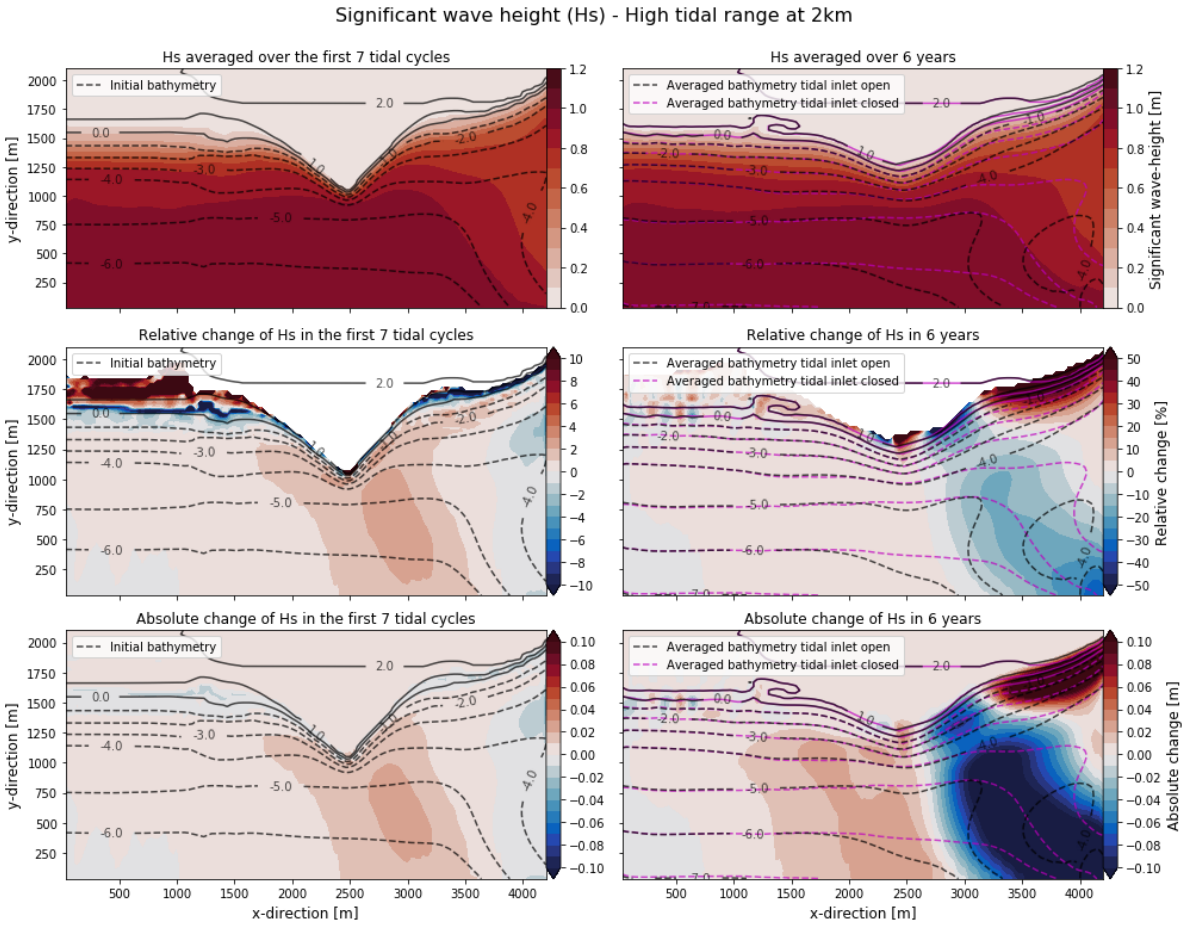

Figure C.4: Significant wave height (hs) high tidal range at 2km from the tidal inlet. The first column shows the significant wave height averaged over the first 7 tidal cycles and the second column shows the hs averaged over 6 years. The first row shows the averaged hs, the second row shows the relative difference in hs between the tidal inlet being open and closed. The third row shows the absolute difference in hs between the tidal inlet being open and closed.

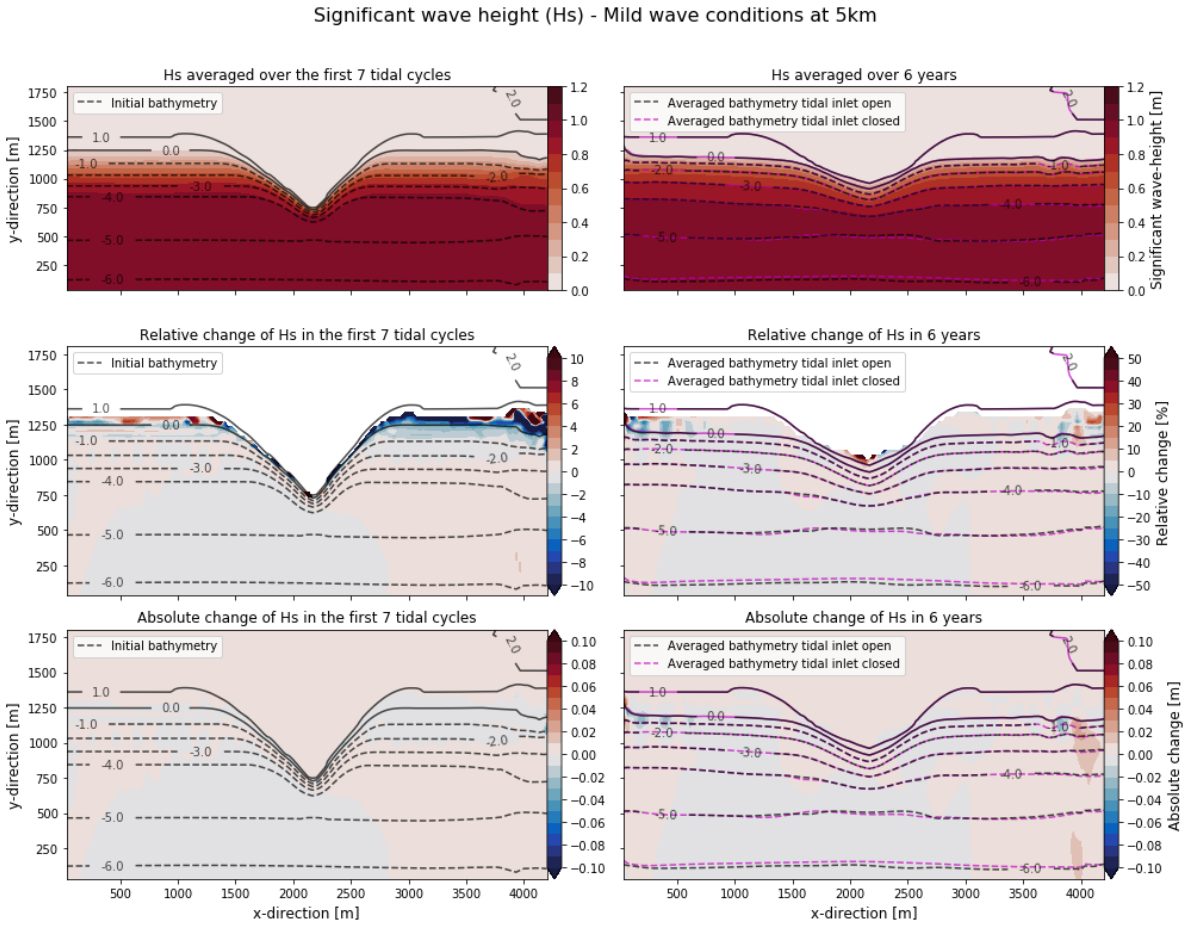

Figure C.5: Significant wave height (hs) mild wave conditions at 5km from the tidal inlet. The first column shows the significant wave height averaged over the first 7 tidal cycles and the second column shows the hs averaged over 6 years. The first row shows the averaged hs, the second row shows the relative difference in hs between the tidal inlet being open and closed. The third row shows the absolute difference in hs between the tidal inlet being open and closed.

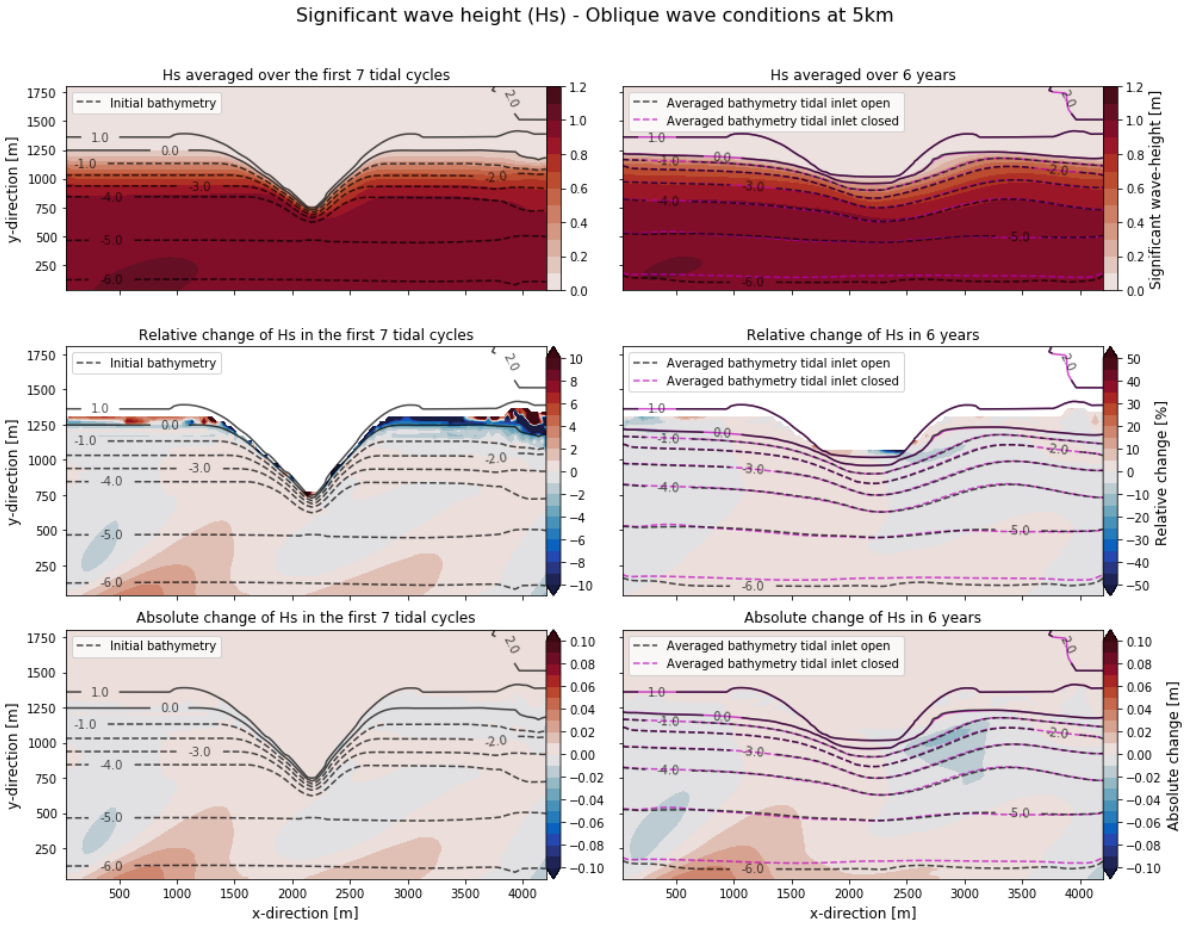

Figure C.6: Significant wave height (hs) oblique wave conditions at 5km from the tidal inlet. The first column shows the significant wave height averaged over the first 7 tidal cycles and the second column shows the hs averaged over 6 years. The first row shows the averaged hs, the second row shows the relative difference in hs between the tidal inlet being open and closed. The third row shows the absolute difference in hs between the tidal inlet being open and closed.

C.2. Wave length

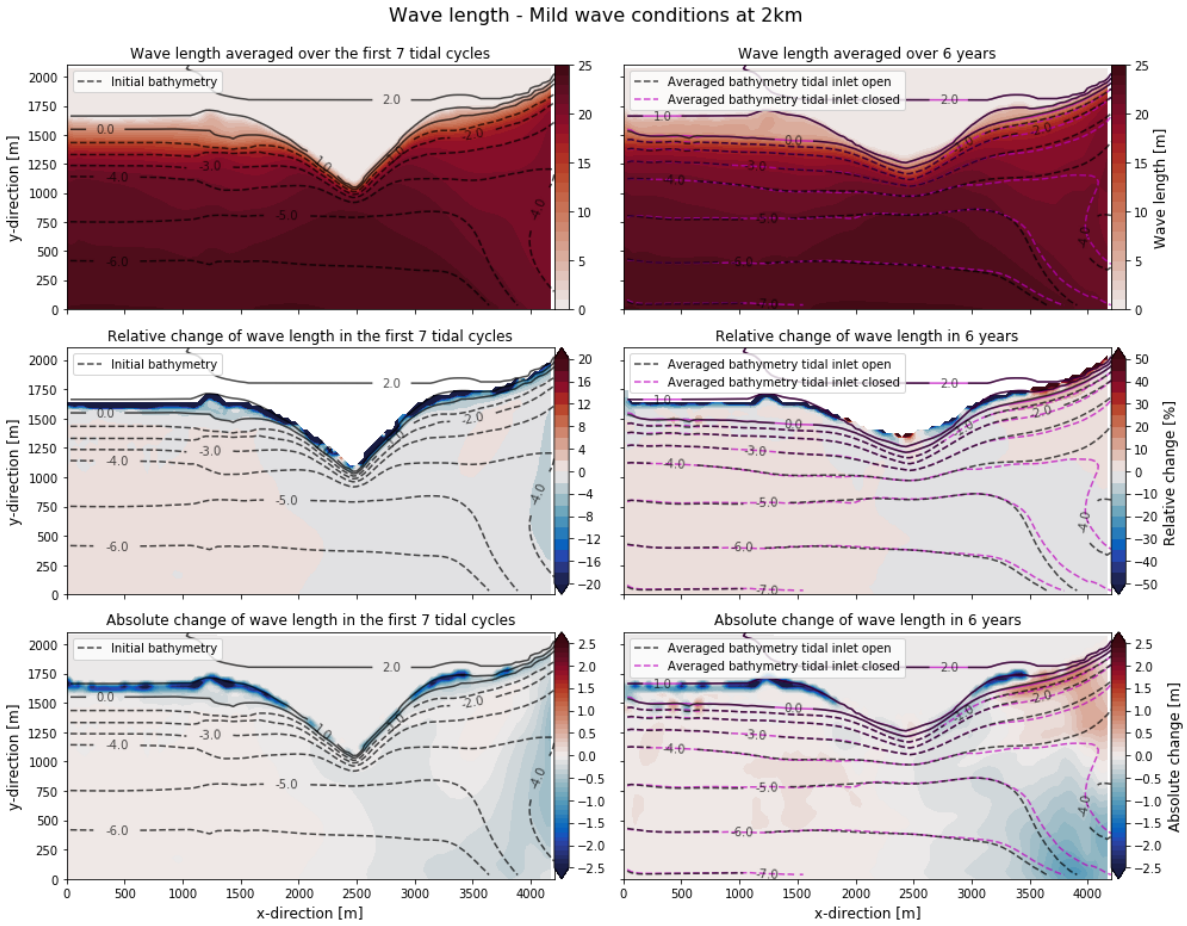

Figure C.7: Wave length mild wave conditions at 2km from the tidal inlet. The first column shows the wave length averaged over the first 7 tidal cycles and the second column shows the wave length averaged over 6 years. The first row shows the averaged wave length, the second row shows the relative difference in the wave length between the tidal inlet being open and closed. The third row shows the absolute difference in the wave length between the tidal inlet being open and closed.

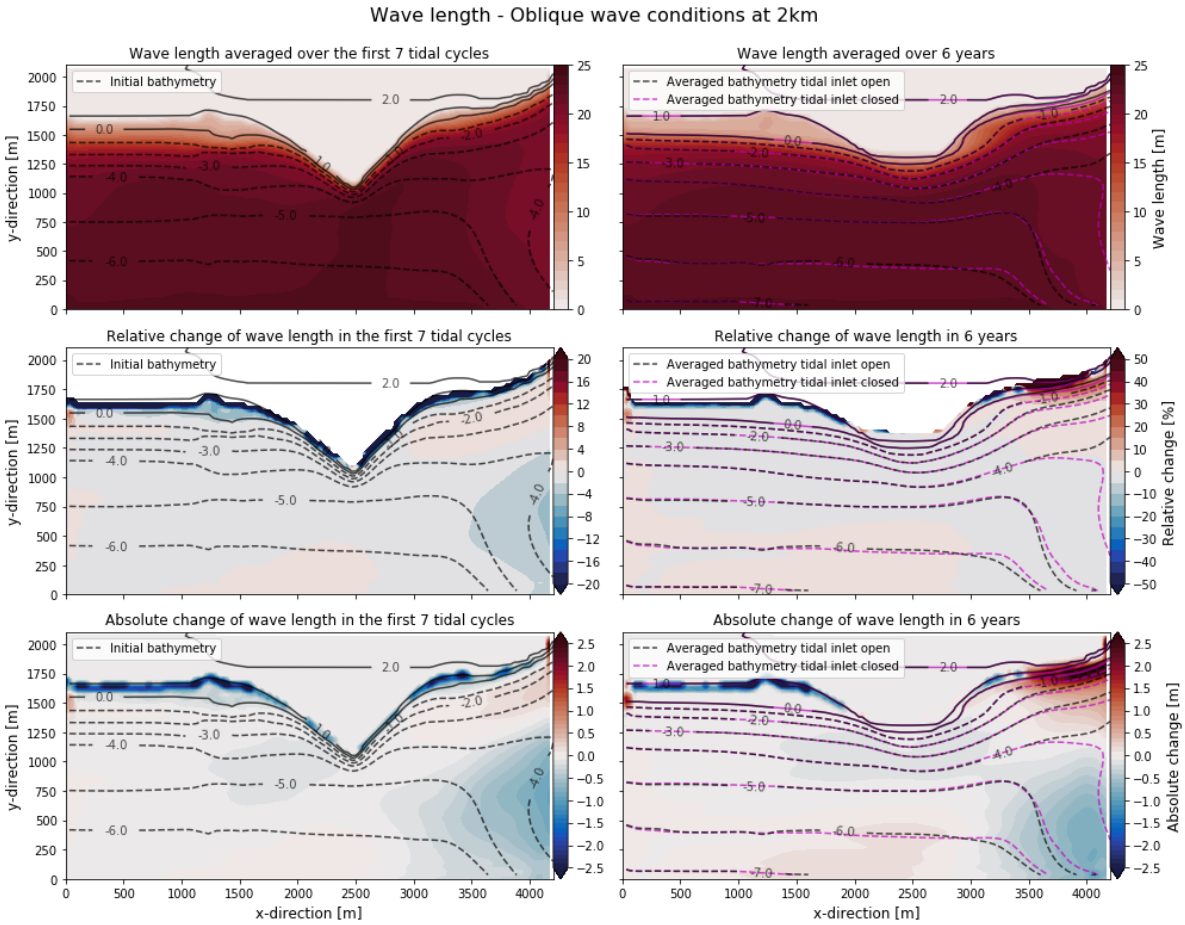

Figure C.8: Wave length oblique wave conditions at 2km from the tidal inlet. The first column shows the wave length averaged over the first 7 tidal cycles and the second column shows the wave length averaged over 6 years. The first row shows the averaged wave length, the second row shows the relative difference in the wave length between the tidal inlet being open and closed. The third row shows the absolute difference in the wave length between the tidal inlet being open and closed.

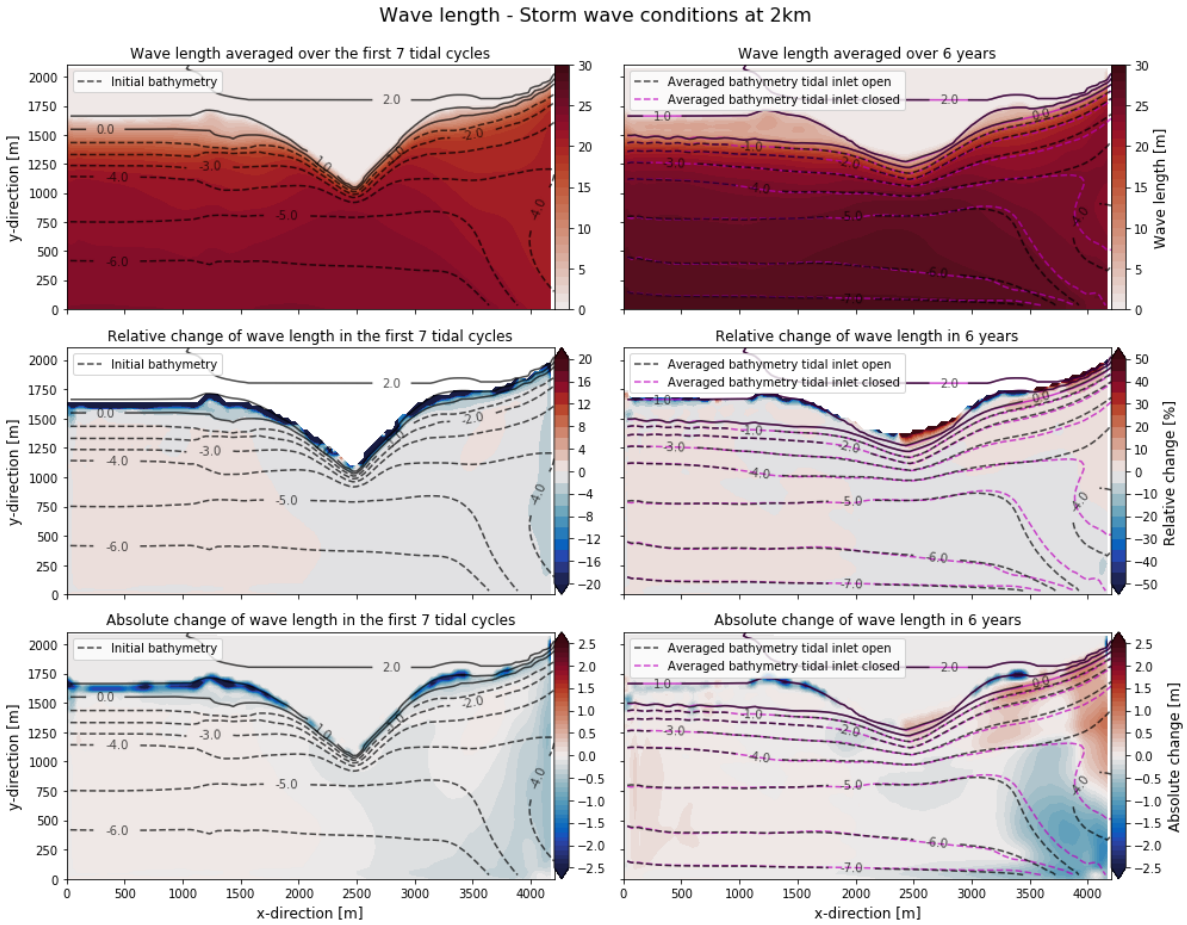

Figure C.9: Wave length storm wave conditions at 2km from the tidal inlet. The first column shows the wave length averaged over the first 7 tidal cycles and the second column shows the wave length averaged over 6 years. The first row shows the averaged wave length, the second row shows the relative difference in the wave length between the tidal inlet being open and closed. The third row shows the absolute difference in the wave length between the tidal inlet being open and closed.

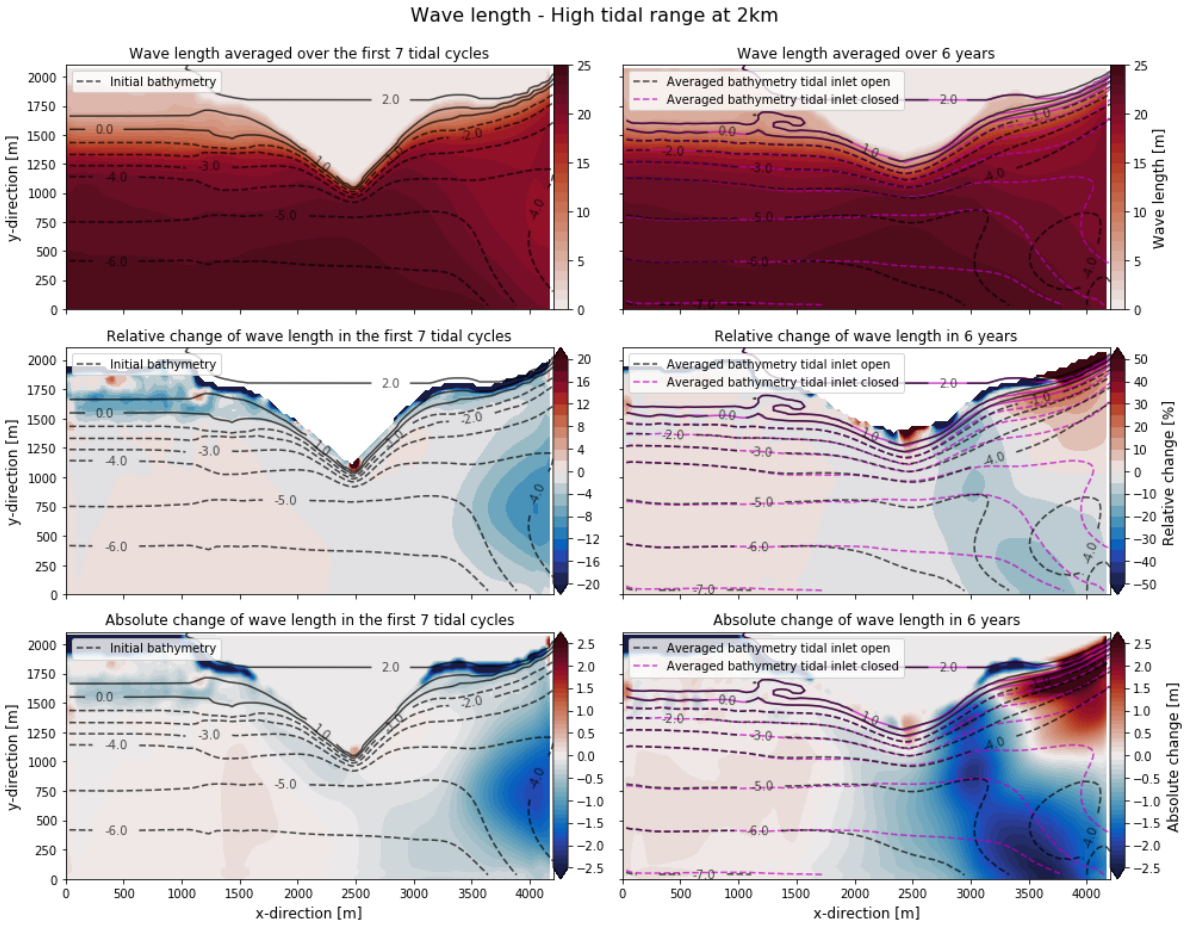

Figure C.10: Wave length high tidal range at 2km from the tidal inlet. The first column shows the wave length averaged over the first 7 tidal cycles and the second column shows the wave length averaged over 6 years. The first row shows the averaged wave length, the second row shows the relative difference in the wave length between the tidal inlet being open and closed. The third row shows the absolute difference in the wave length between the tidal inlet being open and closed.

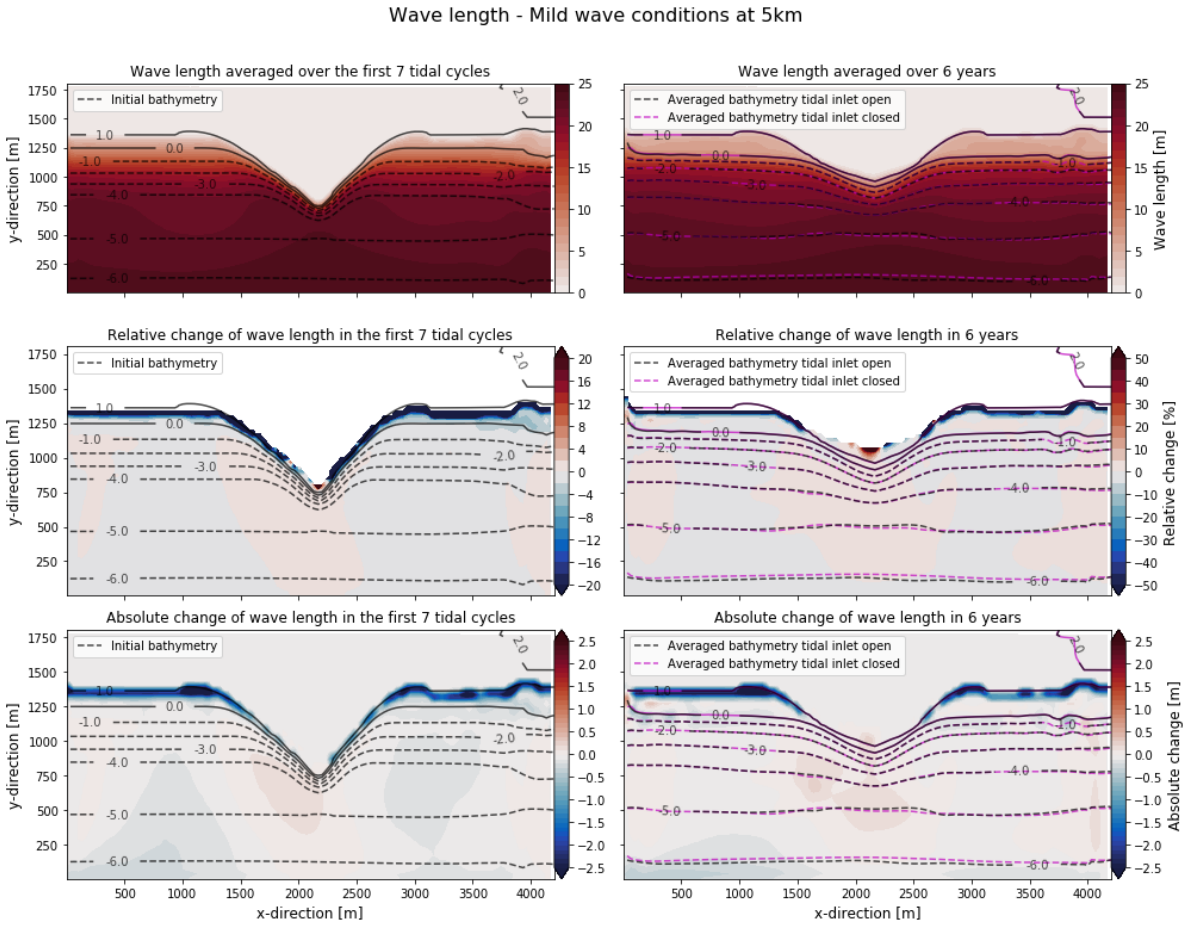

Figure C.11: Wave length mild wave conditions at 5km from the tidal inlet. The first column shows the wave length averaged over the first 7 tidal cycles and the second column shows the wave length averaged over 6 years. The first row shows the averaged wave length, the second row shows the relative difference in the wave length between the tidal inlet being open and closed. The third row shows the absolute difference in the wave length between the tidal inlet being open and closed.

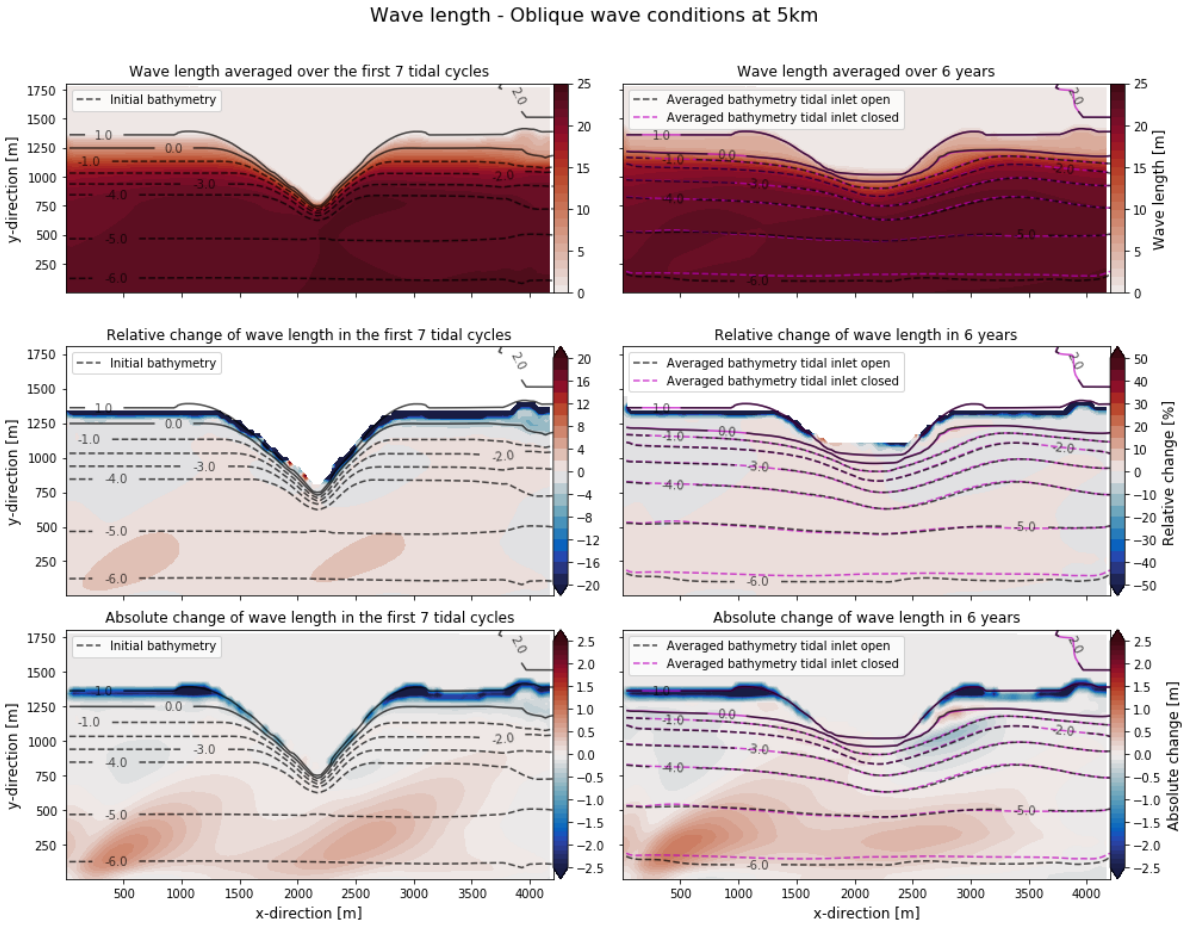

Figure C.12: Wave length oblique wave conditions at 5km from the tidal inlet. The first column shows the wave length averaged over the first 7 tidal cycles and the second column shows the wave length averaged over 6 years. The first row shows the averaged wave length, the second row shows the relative difference in the wave length between the tidal inlet being open and closed. The third row shows the absolute difference in the wave length between the tidal inlet being open and closed.

C.3. Wave direction

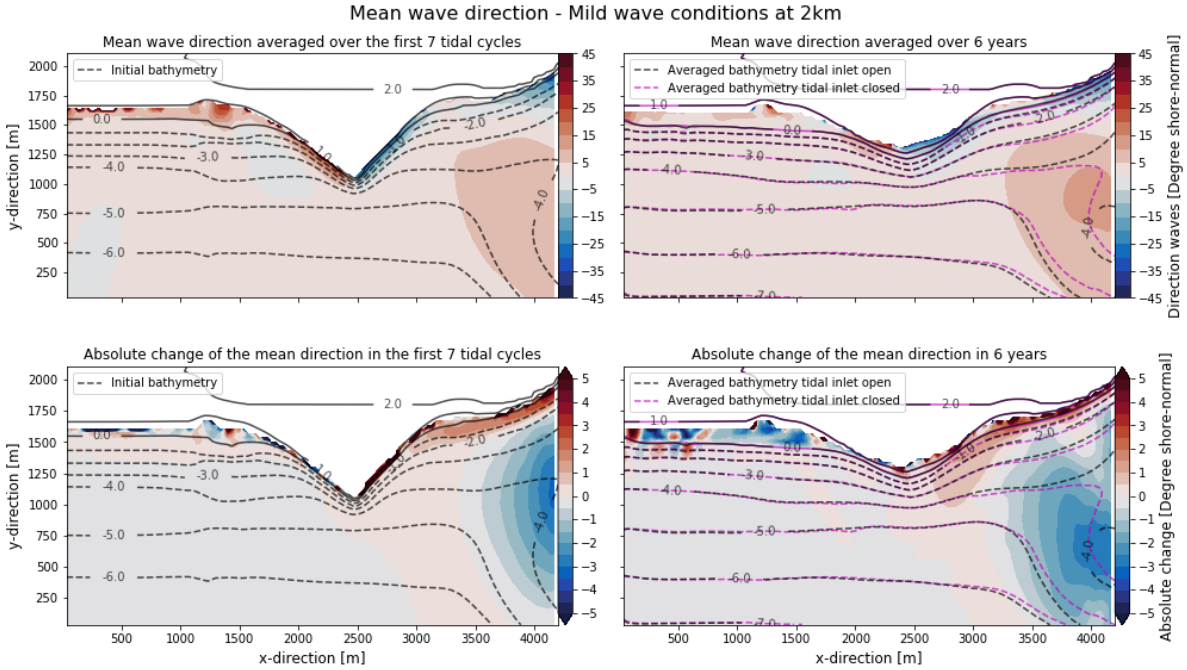

Figure C.13: Peak wave direction for storm wave conditions at 2km from the tidal inlet. The first column shows the peak wave direction averaged over the first 7 tidal cycles and the second column shows the peak wave direction averaged over 6 years. The first row shows the averaged peak wave direction, the second row shows the relative difference in the peak wave direction between the tidal inlet being open and closed. The third row shows the absolute difference in the peak wave direction between the tidal inlet being open and closed.

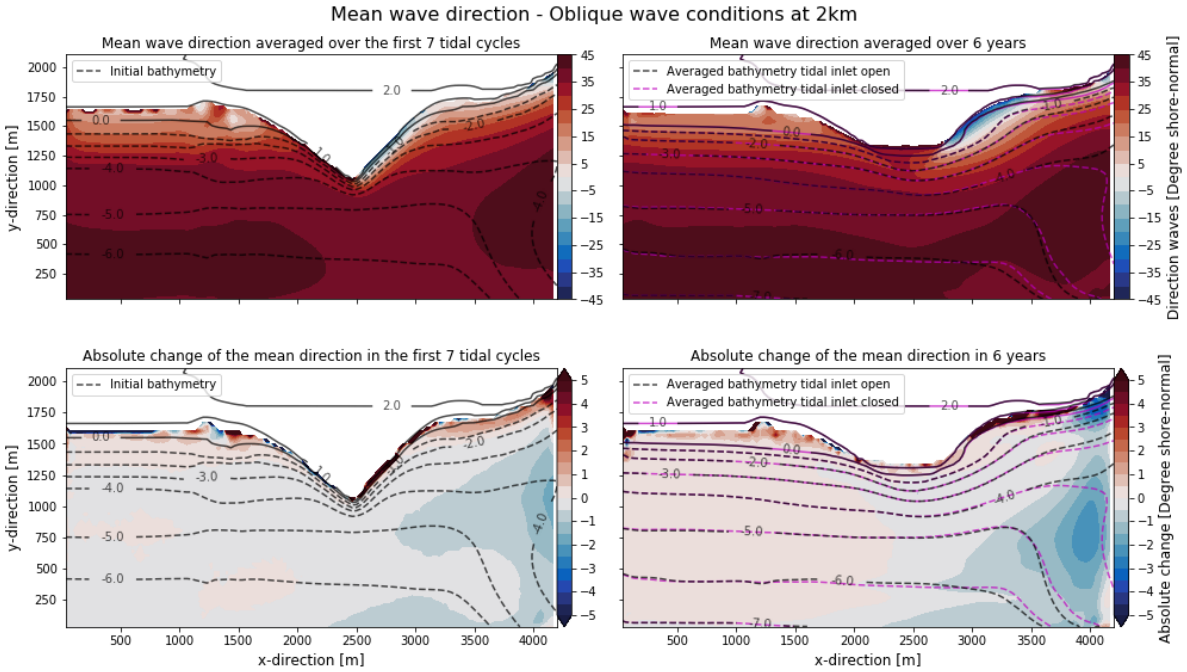

Figure C.14: Peak wave direction for oblique wave conditions at 2km from the tidal inlet. The first column shows the peak wave direction averaged over the first 7 tidal cycles and the second column shows the peak wave direction averaged over 6 years. The first row shows the averaged peak wave direction, the second row shows the relative difference in the peak wave direction between the tidal inlet being open and closed. The third row shows the absolute difference in the peak wave direction between the tidal inlet being open and closed.

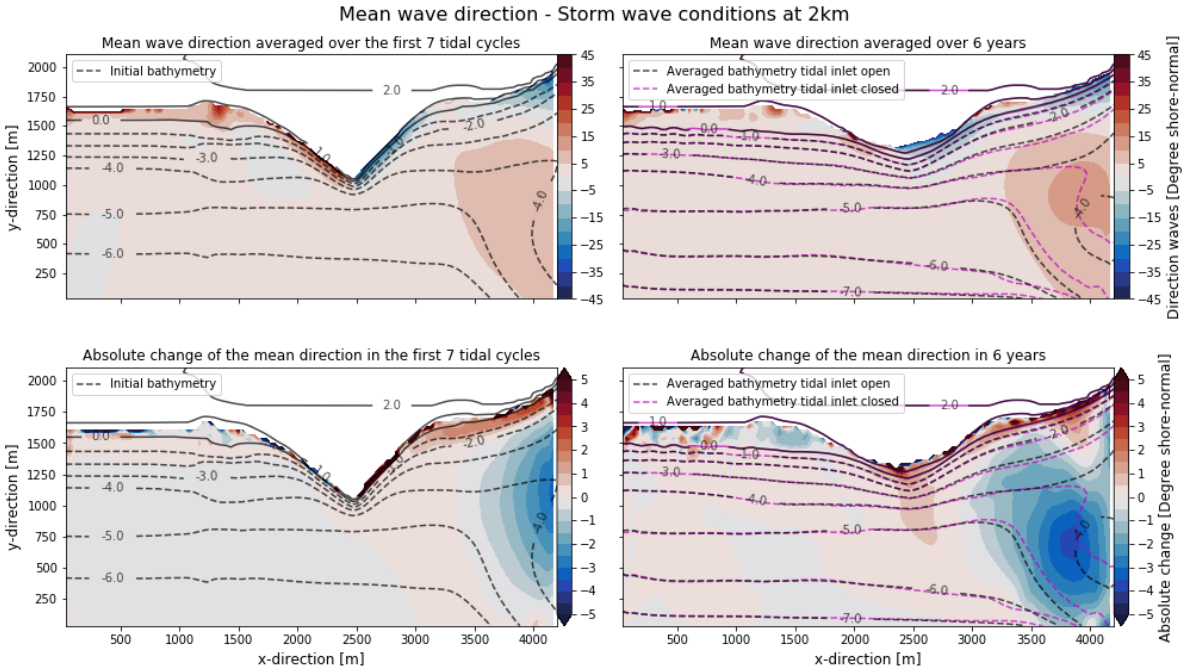

Figure C.15: Peak wave direction for storm wave conditions at 2km from the tidal inlet. The first column shows the peak wave direction averaged over the first 7 tidal cycles and the second column shows the peak wave direction averaged over 6 years. The first row shows the averaged peak wave direction, the second row shows the relative difference in the peak wave direction between the tidal inlet being open and closed. The third row shows the absolute difference in the peak wave direction between the tidal inlet being open and closed.

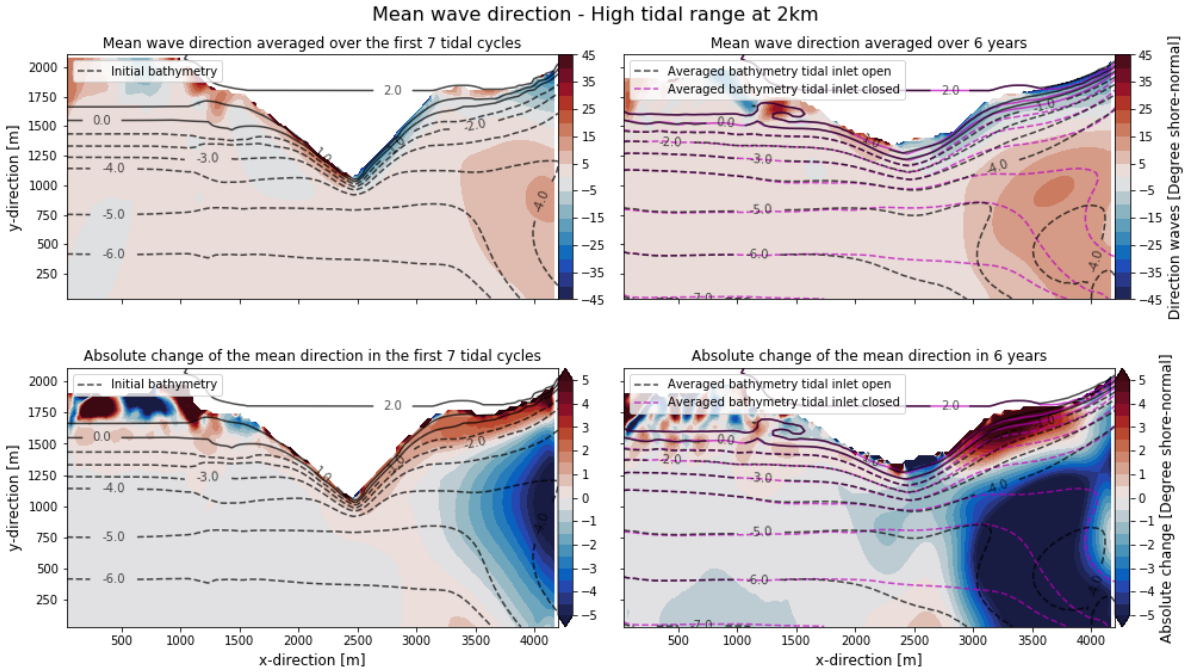

Figure C.16: Peak wave direction for high tidal range at 2km from the tidal inlet. The first column shows the peak wave direction averaged over the first 7 tidal cycles and the second column shows the peak wave direction averaged over 6 years. The first row shows the averaged peak wave direction, the second row shows the relative difference in the peak wave direction between the tidal inlet being open and closed. The third row shows the absolute difference in the peak wave direction between the tidal inlet being open and closed.

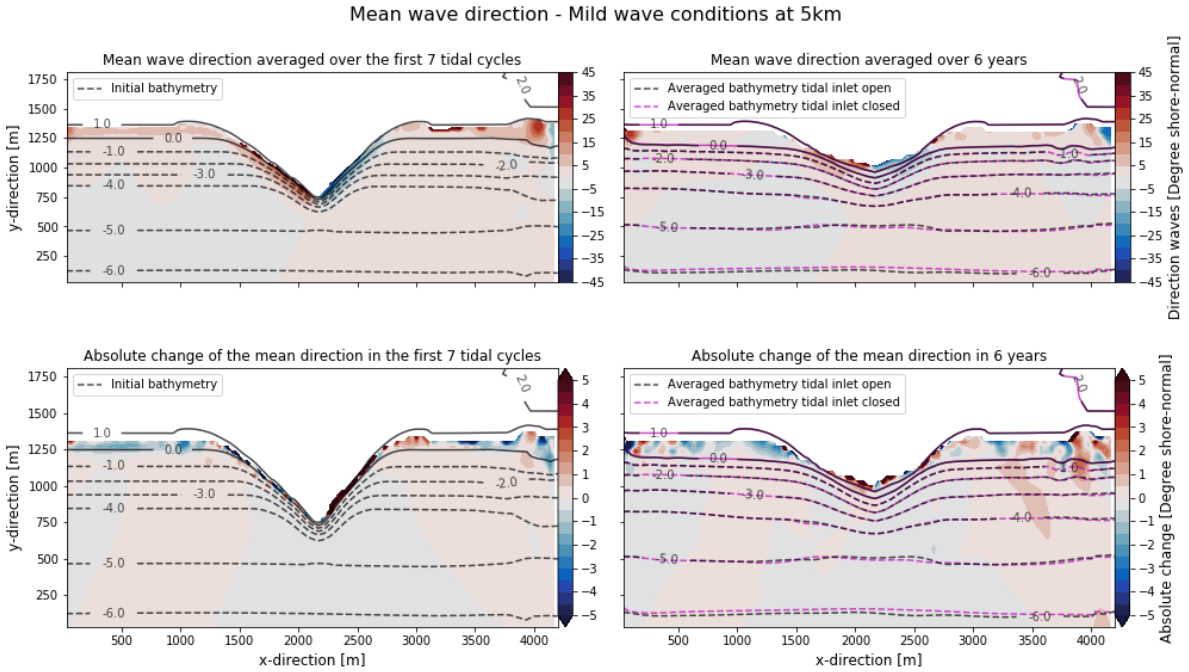

Figure C.17: wave direction for mild wave conditions at 5km from the tidal inlet. The first column shows the peak wave direction averaged over the first 7 tidal cycles and the second column shows the peak wave direction averaged over 6 years. The first row shows the averaged peak wave direction, the second row shows the relative difference in the peak wave direction between the tidal inlet being open and closed. The third row shows the absolute difference in the peak wave direction between the tidal inlet being open and closed.

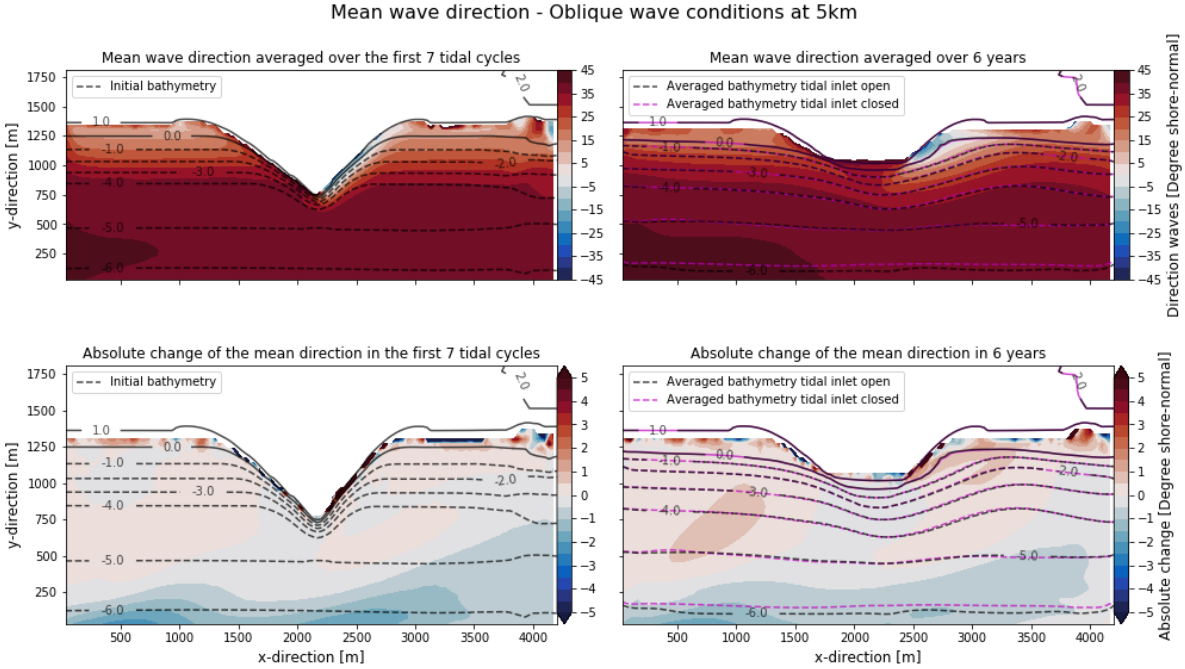

Figure C.18: wave direction for oblique wave conditions at 5km from the tidal inlet. The first column shows the peak wave direction averaged over the first 7 tidal cycles and the second column shows the peak wave direction averaged over 6 years. The first row shows the averaged peak wave direction, the second row shows the relative difference in the peak wave direction between the tidal inlet being open and closed. The third row shows the absolute difference in the peak wave direction between the tidal inlet being open and closed.

D

Total alongshore sediment transport

As discussed in the methodology, only the transport owing to the mega-nourishment and the tidal inlet are of interest. Therefore the transport as a result of the ebb-tidal delta is discarded.

Mild wave conditions

With the mega-nourishment at 5km from the tidal inlet (top right figure) it can be seen that the total sediment transport is symmetric around the centroid of the mega-nourishment (Figure D.1). This suggests that mega-nourishment is located outside of the influence of the tidal inlet. Additionally, the center right figure shows that the total alongshore sediment transport (referred to as TAST) is similar with the tidal inlet being opened and closed. The absolute difference (purple line) between the TAST with the tidal inlet being open and closed is about zero (RTF TAST). This further emphasizes that the mega-nourishment at 5km from the tidal inlet is not influenced by flows owing to the tidal inlet. Moreover, the TAST is also symmetrical in this figure. The TAST has a trough of about -540 m^3/6y/m at a distance of 482 meters from the centroid of the mega-nourishment and a peak of 530 m^3/6y/m at a distance of 350 meters. The TAST follows the shoreline orientation as shown in the bottom right figure (see Figure D.1).

With the mega-nourishment at 2km from the tidal inlet, it can be seen in the top left and center left figure (see Figure D.1) that the magnitude of the total sediment transport is higher on the inlet-side of the mega-nourishment than on the non-inlet-side. This is consistent with the tide averaged currents increasing in magnitude towards the tidal inlet (see Figure 4.5). The TAST first increases in magnitude towards the non-inlet-side (see center left figure) until it has reached a peak of -500 m^3/6y/m at a distance of 480 meter from the centroid of the mega-nourishment. After this peak the TAST gradually approaches a zero TAST towards the boundary.

On the inlet-side of the mega-nourishment, the total sediment transport is not similar for the tidal inlet being open and closed. With an open tidal inlet the TAST first increases in magnitude until it has reached a local maximum of 800 m^3/6y/m at a distance of 480 meter from the centroid of the mega-nourishment. After this local peak the TAST slightly reduces to 730 m^3/6y/m at a distance of 790 meter from the centroid of the mega-nourishment. The local maximum and minimum of the tidal inlet being closed are 720 m^3/6y/m at a distance of 450 meters and 590 m^3/6y/m at a distance of 920 meters from the centroid of the mega-nourishment. The maximum TAST (at x=4133 m) is 1400 m^3/6y/m for the tidal inlet being open and 820 m^3/6y/m for the tidal inlet being closed. Furthermore, the TAST line follows the shoreline orientation.

Additionally, in the center left figure, it can be seen that the TAST on the non-inlet-side side is equal for the tidal inlet being open and closed. Whereas the transport on the inlet-side of

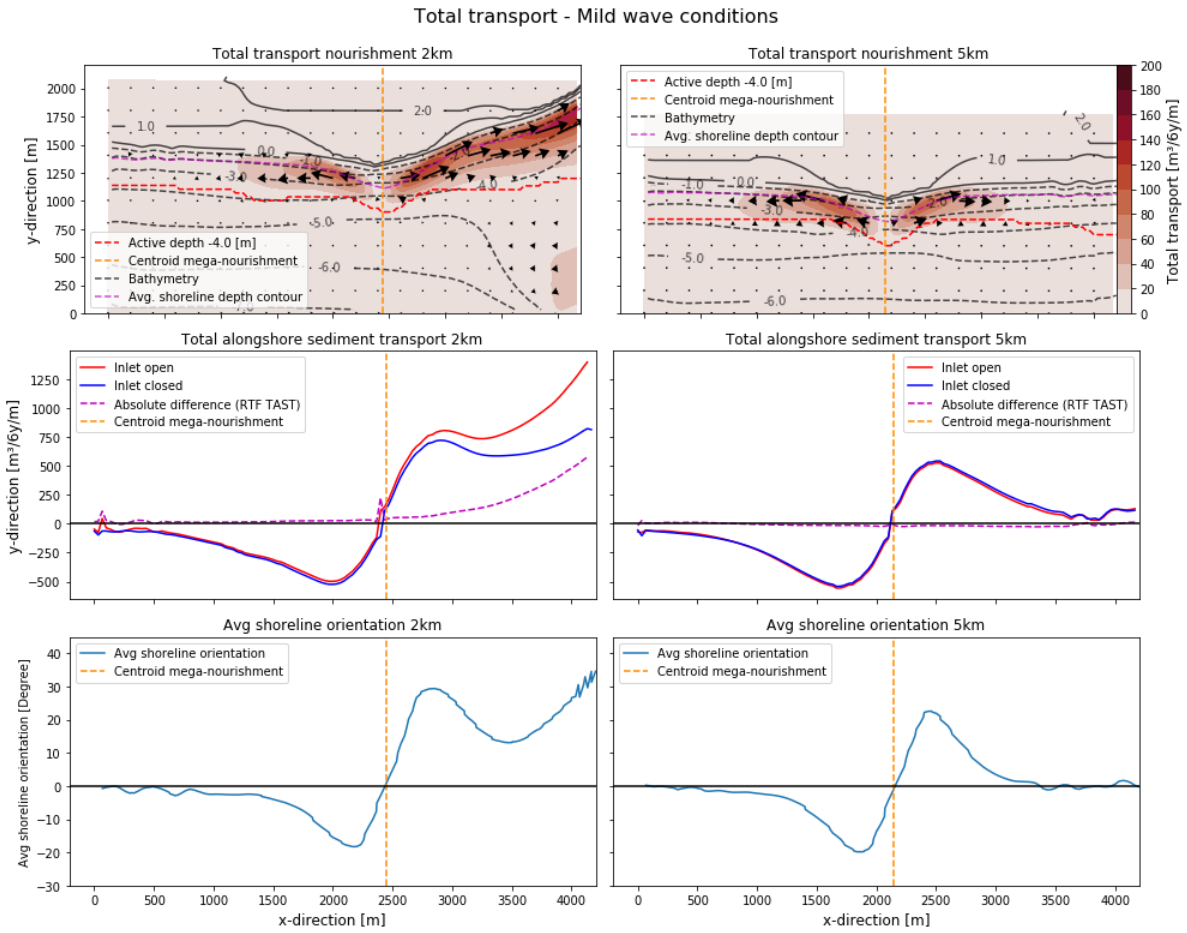

Figure D.1: Total alongshore sediment transport mild wave conditions over 6 years. The top, center and bottom row show the total sediment transport, total alongshore sediment transport (TAST) and average shoreline orientation respectively. The left and right column show this for the mega-nourishment at 2km and 5km from the tidal inlet. The centroid of the mega-nourishment at t=0 is shown with the orange dashed line. The red and blue line in the center row figures show the TAST for the tidal inlet being open and closed. The purple dashed line shows the absolute difference between the former and latter.

the mega-nourishment is higher with the tidal inlet being open and increases in magnitude towards the tidal inlet. This suggests that the influence of the tidal inlet flow increases towards the tidal inlet. Likewise, the transport does not decrease for the tidal inlet being closed. This suggests that the transport increases owing to the shoreline orientation relative to the angle of incidence of the waves (see bottom left figure in Figure D.1).

Oblique waves conditions

In Figure D.2 the total sediment transport for oblique wave conditions are shown. With the mega-nourishment at 5km from the tidal inlet (top right figure) it can be seen that the total sediment transport is much higher along the shore than for the mild wave conditions (see Figure D.1). Oblique waves will generate an alongshore current which will result in an alongshore sediment transport averaging in about 1200 m^3/6y/m. The TAST (see center right figure) has a trough of about -600 m^3/6y/m at a distance of 300 meters to the non-inlet-side of the mega-nourishment and a peak of 1450 m^3/6y/m at a distance of 200 meters to the inlet-side. The waves have an angle of 45 degrees relative to the shore, towards the inlet-side. This wave angle will result in the highest TAST compared to the other simulations, as the TAST scales with the sinus of twice the wave angle (s,ϕ-curve). This means that the TAST is already maximum along the non perturbed shoreline. Therefore the TAST decreases significantly to the non-inlet-side of the mega-nourishment, as the non-inlet-side of the mega-nourishment decreases the incident wave angle.

To the inlet-side the TAST has a peak which is higher than the TAST at either boundary. After the peak, the transport reduces again since the incident wave angle becomes larger than 45 degrees. The TAST with the tidal inlet being open and closed shows a similar behavior. This coupled with TAST decreasing owing to the wave angle, shows that the tidal inlet has no effect on the total alongshore sediment transport with the mega-nourishment at a distance of 5km from the tidal inlet.

With the mega-nourishment at 2km from the tidal inlet, it can be seen in the center left figure, that the transport is equal for the tidal inlet being open and closed. Furthermore, the non-inlet-side of the mega-nourishment has a similar shape and magnitude as the non-inlet-side of the mega-nourishment at a distance of 5km from the tidal inlet (center right figure). Emphasizing that the non-inlet-side of the mega-nourishment is not influenced by the flow induced by the tidal inlet. In the mild wave condition it was shown that the transport increases towards the tidal inlet for both the tidal inlet being open as well as closed. However, this is not the case for the oblique wave conditions. The transport towards the tidal inlet with the inlet being closed is in fact lower than at 5km. The wave angle increases after the centroid of the mega-nourishment to more than 45 degrees relative to shore-normal resulting in a reduced TAST. Similarly the TAST with the tidal inlet being open increases towards the tidal inlet. The absolute difference between the tidal inlet being open and closed is again owing to the RTF currents (purple line).

The magnitude of the TAST as a result of the RTF currents (about 400 m^3/6y/m) are however lower than for the mild wave conditions (see the magenta line in the bottom left figure in Figure D.1 which is about 600 m^3/6y/m). Moreover, the effect owing to the tidal inlet diminishes faster (about 800 meters from the tidal inlet) than compared to the mild wave conditions (about 2 kilometers from the tidal inlet). This is also consistent with the reduction in RTF currents as seen in Figure 4.5. Consequently, the most important processes for oblique wave conditions are the incident wave angle and RTF currents.

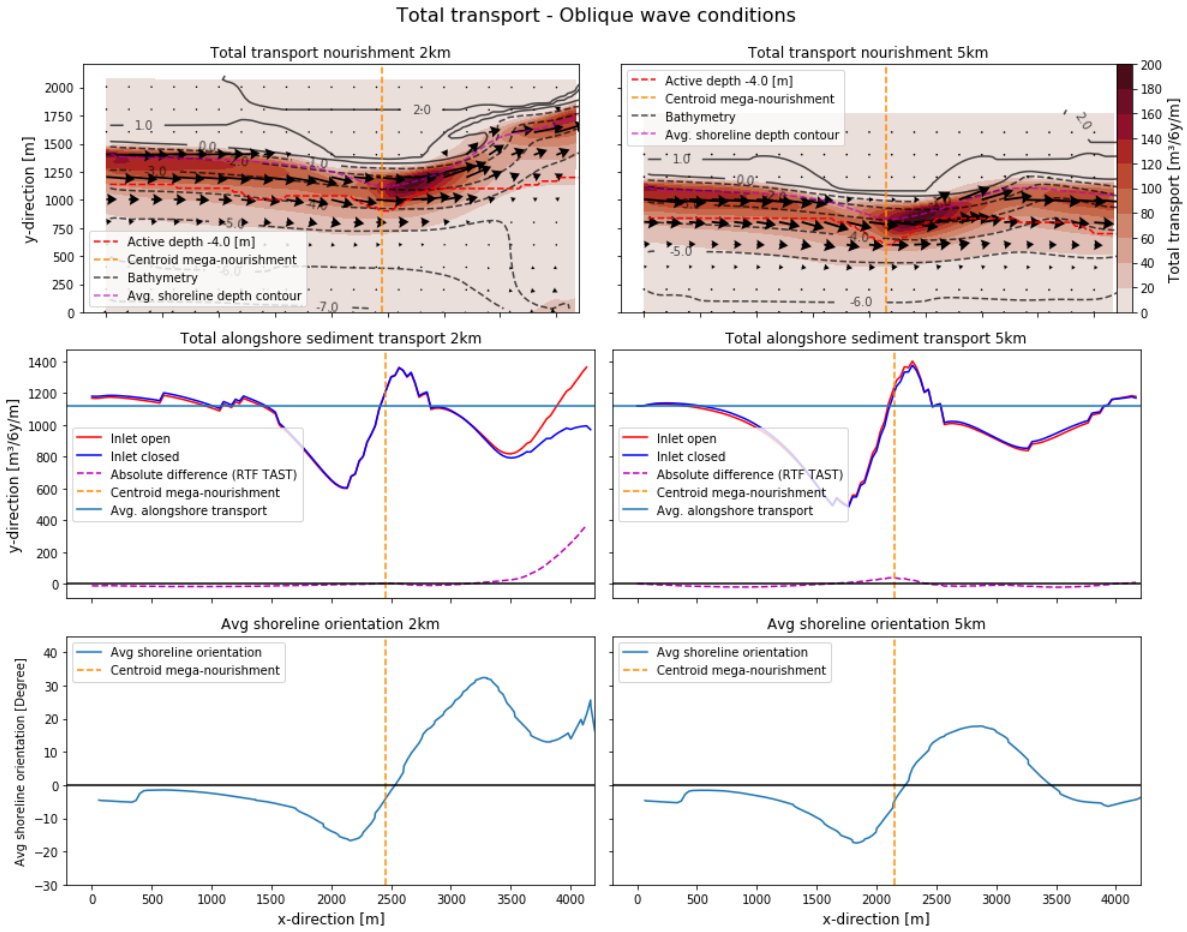

Figure D.2: Total alongshore sediment transport oblique wave conditions over 6 years. The top, center and bottom row show the total sediment transport, total alongshore sediment transport (TAST) and average shoreline orientation respectively. The left and right column show this for the mega-nourishment at 2km and 5km from the tidal inlet. The centroid of the mega-nourishment at t=0 is shown with the orange dashed line. The red and blue line in the center row figures show the TAST for the tidal inlet being open and closed. The purple dashed line shows the absolute difference between the former and latter.

Storm wave conditions

In Figure D.3 the total sediment transport for storm wave conditions are shown. With the mega-nourishment at 5km from the tidal inlet (center right figure) it can be seen that the TAST is roughly symmetric around the centroid of the mega-nourishment. The shape as well as the magnitude are similar for both sides. The TAST has a trough of about -630 m^3/6y/m at a distance of 480 meters to the non-inlet-side of the mega-nourishment (see center right figure) and a peak of 640 m^3/6y/m at a distance of 390 meters to the inlet-side. The TAST first increases in magnitude away from the mega-nourishment until the location of the peak. After this peak the TAST reduces, approaching the zero transport line. The TAST follows the average shoreline orientation (bottom right figure). Furthermore, the TAST with the tidal inlet being open and closed are similar, hence the tidal inlet does not influence the mega-nourishment.

With the mega-nourishment at 2km from the tidal inlet, it can be seen in the top left figure that the magnitude of the total sediment transport is higher on the inlet-side of the mega-nourishment than on the non-inlet-side. Similarly this can be seen in the center left figure (see Figure D.3). The TAST on the non-inlet-side of the mega-nourishment is similar for the tidal inlet being open and closed. The TAST first increases in magnitude towards the non-inlet-side until it has reached a trough of -600 m^3/6y/m at a distance of 480 meter. After which the TAST approaches a zero total alongshore sediment transport. This TAST is roughly similar in shape and magnitude to the TAST found with the mega-nourishment at 5km from the tidal inlet.

On the inlet-side of the mega-nourishment, the TAST is not similar for the tidal inlet being open and closed. With an opened tidal inlet the TAST first increases in magnitude until it has reached a local maximum of 1000 m^3/6y/m at a distance of 520 meter from the mega-nourishment. After this the TAST decreases to a local minimum of 925 m^3/6y/m at a distance of 2450 meter from the mega-nourishment and finally increases in magnitude towards the tidal inlet. With a closed tidal inlet the magnitude of the local minimum and maximum are lower. The local maximum is 850 m^3/6y/m at a distance of 490 meter from the mega-nourishment. However, this TAST is higher than the trough found on the non-inlet-side (-600 m^3/6y/m). Furthermore, the maximum TAST (at x=4133 m) is 1590 m^3/6y/m for the tidal inlet being open and 980 m^3/6y/m for the tidal inlet being closed

It can be seen in the bottom left figure that the TAST follows the shoreline orientation, as the alongshore transport is proportional to the sinus of twice the angle of the waves relative to the shoreline (s,ϕ-curve). The shoreline orientation on the non-inlet-side is slightly lower than on the inlet-side and as a result so are the TAST magnitudes. On the inlet-side the shoreline first increases, then decreases after which it increases again. The TAST with the tidal inlet being closed also follows this line. Therefore, it can be concluded that the shoreline orientation is an important process in the TAST. The difference in TAST between the tidal inlet being open and closed is owing to the tidal inlet. This is shown with the purple line in the center right figure. This effect increases towards the tidal inlet. As a result the most important processes in the TAST for the storm wave conditions are the angle of the waves with respect to the shoreline and the RTF currents owing to the tidal inlet.

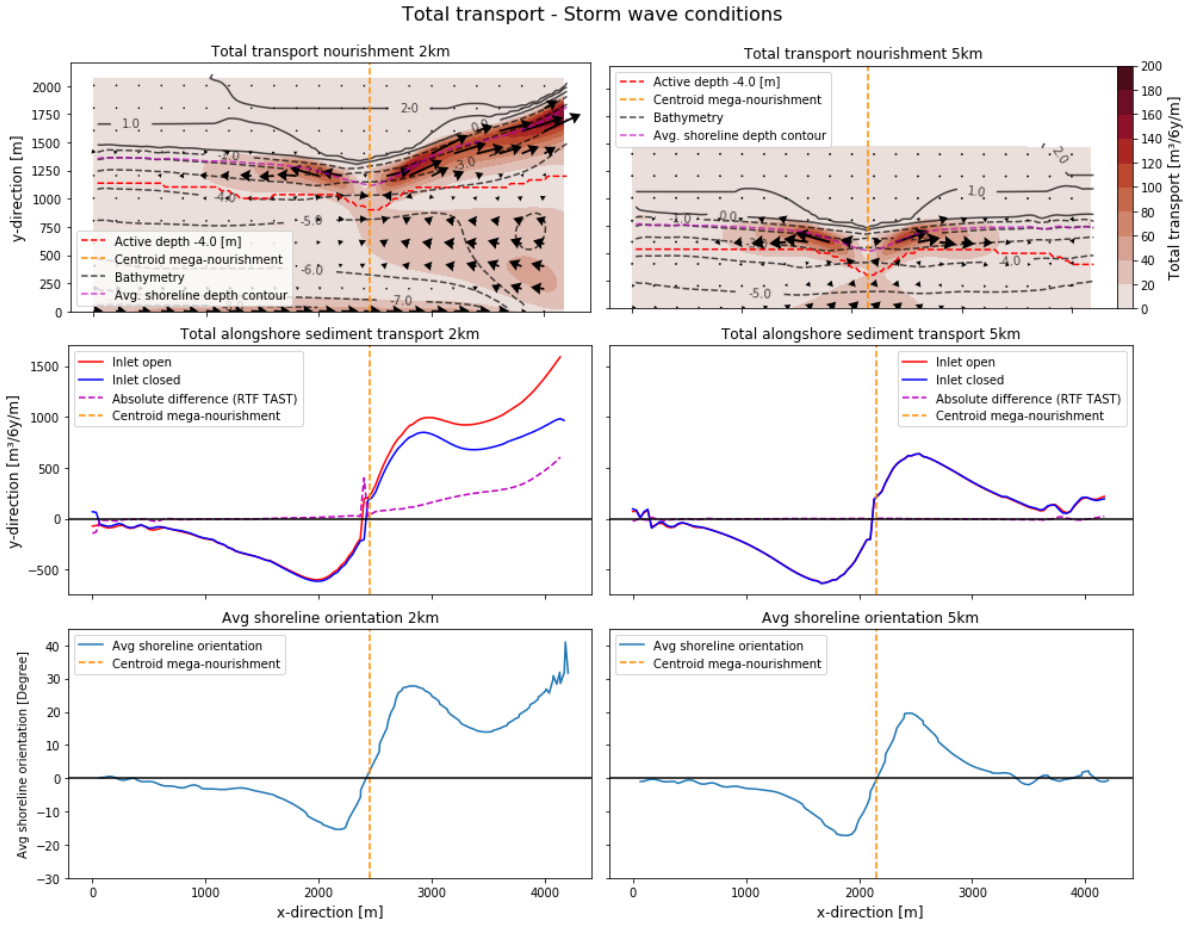

Figure D.3: Total alongshore sediment transport storm wave conditions over 6 years. The top, center and bottom row show the total sediment transport, total alongshore sediment transport (TAST) and average shoreline orientation respectively. The left and right column show this for the mega-nourishment at 2km and 5km from the tidal inlet. The centroid of the mega-nourishment at t=0 is shown with the orange dashed line. The red and blue line in the center row figures show the TAST for the tidal inlet being open and closed. The purple dashed line shows the absolute difference between the former and latter.

High tidal range

In Figure D.4 the TAST for the high tidal range are shown. With the mega-nourishment at 5km from the tidal inlet (center right figure) it can be seen that the TAST is roughly symmetric around the centroid of the mega-nourishment. The shape as well as the magnitude are similar for both sides. The TAST to the non-inlet-side of the mega-nourishment has a maximum in magnitude of -520 m^3/6y/m at a distance of 480 meter from the mega-nourishment. After which it gradually reduces to a zero TAST. To the inlet-side of the mega-nourishment there is a maximum of 520 m^3/6y/m at a distance of 390 meter from the mega-nourishment. The shape of the total transport at 5km follows the shoreline orientation (see bottom right figure). This suggests that the sediment is diffused by the angle of the waves relative to the shoreline orientation resulting in a alongshore current.

With the mega-nourishment at 2km from the tidal inlet, it can be seen in the top left figure that the magnitude of the total sediment transport is higher on the inlet-side of the mega-nourishment than on the non-inlet-side. Similarly this can be seen in the center left figure (see Figure D.4). The TAST is not similar on both the non-inlet-side and inlet-side of the mega-nourishment with the tidal inlet being open and closed. On the non-inlet-side the maximum magnitude of the TAST for the tidal inlet being open (-440 m^3/6y/m) is lower than for the tidal inlet being closed (-520 m^3/6y/m), both are located at a distance of 480 meter from the mega-nourishment. The non-inlet-side behaves similarly as the non-inlet-side of the mega-nourishment at 5km from the tidal inlet, with the tidal inlet being closed.

On the inlet-side of the mega-nourishment the largest changes occur. With an open tidal inlet the TAST first increases in magnitude until it has reached a local maximum of 810 m^3/6y/m at a distance of 350 meter from the mega-nourishment. This is higher than the TAST of 680 m^3/6y/m for the tidal inlet being closed. After this the transport decreases to a local minimum of 470 m^3/6y/m at a distance of 820 meter from the tidal inlet, which is lower than the TAST of 520 with the tidal inlet being closed. After this the TAST increases towards the tidal inlet with a TAST of 2310 m^3/6y/m. This is much higher than the TAST of 720 m^3/6y/m for the tidal inlet being closed.

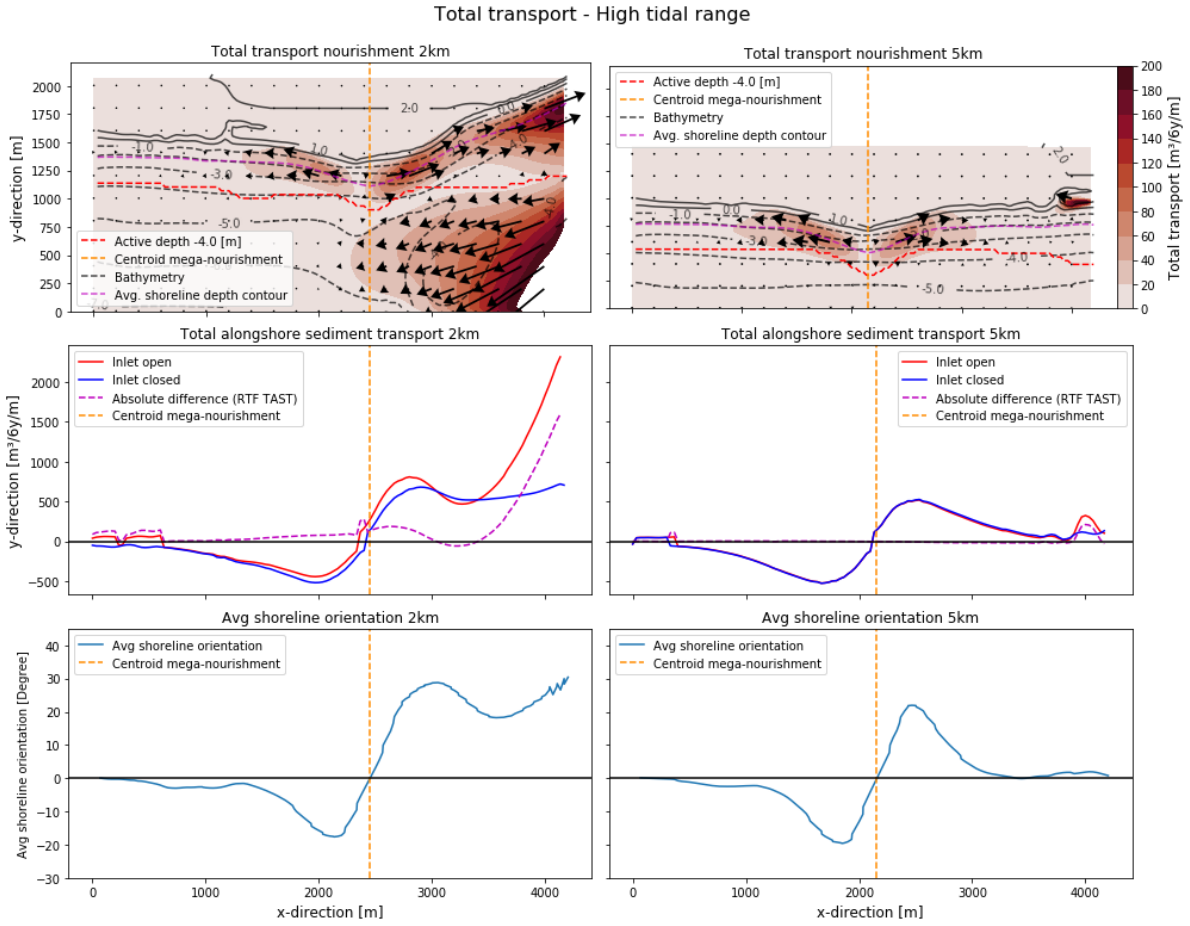

Figure D.4: Total alongshore sediment transport high tidal range over 6 years. The top, center and bottom row show the total sediment transport, total alongshore sediment transport (TAST) and average shoreline orientation respectively. The left and right column show this for the mega-nourishment at 2km and 5km from the tidal inlet. The centroid of the mega-nourishment at t=0 is shown with the orange dashed line. The red and blue line in the center row figures show the TAST for the tidal inlet being open and closed. The purple dashed line shows the absolute difference between the former and latter.

Real tides

In Figure D.5 the TAST for the real tide is shown. With the mega-nourishment at 5km from the tidal inlet (top right figure) it can be seen that the total sediment transport is symmetric around the centroid of the mega-nourishment. This suggests that the mega-nourishment is outside the sphere of influence of the tidal inlet. The shape and the magnitude are similar for both sides. The TAST (see center right figure) to the non-inlet-side of the mega-nourishment has a maximum in magnitude of -540 $m^3/6y/m$ at a distance of 480 meter from the mega-nourishment. After which it gradually reduces to a zero TAST. The inlet-side of the mega-nourishment has a peak TAST of 520 $m^3/6y/m$ at a distance of 390 meter from the mega-nourishment. The shape of the TAST with the mega-nourishment at 5km from the tidal inlet follows the shoreline orientation as shown in the bottom right figure.

With the mega-nourishment at 2km from the tidal inlet, it can be seen in the top left figure that the magnitude of the total sediment transport is higher on the inlet-side of the mega-nourishment than on the non-inlet-side. Similarly this can be seen in the center left figure (see Figure D.5). The TAST on the non-inlet-side of the mega-nourishment is similar for the tidal inlet being open and closed. The TAST first increases in magnitude towards the non-inlet-side until it has reached a maximum of -500 $m^3/6y/m$ at a distance of 480 meter from the centroid of the mega-nourishment. After this peak, away from the centroid of the mega-nourishment, the TAST gradually reduces towards a zero transport.

On the inlet-side of the mega-nourishment, the TAST is not similar for the tidal inlet being open and closed. With an open tidal inlet the TAST first increases in magnitude until it has reached a local maximum of 780 $m^3/6y/m$ at a distance of 480 meter from the centroid of the mega-nourishment. After this local peak the TAST slightly reduces to 700 $m^3/6y/m$ at a distance of 820 meter from the centroid of the mega-nourishment. The local maximum and minimum of the tidal inlet being closed are 700 $m^3/6y/m$ at a distance of 450 meters and 570 $m^3/6y/m$ at a distance of 950 meters from the centroid of the mega-nourishment respectively. The maximum TAST (at x=4133 m) is 1330 $m^3/6y/m$ for the tidal inlet being open and 800 $m^3/6y/m$ for the tidal inlet being closed. Furthermore, the TAST line follows the shoreline orientation.

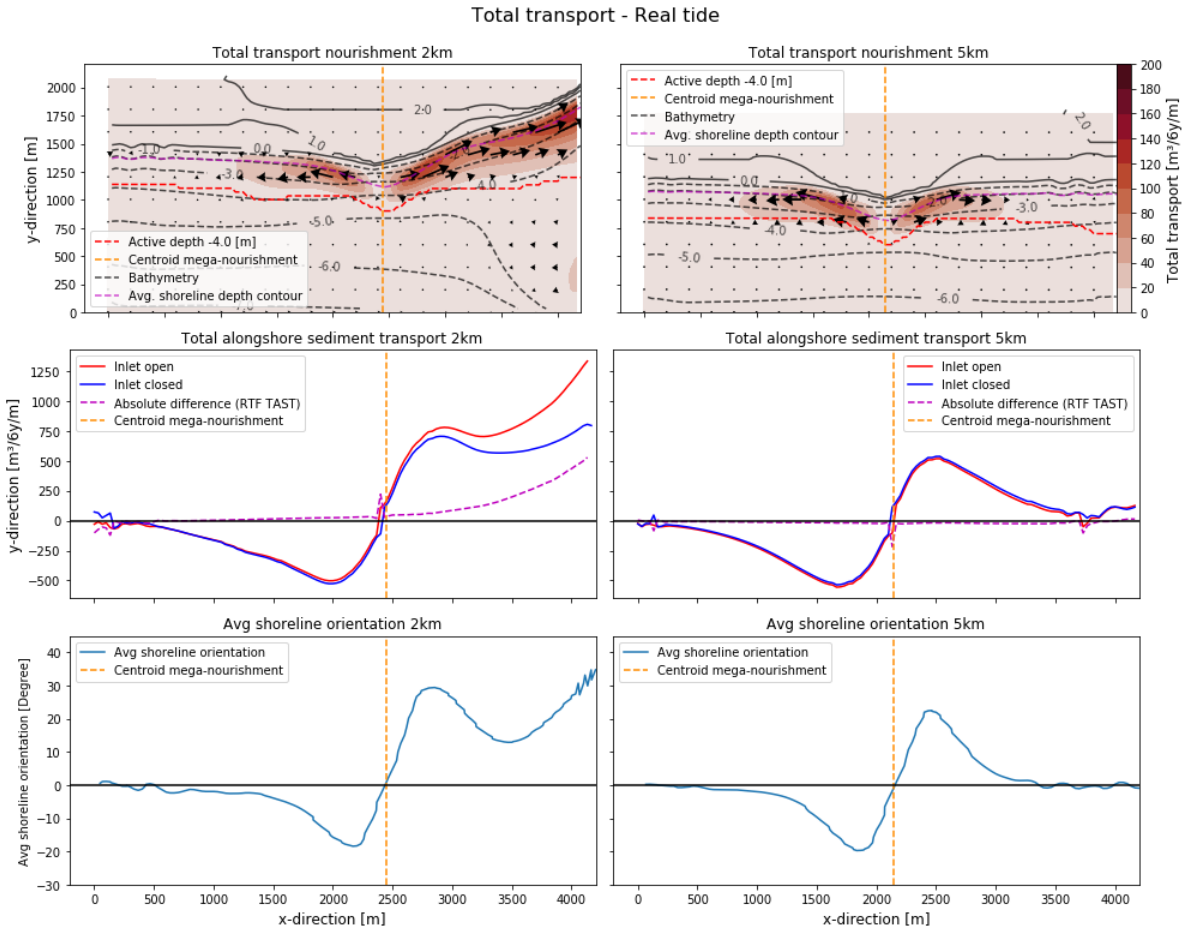

Figure D.5: Total alongshore sediment transport real tides over 6 years. The top, center and bottom row show the total sediment transport, total alongshore sediment transport (TAST) and average shoreline orientation respectively. The left and right column show this for the mega-nourishment at 2km and 5km from the tidal inlet. The centroid of the mega-nourishment at t=0 is shown with the orange dashed line. The red and blue line in the center row figures show the TAST for the tidal inlet being open and closed. The purple dashed line shows the absolute difference between the former and latter.

Real waves

In FigureD.6 the TAST for the real waves is shown. With the mega-nourishment at an alongshore distance of 5km from the tidal inlet it can be seen that the TAST is not symmetric around the centroid of the mega-nourishment. The average TAST is shifted up, to about 230 m^3/6y/m. The real wave conditions have waves coming from all directions instead of just one. The majority of the waves come from -80 to 0 degrees relative to shore-normal (see Figure 3.8). The mean wave direction is about -15 degrees relative to shore-normal. Also the highest waves come from -80 to 0 degrees relative to shore normal. Therefore, the upwards shift of the TAST is generated by angle of incidence of the waves.

The trough to the non-inlet-side of the centroid of the mega-nourishment is located at an alongshore distance of 410 meter, with a TAST of -275 m^3/6y/m. The peak to the inlet-side is located at an alongshore distance of 320 meter from the centroid of the mega-nourishment, with a TAST of 610 m^3/6y/m. The shape of the TAST follows the shoreline orientation as can be seen in the bottom right figure. Furthermore, there is no significant difference between the TAST values for the tidal inlet being open and closed.

With the mega-nourishment at 2km from the tidal inlet it can be seen that the TAST again is shifted upwards. This shift is again with about 230 m^3/6y/m. In the top left figure it can be seen that the magnitude of the TAST is higher on the inlet-side of the mega-nourishment than on the non-inlet-side. Similarly this can be seen in the center left figure. The TAST on the non-inlet-side is similar for the tidal inlet being open and closed. The TAST first increases in magnitude towards the non-inlet-side until it has reached a maximum of -225 m^3/6y/m at an alongshore distance of 116 meter from the mega-nourishment. After this peak, away from the centroid of the mega-nourishment, the TAST gradually reduces towards a zero transport.

There is a increasingly difference between the tidal inlet being open and closed towards the tidal inlet, to the inlet-side of the mega-nourishment located at an alongshore distance of 2km from the tidal inlet. With a open tidal inlet the local maximum, local minimum and absolute maximum are located at an alongshore distance of 450, 850 and 1680 meter from the mega-nourishment respectively. With a TAST value of 800, 650 and 1100 m^3/6y/m respectively. This is higher than for the tidal inlet being closed which resulted in TAST values of 760, 570, 690 m^3/6y/m for the local maximum, local minimum and absolute maximum respectively. The TAST line for the open tidal inlet has the same shape as the shoreline orientation. Again indicating that the TAST follows the shoreline orientation. An open tidal inlet also follows the shoreline orientation but has an added contribution owing to the tidal inlet.

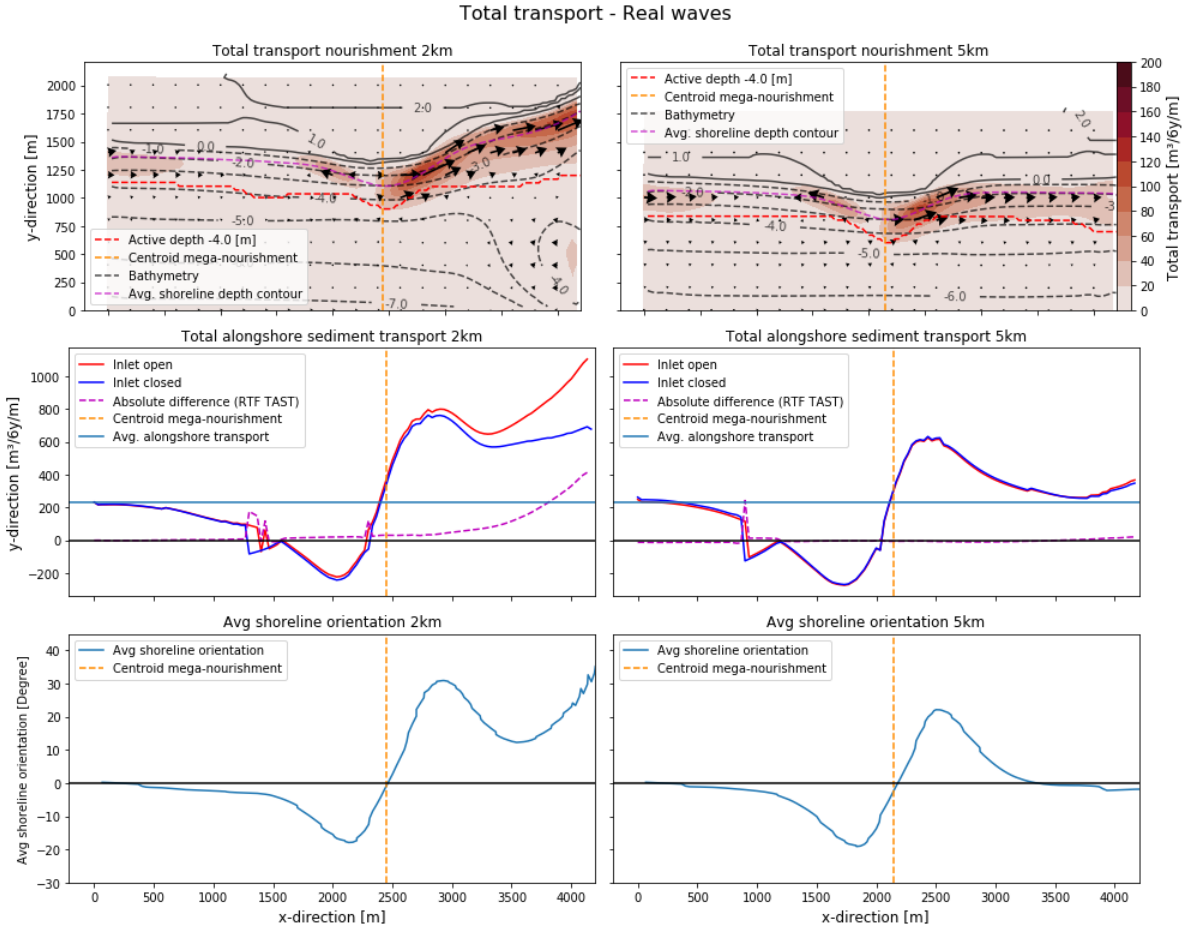

Figure D.6: Total alongshore sediment transport real waves over 6 years. The top, center and bottom row show the total sediment transport, total alongshore sediment transport (TAST) and average shoreline orientation respectively. The left and right column show this for the mega-nourishment at 2km and 5km from the tidal inlet. The centroid of the mega-nourishment at t=0 is shown with the orange dashed line. The red and blue line in the center row figures show the TAST for the tidal inlet being open and closed. The purple dashed line shows the absolute difference between the former and latter.

E

Morphological development of the mega-feeder nourishment

The research question regarding the development of the mega-nourishment over time will be investigated in this chapter. As described in the methodology the change over time compared to the initial shoreline is analysed.

Mild wave conditions

In Figure E.1 the development of the shoreline (0 meter depth contour) can be seen. The mega-nourishment at 5km from the tidal inlet is shown in Figure E.1b. With the mega-nourishment at 5km from the tidal inlet it can be seen in the top left figure that the nourishment erodes quickly at first (2008 to 2010) but slows down as time progresses. The shoreline retreat from 2008 to 2010 is 150 meter, from 2010 to 2012 is 70 meter and from 2012 to 2014 is 55 meter. This retreat is the similar for the tidal inlet being open and closed. The adjacent accreding coast accretes fast until 2010 (up to 100 meter) after which there is not much accretion from 2010 to 2014 compared to the first two years (2008 to 2010). The accretion is uniform along the adjacent coast for the first two years. The depth contours are closer to each other, indicating a steeper slope near the shore compared to the initial bathymetry (top right figure).

In the bottom row (see Figure E.1b) the accretion and erosion patterns are symmetrical around the centroid of the mega-nourishment. During the first year there is a spatially uniform accretion pattern in the zones which accrede (adjacent coast). After 2010 accretion is no longer uniform in the alongshore direction, but spreads out away from the mega-nourishment. The shoreline change over time (see bottom right figure) is similar for the tidal inlet being open and closed.

With the mega-nourishment at 2km from the tidal inlet (see Figure E.1a) it can be seen in the top row that the tip of the mega-nourishment erodes fast during the first few years (from 2008 to 2010) and then slows down over time. The shoreline retreat from 2008 to 2010, from 2010 to 2012 and from 2012 to 2014 are 150, 70 and 55 meter respectively for the tidal inlet being open. Furthermore, the tip of the mega-nourishment slowly propagates towards the non-inlet-side as the inlet-side erodes more than the non-inlet-side. On the non-inlet-side the adjacent beach accretes by up to 100 meters for the first two years (2008 to 2010) after which the accretion slows down significantly. The bathymetry for the tidal inlet being open and closed are different from each other. This is most apparent by looking at the -4.0 meter depth contour.

In the bottom row (see Figure E.1a) the erosion and sedimentation patterns are not symmetrical around the centroid of the mega-nourishment. The inlet-side erodes more than the

non-inlet-side. Also the inlet-side does not show uniform accretion in the alongshore direction during the first two years (2008 to 2010), whereas the non-inlet-side does. The shoreline at the inlet-side only erodes/accretes for about 33.3 meters during 6 years. There is a slight erosion towards the tidal inlet.

By investigating the bottom right figure it can be seen that there is not much difference in the position of the shoreline with the tidal inlet open and closed. However, towards the tidal inlet on the inlet-side of the mega-nourishment there is more shoreline retreat with the tidal inlet being open than closed. This pattern starts at 2010 to 2011 and increases in size with time progressing. There is a difference of at most 33.3 meter in the shoreline between the tidal inlet being open and closed. Emphasizing that there is not much of a difference in shoreline between between the tidal inlet being open and closed. There is no pattern elsewhere in the domain except for noise.

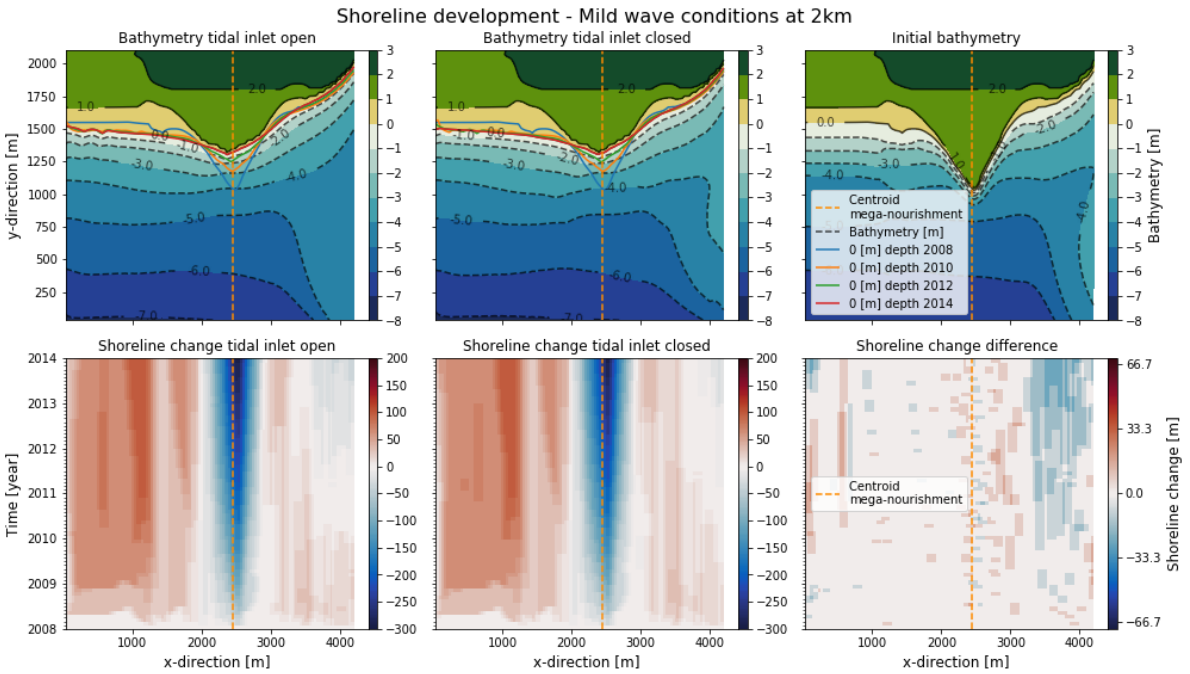

(a) Shoreline development mild wave conditions at 2 km

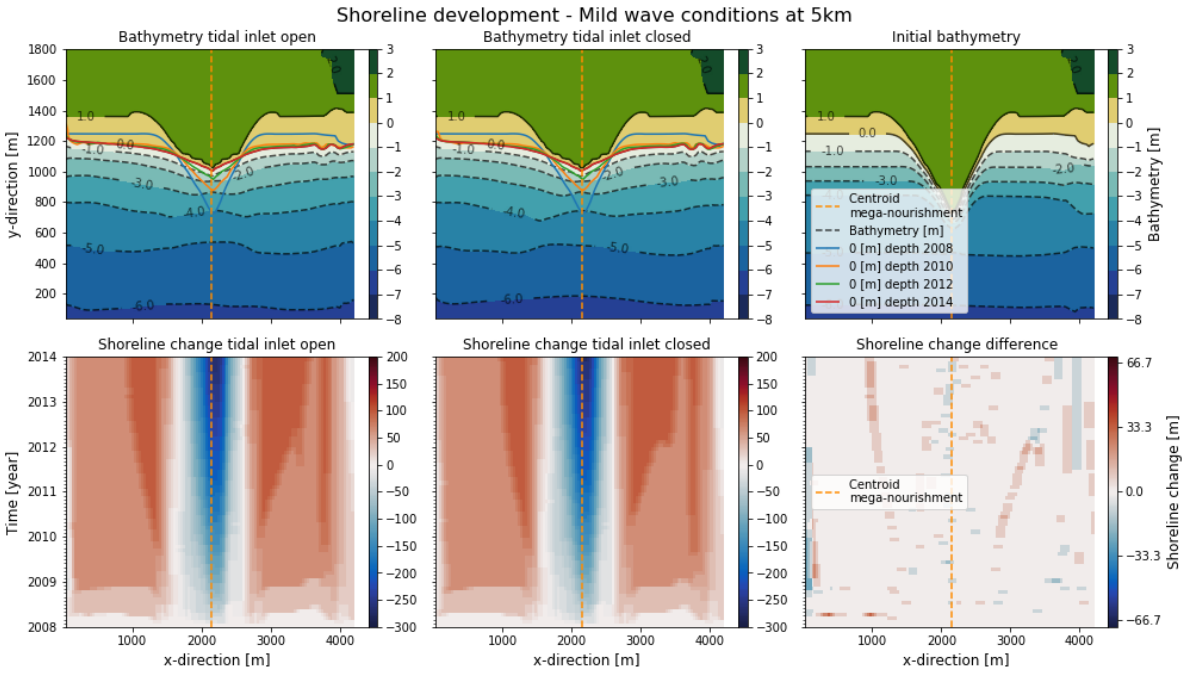

(b) Shoreline development mild wave conditions at 5 km

Figure E.1: Shoreline development for the mild wave conditions. The first row shows the bathymetry and the shoreline over time. The blue, orange, green, red and dashed orange lines shows the zero meter depth contour at the years 2008, 2010, 2012, 2014 and centroid of the mega-nourishment respectively. The second row shows the gained or lost shore with respect to the initial shoreline. Red shades indicates gained shore compared to the first time step (2008) and blue shows shore being lost. Furthermore, the first column shows the results for the tidal inlet being open. The second column shows the results for the tidal inlet being closed. At last the top right figure shows the initial bathymetry and the bottom left figure shows the difference between the gained shoreline between the tidal inlet being open and closed.

Oblique wave conditions

In Figure E.2 the development of the shoreline can be seen. The mega-nourishment at 5km from the tidal inlet is shown in Figure E.2b. With the mega-nourishment at 5km from the tidal inlet it can be seen in the top left figure that the nourishment erodes quickly at first (2008 to 2010) but slows down as time progresses. The shoreline retreat from 2008 to 2010, 2010 to 2012 and 2012 to 2014 are 215, 60 and 30 meter respectively. This retreat is similar for the tidal inlet being open and closed. Furthermore, it can be seen that a spit is formed at about 2010 to 2012 after which the shoreline combines again at about 2013. The presence of the mega-nourishment can be seen in the final bathymetry, where all depth contours up to a depth of -5 meter are curved following the 0 meter depth contour. There is a strong uniform accretion (up to 150 meters) in the adjacent coast (0 to about 1500 meter in the x-direction) from 2008 to 2010. After which the accretion slows down significantly in the years thereafter. On the inlet-side from 2300 to 3100 meter in the x-direction, the gained shoreline is more gradual owing to the spit. Furthermore, the depth contours are closer to each other, indicating a steeper slope near the shore compared to the initial bathymetry (top right figure).

In the bottom row it can be seen that the erosion and mainly the accretion patterns are not symmetrical around the centroid of the mega-nourishment. As seen in the top row a spit has formed at about 2010. The accretion related to the spit can also be seen in the bottom row, however, the exact time when the spit is detached and merged again with the downstream shore line (to the inlet-side of the spit) cannot be seen in this figure. This accretion starts at about July 2008 and grows in magnitude over time. Furthermore, this accretion pattern grows in the alongshore direction too. The mega-nourishment creates a shadow zone for the waves and thus the wave height is reduced to the inlet-side of the mega-nourishment (see the top right figure in Figure C.6). This shadow zone creates a spot for the sediment to accumulate. During the first year there is a spatially uniform accretion pattern from 0 to 1500 meter in the x-direction. After 2009 the accretion slowly spreads out away from the mega-nourishment. The shoreline change over time (see bottom right figure) is about the same for the tidal inlet being open and closed. On the inlet-side an accretion pattern is propagating to the inlet-side. However, the magnitude is insignificant.

With the mega-nourishment at 2km from the tidal inlet (see Figure E.2a) it can be seen in the top row that the tip of the mega-nourishment erodes fast during the first few years (2008 to 2010) and slows down over time. The shoreline retreat from 2008 to 2010, from 2010 to 2012 and from 2012 to 2014 are 200, 60 and 30 meters respectively. A spit is formed starting in about 2010. Over the years from 2010 to 2014 the spit has not merged with the coast. To the inlet-side of the spit the coast erodes compared to the initial shoreline. Furthermore, there is a strong accretion (up to 100 meters) in the adjacent coast (0 to about 2000 meter in the x-direction) from 2008 to 2010. After which the accretion slows down significantly in the years thereafter. The shoreline on the non-inlet-side of the mega-nourishment is similar for the tidal inlet being closed and open, and for the mega-nourishment at 2km and 5km from the tidal inlet.

In the bottom row (see Figure E.2a) it can be seen that also for the mega-nourishment at 2km from the tidal inlet, the accretion and erosion patterns are not symmetrical around the centroid of the mega-nourishment. Furthermore, it becomes clear that the spit is growing in magnitude and size in the alongshore direction over time. The width owing to the spit related accretion is about 500 meters wide. This is smaller than the width with the mega-nourishment at 5km from the tidal inlet of 700 meter. The magnitude is higher for the mega-nourishment at 2km from the tidal inlet compared to 5km. Furthermore, there is erosion to the inlet-side of the tip of the spit starting at about the year 2010 with the mega-nourishment at 2km from the tidal inlet.

By investigating the bottom right figure (see Figure E.2a) it can be seen that in general there is not much of a difference in the domain. However, towards the tidal inlet an erosion pattern emerges. This erosion pattern starts at about the year 2009 and then increases over time. There is a difference of 33.3 meters the majority of the time but this increases towards 66.7

meters from 2012 and thereafter. In the end (2014) there is a large difference between in the shoreline between the tidal inlet being open and closed.

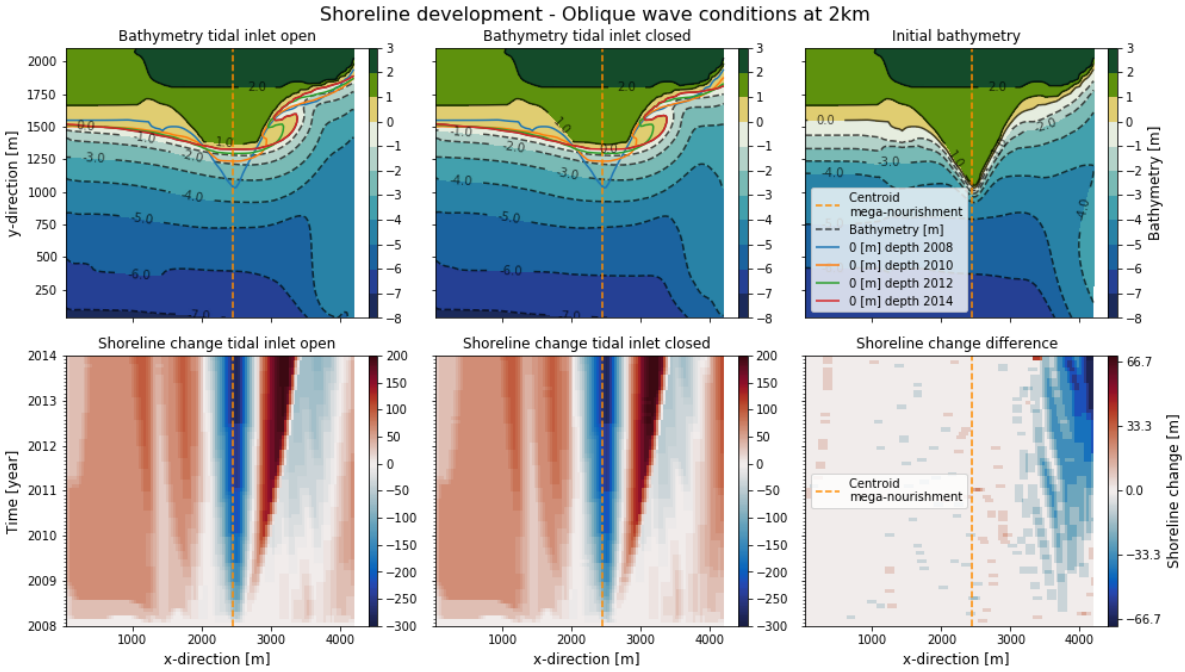

(a) Shoreline development oblique wave conditions at 2 km

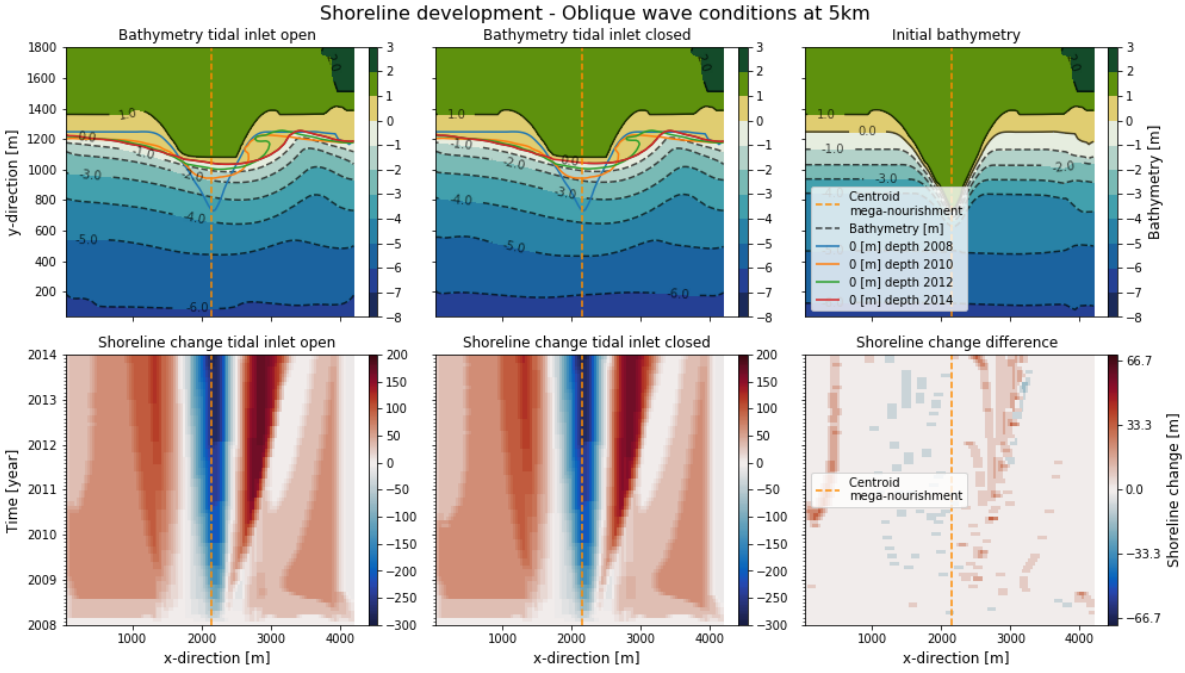

(b) Shoreline development oblique wave conditions at 5 km

Figure E.2: Shoreline development for oblique wave conditions. The first row shows the bathymetry and the shoreline over time. The blue, orange, green, red and dashed orange lines shows the zero meter depth contour at the years 2008, 2010, 2012, 2014 and centroid of the mega-nourishment respectively. The second row shows the gained or lost shore with respect to the initial shoreline. Red shades indicates gained shore compared to the first time step (2008) and blue shows shore being lost. Furthermore, the first column shows the results for the tidal inlet being open. The second column shows the results for the tidal inlet being closed. At last the top right figure shows the initial bathymetry and the bottom left figure shows the difference between the gained shoreline between the tidal inlet being open and closed.

Storm wave conditions

In Figure E.3 the development of the shoreline can be seen for the storm wave conditions simulations. The mega-nourishment at 5km from the tidal inlet is shown in Figure E.3b. With the mega-nourishment at 5km from the tidal inlet it can be seen in the top left figure that the mega-nourishment erodes quickly at first (2008 to 2010) but slows down as time progresses. The shoreline retreat from 2008 to 2010, from 2010 to 2012 and from 2012 to 2014 are 160, 70 and 40 meters respectively. The tip of the mega-nourishment stays at the line indicating the centroid of the mega-nourishment. Furthermore, the adjacent coast next to the erosion of the mega-nourishment, accretes by up to 100 meter from 2008 to 2010. After this the accretion of the shore slows down significantly to up to several tens of meters per two years. Furthermore, the depth contours are closer to each other, indicating a steeper slope near the shore compared to the initial bathymetry (see top right figure).

In the bottom row the accretion and erosion patterns are symmetrical around the centroid of the mega-nourishment. During the first 1.5 years there is a spatially uniform accretion in the alongshore direction. After 1.5 years the accretion spreads out away from the mega-nourishment. The maximum accretion at the year 2014 is 133.3 meters and the maximum erosion is -300 meters. It can be seen by investigating the bottom right figure (see Figure E.3b), that there is no difference between the tidal inlet being open and closed for the storm wave conditions. No pattern can be recognized (see bottom right figure).

With the mega-nourishment at 2km from the tidal inlet (see Figure E.3a) it can be seen in the top row that the tip of the mega-nourishment erodes fast the first 2 years (2008 to 2010) and slows down over time. The shoreline retreat from 2008 to 2010, from 2010 to 2012 and from 2012 to 2014 are 150, 75 and 45 meters respectively. Furthermore, the tip of the mega-nourishment propagates towards the non-inlet-side as the inlet-side erodes more. On the non-inlet-side the adjacent beach accretes by up to 100 meters for the first two years (2008 to 2010) after which the accretion slows down significantly. The bathymetry for the tidal inlet being open and closed are different from each other. This is most apparent by looking at the -4.0 meter depth contour.

In the bottom row (see Figure E.3a) it can be seen that the accretion and erosion patterns are not symmetrical around the centroid of the mega-nourishment. The adjacent coast on the inlet-side of the centroid of the mega-nourishment accretes more than the non-inlet-side. At the last time step in 2014 the maximum accretion on the non-inlet-side is 133.3 meter while on the inlet-side it is 66.7 meter. In the first few years (2008 to 2010) there is accretion on the inlet-side at the adjacent coast. However, towards the tidal inlet there is erosion from 2012 to 2014. At the adjacent coast on the non-inlet-side there is a spatially uniform accretion pattern in the alongshore direction from 2008 to about July 2009. After this the accretion pattern spreads out from the mega-nourishment.

In the bottom right figure (see Figure E.3a) the change in shoreline between the tidal inlet being open and closed is shown. There is a general erosion pattern on the inlet-side of the centroid of the mega-nourishment. This erosion pattern has a maximum value of 33.3 meter which means that there is more shoreline lost with the tidal inlet being open than closed.

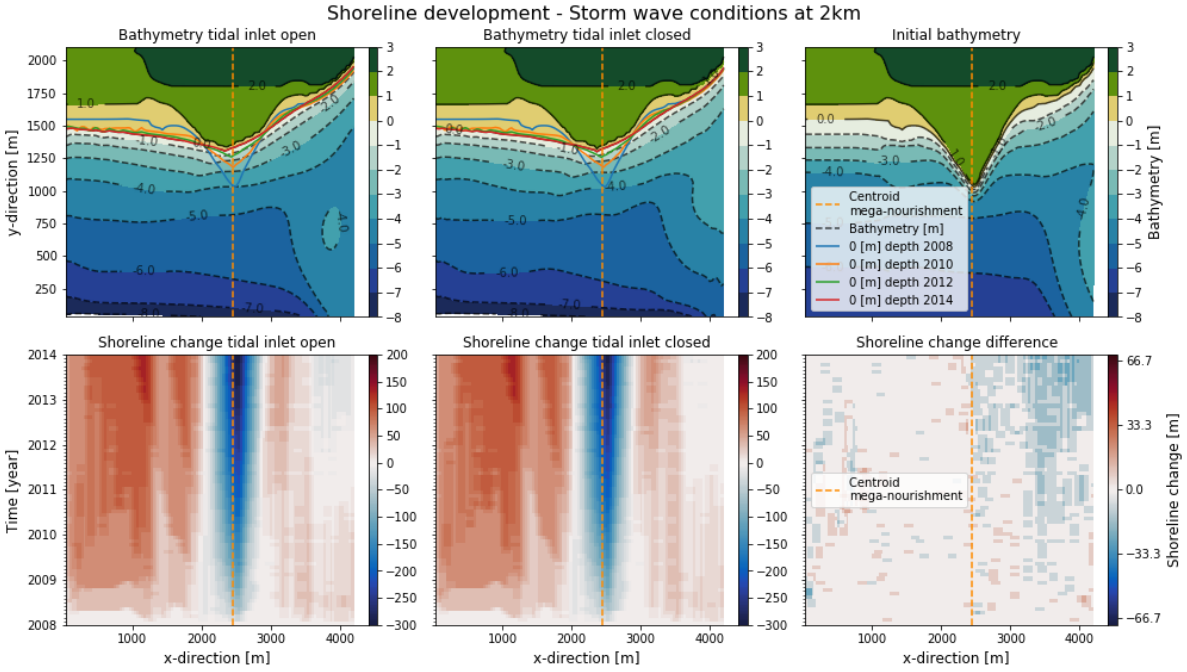

(a) Shoreline development storm wave conditions at 2 km

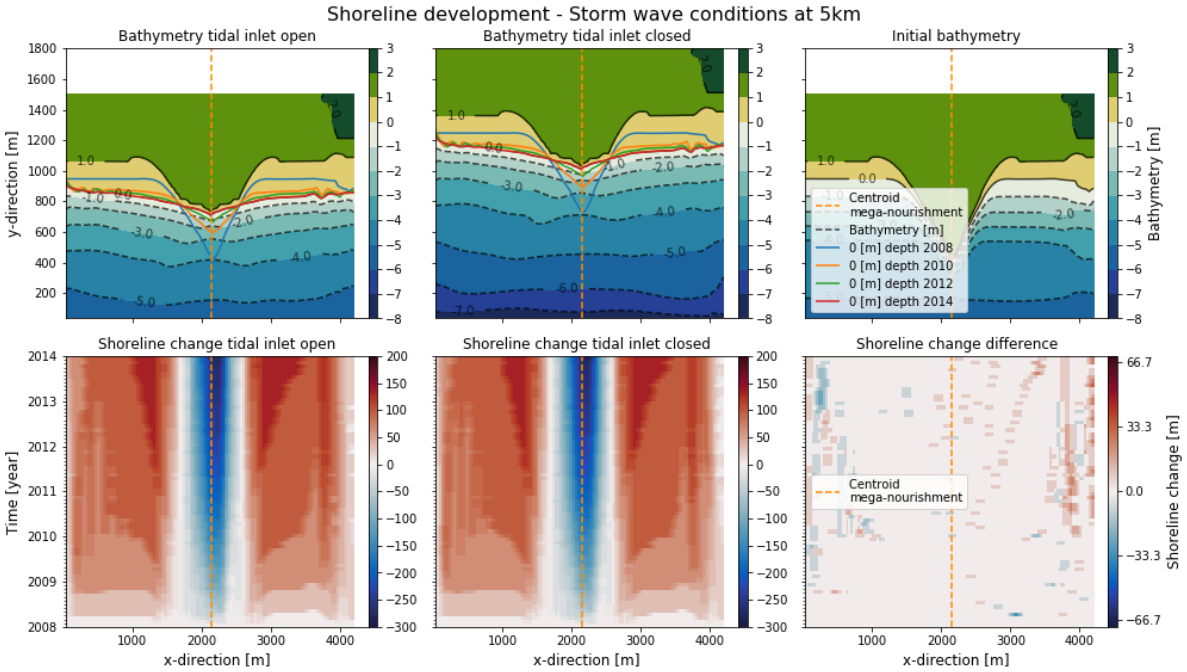

(b) Shoreline development storm wave conditions at 5 km

Figure E.3: Shoreline development for storm wave conditions. The first row shows the bathymetry and the shoreline over time. The blue, orange, green, red and dashed orange lines shows the zero meter depth contour at the years 2008, 2010, 2012, 2014 and centroid of the mega-nourishment respectively. The second row shows the gained or lost shore with respect to the initial shoreline. Red shades indicates gained shore compared to the first time step (2008) and blue shows shore being lost. Furthermore, the first column shows the results for the tidal inlet being open. The second column shows the results for the tidal inlet being closed. At last the top right figure shows the initial bathymetry and the bottom left figure shows the difference between the gained shoreline between the tidal inlet being open and closed.

High tidal range

In Figure E.4 the development of the shoreline can be seen for the storm wave conditions simulations. The mega-nourishment at 5km from the tidal inlet is shown in Figure E.4b. With the mega-nourishment at 5 km from the tidal inlet it can be seen in the top left figure that the mega-nourishment erodes quickly at first (2008 to 2010) but slows down as time progresses. The shoreline retreat from 2008 to 2010, from 2010 to 2012 and from 2012 to 2014 are 150, 70 and 55 meters respectively. The tip of the mega-nourishment stays at the line indicating the centroid of the nourishment. Furthermore, the adjacent coast next to the erosion of the mega-nourishment accretes slowly over time. The +1.0 meter depth contour accretes more than the 0 meter depth contour. Moreover, the depth contours are closer to each other, indicating a steeper slope near the shore compared to the initial bathymetry (see top right figure).

In the bottom row (see Figure E.4b) it can be seen that the erosion and accretion patterns are symmetrical around the centroid of the mega-nourishment. There is a strong erosion near the centroid of the mega-nourishment with a maximum shoreline of 300 meter being lost. The adjacent coast gains shore of up to 33.3 meter up to the year 2011, after which there is increased accretion of 66.6 meter which spreads out from the mega-nourishment over time. There is no significant difference between the tidal inlet being open and closed and also no patterns are evolving (see bottom right figure in Figure E.4b).

In Figure E.4a the shoreline development with the mega-nourishment at 2km from the tidal inlet is shown. In the top row it can be seen that the tip of the mega-nourishment first erodes quickly (2008 to 2010) and then slows down over time. The shoreline retreat from 2008 to 2010, from 2010 to 2012 and from 2012 to 2014 are 150, 70, 55 meters respectively for both the tidal inlet being open and closed. The location of the tip of the mega-nourishment shifts towards the non-inlet-side over time as the inlet-side near the tip of the mega-nourishment erodes more than the non-inlet-side. The +1.0 meter depth contour accretes more than the 0.0 meter depth contour over time, indicating that more sediment is higher up in the beach profile. The depth contour lines are closer to each other. As a result the beach slope became steeper over time compare to the initial bathymetry. The bathymetry from the tidal inlet being open and closed are different. With the tidal inlet being open the ebb-tidal delta has grown (see -5.0 meter depth contour in the top left figure) and a shoal has been created (see x=3000 meter and y=500 meter). Furthermore, a deeper flood channel (compared to the closed tidal inlet) has formed between the ebb-tidal delta and the shore.

At last the figures in the bottom row (see Figure E.4a) shows the change in shoreline over time with the mega-nourishment located 2km from the tidal inlet. The erosion and accretion patterns are not symmetrical around the centroid of the mega-nourishment. At the location of the mega-nourishment there is more erosion on the inlet-side of the centroid of the mega-nourishment than on the non-inlet-side. Furthermore, on the non-inlet-side of the mega-nourishment at the adjacent coast there is an accretion of 33.3 meters which is somewhat uniform in time over the entire duration of the simulation. On the inlet-side for the tidal inlet being open there is accretion at the adjacent coast towards the mega-nourishment and erosion towards the tidal inlet. With the tidal inlet being closed the accretion and erosion patterns to the inlet-side of the mega-nourishment are less pronounced than for the tidal inlet being open. This difference is also more apparent in the bottom right figure (see Figure E.4a). In this figure there is a clear pattern of more shoreline gained on the inlet-side close to the mega-nourishment over time. Meanwhile further to the inlet-side there is more shoreline retreat of up to 66.7 meter over time with the tidal inlet being open. The maximum difference between the shoreline with the tidal inlet being open and closed near the tidal inlet is 100 meter of shoreline retreat.

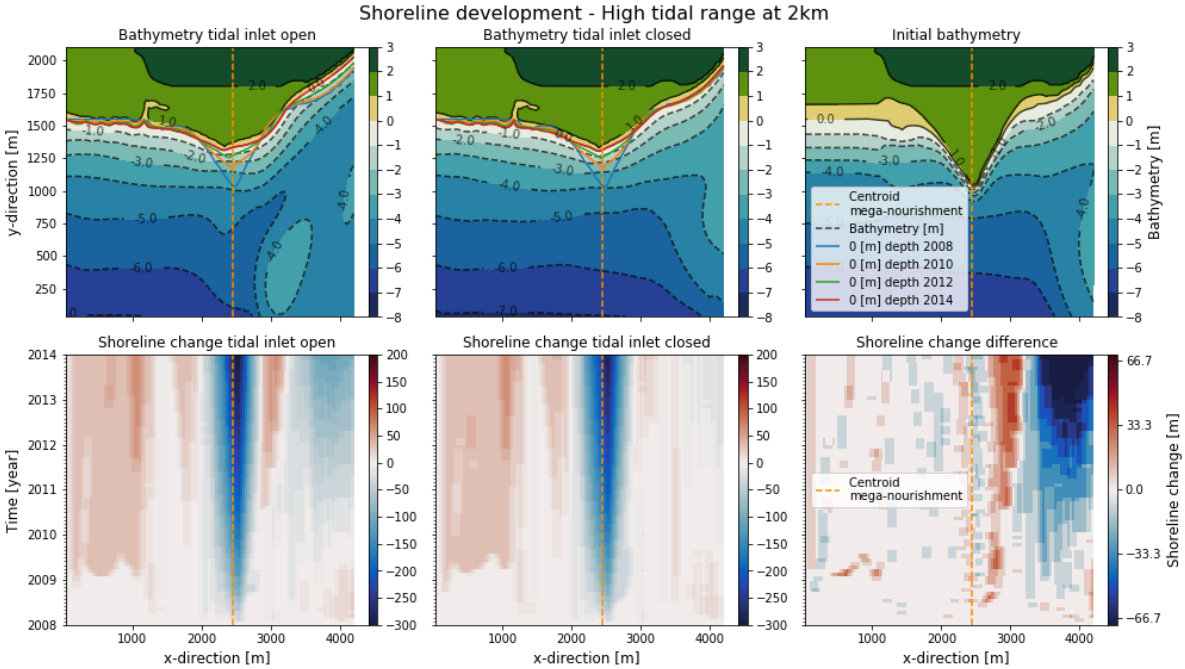

(a) Shoreline development oblique wave conditions at 2 km

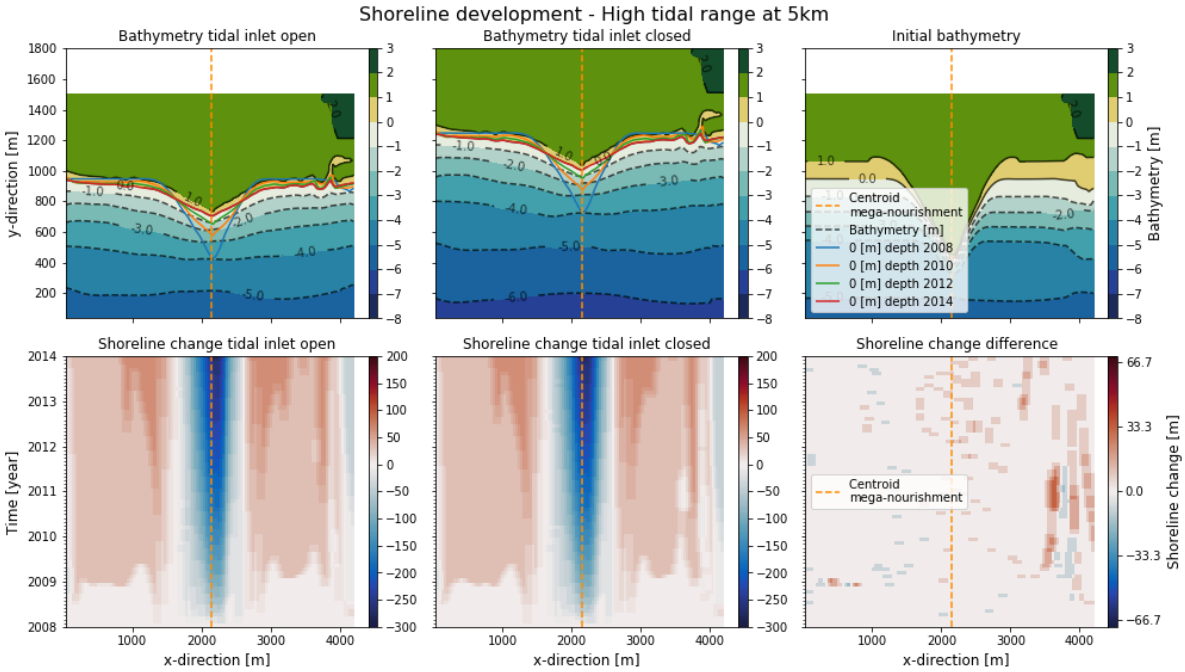

(b) Shoreline development high tidal range at 5 km

Figure E.4: Shoreline development for a high tidal range. The first row shows the bathymetry and the shoreline over time. The blue, orange, green, red and dashed orange lines shows the zero meter depth contour at the years 2008, 2010, 2012, 2014 and centroid of the mega-nourishment respectively. The second row shows the gained or lost shore with respect to the initial shoreline. Red shades indicates gained shore compared to the first time step (2008) and blue shows shore being lost. Furthermore, the first column shows the results for the tidal inlet being open. The second column shows the results for the tidal inlet being closed. At last the top right figure shows the initial bathymetry and the bottom left figure shows the difference between the gained shoreline between the tidal inlet being open and closed.

Real tide

In Figure E.5 the development of the shoreline (0 meter depth contour) is shown. The mega-nourishment at 5km from the tidal inlet can be seen in Figure E.5b. With the mega-nourishment at 5km from the tidal inlet it can be seen in the top left figure that the nourishment erodes quickly at first (2008 to 2010) and then slows down over time. The shoreline retreat from 2008 to 2010, from 2010 to 2012 and from 2012 to 2014 are 150, 70 and 55 respectively. This retreat is similar for the tidal inlet being open and closed. The adjacent coast accretes fast until 2010 after which the accretion slows down. This accretion is uniform along the adjacent coast for the first two years. In the finial bathymetry (see the top right and top center figures) it can be seen that the depth contours near the shore are closer to each other, indicating that the beach slope is steeper than in the initial bathymetry.

In the bottom row (see Figure E.5b) the accretion and erosion patterns are symmetrical around the centroid of the mega-nourishment. During the first two years there is a spatially uniform accretion pattern at the adjacent coast. After about July 2010 the accretion pattern is not uniform anymore but spreads out from the mega-nourishment. The difference in shoreline between the tidal inlet being open and closed are the same (see the bottom right figure). No patterns or developing patterns can be recognized.

With the mega-nourishment at 2km from the tidal inlet (see Figure E.5a) it can bee seen in the top row that the tip of the mega-nourishment erodes fast from 2008 to 2010 and then slows down over time. The shoreline retreat from 2008 to 2010, from 2010 to 2012 and from 2012 to 2014 are 150, 70 and 55 meters respectively for the tidal inlet being open. Furthermore the centroid of the mega-nourishment propagates towards the non-inlet-side as time progresses since the inlet-side erodes more than the non-inlet-side. On the non-inlet-side the adjacent beach accretes by up to 100 meters for the first 2 years (2008 to 2010) after which the accretion slows down significantly. The bathymetry for the tidal inlet being open and closed are different from each other. This is most apparent when looking at the -4.0 meter depth contour.

In the bottom row (see Figure E.5a) the erosion and accretion patterns are not symmetrical around the centroid of the mega-nourishment. The inlet-side erodes more than the non-inlet-side. Also the inlet-side does not show uniform accretion in the alongshore direction during the first two years (2008 to 2010), whereas the non-inlet-side does. The shoreline at the inlet-side only erodes/accretes for about 33.3 meters during 6 years. Furthermore, there is a slight erosion towards the tidal inlet.

By investigating the bottom right figure it can be seen that there is not much difference in the position of the shoreline with the tidal inlet being open and closed. However, towards the tidal inlet on the inlet-side of the mega-nourishment there is more shoreline retreat with the tidal inlet being open than closed. This pattern starts at 2010 to 2011 and increases in size with time progressing. There is a difference of at most 33.3 meter in the shoreline between the tidal inlet being open and closed. Emphasizing that there is not much of a difference in shoreline between between the tidal inlet being open and closed. There is no pattern elsewhere in the domain except for noise.

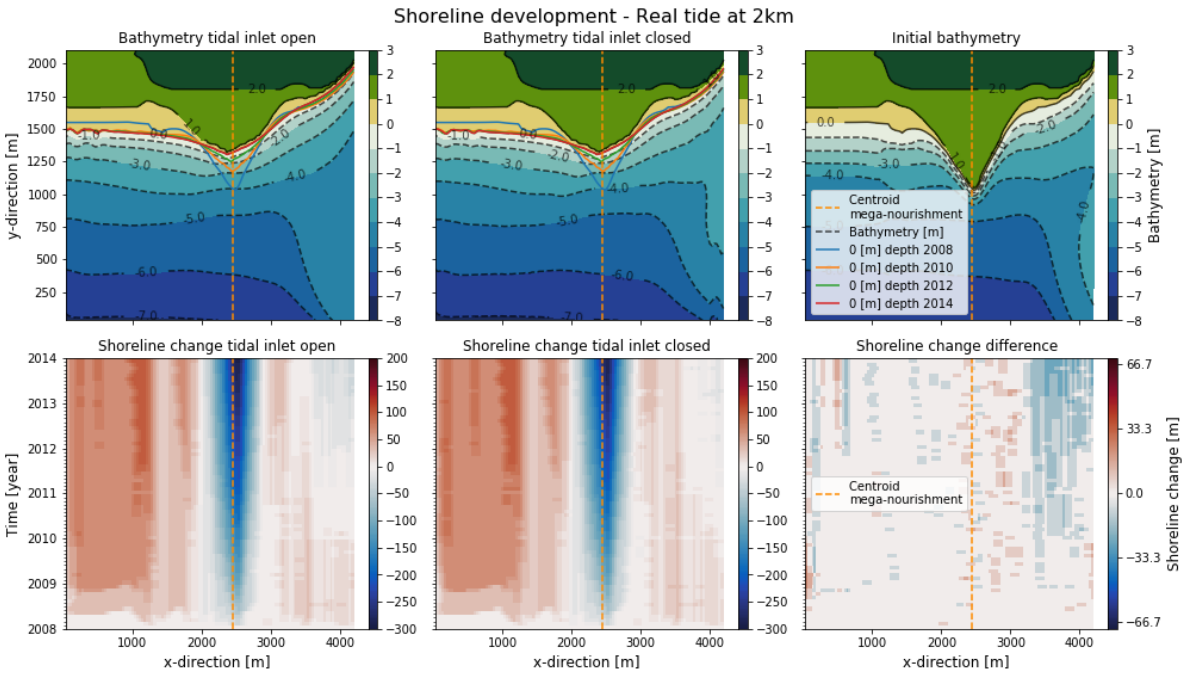

(a) Shoreline development real tide at 2 km

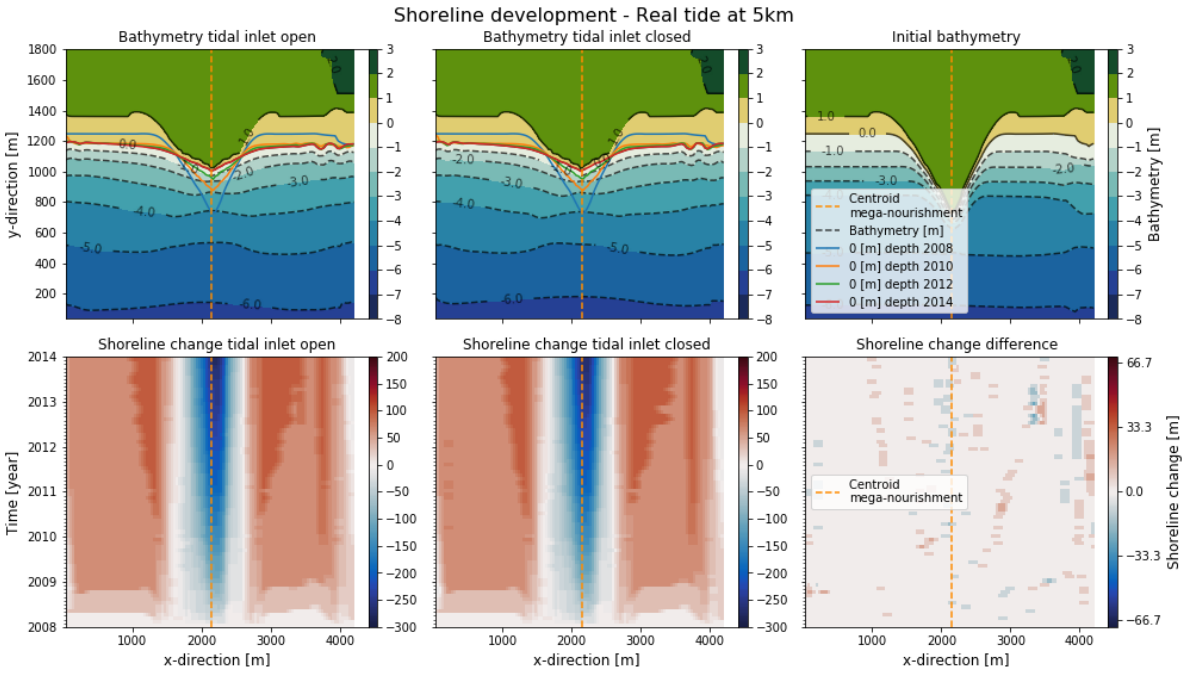

(b) Shoreline development real tide at 5 km

Figure E.5: Shoreline development for real tide. The first row shows the bathymetry and the shoreline over time. The blue, orange, green, red and dashed orange lines shows the zero meter depth contour at the years 2008, 2010, 2012, 2014 and centroid of the mega-nourishment respectively. The second row shows the gained or lost shore with respect to the initial shoreline. Red shades indicates gained shore compared to the first time step (2008) and blue shows shore being lost. Furthermore, the first column shows the results for the tidal inlet being open. The second column shows the results for the tidal inlet being closed. At last the top right figure shows the initial bathymetry and the bottom left figure shows the difference between the gained shoreline between the tidal inlet being open and closed.

Real waves

In Figure E.6 the development of the shoreline (0 meter depth contour) is shown. With the mega-nourishment at 5km from the tidal inlet it can be seen in the top left figure (see Figure E.6b) that the nourishment erodes quickly at first (2008 to 2010) and then slows down over time. The shoreline retreat from 2008 to 2010, from 2010 to 2012 and from 2012 to 2014 are 170, 65 and 40 respectively. This retreat is similar for the tidal inlet being open and closed. The adjacent coast accretes fast until 2010 after which the accretion slows down. This accretion is uniform along the adjacent coast for the first two years. In the finial bathymetry (see the top right and top center figures) it can be seen that the depth contours near the shore are closer to each other, indicating that the beach slope is steeper than in the initial bathymetry.

In the bottom row (see Figure E.6b) it can be seen that during the first 2 years there is a spatially uniform accretion pattern at the adjacent coast. After 2010 a pattern starts to spread out from the centroid of the mega-nourishment. In the bottom right figure it can be seen that there is no significant difference between the tidal inlet being open and closed. This indicates that the tidal inlet does not influence the shoreline development of the mega-nourishment and the coast adjacent to the mega-nourishment.

With the mega-nourishment at 2km from the tidal inlet it can be seen in the top row (see Figure E.6a) that again the tip of the mega-nourishment erodes fast from 2008 to 2010 after which it slows down. The shoreline retreat from 2008 to 2010, from 2010 to 2012 and from 2012 to 2014 are 165, 65, 40 meter respectively. This is about the same as for the mega-nourishment at an alongshore distance of 5km from the tidal inlet. Furthermore, the tip of the mega-nourishment propagates towards the inlet-side over time. As the mean wave angle is -15 degrees relative to shore normal (see chapter 3.3.1).

In the bottom row (see Figure E.6a) it can be seen that the erosion and sedimentation patterns are not symmetrical around the centroid of the mega-nourishment. The inlet-side loses more shoreline than the non-inlet-side. On the non-inlet-side there is a spatially uniform accretion pattern until about 2010 after which a pattern emerges spreading out from the centroid of the mega-nourishment. However, the shoreline on the inlet-side of the mega-nourishment gains less shoreline compared to the non-inlet-side.

The bottom right figure (see Figure E.6a) shows the difference in gained or lost shoreline between the tidal inlet being open and closed. Relatively more shoreline is being lost for the tidal inlet being open compared to closed. This effect is most apparent close to the tidal inlet and does not reach the centroid of the mega-nourishment. It does reach the adjacent coast to the inlet-side of the mega-nourishment.

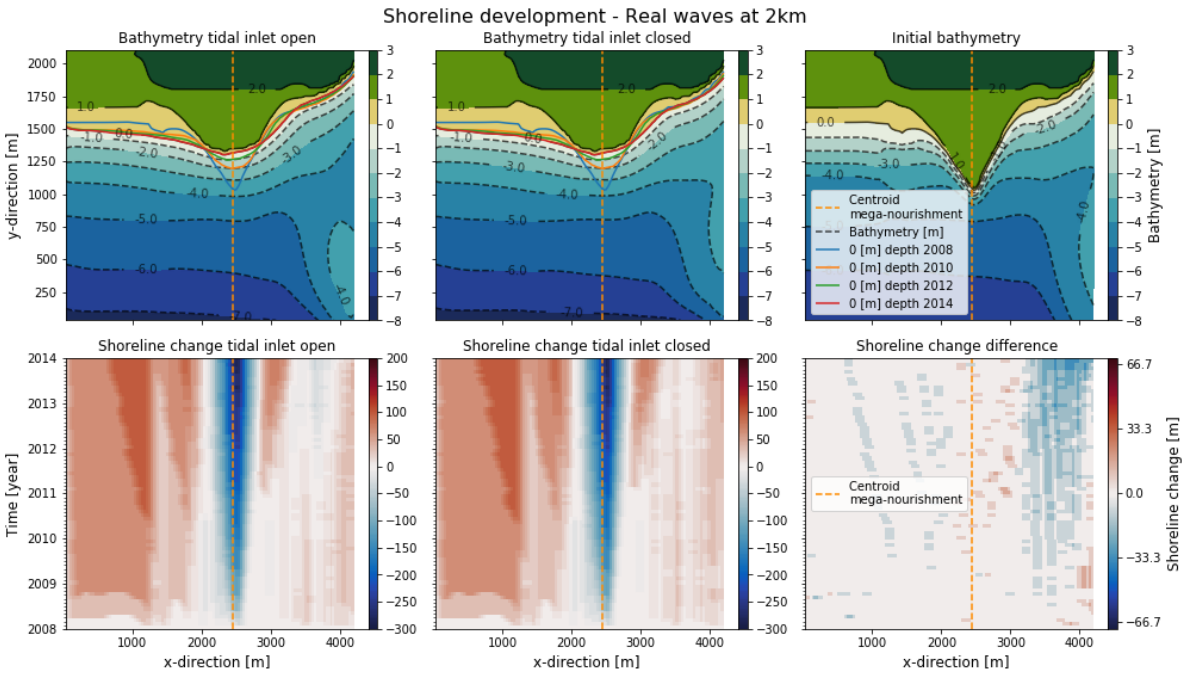

(a) Shoreline development real wave at 2 km

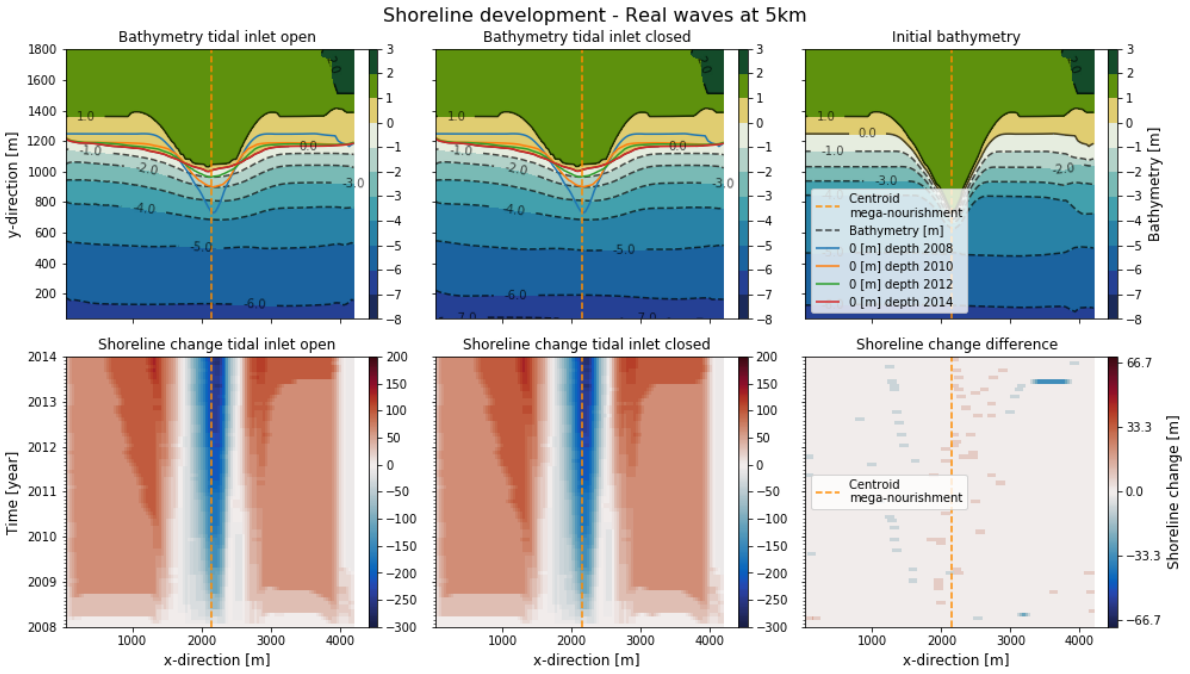

(b) Shoreline development real wave at 5 km

Figure E.6: Shoreline development for real wave. The first row shows the bathymetry and the shoreline over time. The blue, orange, green, red and dashed orange lines shows the zero meter depth contour at the years 2008, 2010, 2012, 2014 and centroid of the mega-nourishment respectively. The second row shows the gained or lost shore with respect to the initial shoreline. Red shades indicates gained shore compared to the first time step (2008) and blue shows shore being lost. Furthermore, the first column shows the results for the tidal inlet being open. The second column shows the results for the tidal inlet being closed. At last the top right figure shows the initial bathymetry and the bottom left figure shows the difference between the gained shoreline between the tidal inlet being open and closed.